A nose - brain preparation to study network interactions within the mammalian olfactory bulb.

Fernando Pérez de los Cobos Pallarés

A nose - brain preparation to study network interactions within the mammalian olfactory bulb.

Fernando Pérez de los Cobos Pallarés

Ludwig-Maximilians Universität München

18.10.2016

Gutachter: Prof. Dr. Veronica Egger

                Prof. Dr. Hans Straka

Tag der mündlichen Prüfung: 07.02.2017

Table of Contents

Abstract

Der Geruchssinn ist auf unterschiedliche Weise für viele Tiere überlebenswichtig. Im Gegensatz zum Menschen sind einige Gruppen von Säugetieren in ihrem Alltag darauf angewiesen, um ihre Umgebung wahrnehmen zu können, nach Essen zu suchen, zu kommunizieren, Feinde aufzuspüren und sich zu paaren. Diese Informationen werden vom Individuum als Geruch, zusammengesetzt aus verschiedenen chemischen Stoffen, aufgenommen. Die Aufnahme der Geruchsstoffe kann nicht ohne die Atmung funktionieren. Das Einatmen von Luft dient also einerseits zur überlebenswichtigen Aufnahme von Sauerstoff in den Körper aber andererseits auch als Mechanismus um Gerüche aus der Umgebung aufzunehmen. Dabei transportiert die Atmung Geruchsstoffe zu einem spezialisierten Riechepithel, wo die chemischen Stoffe von ebenfalls spezialisierten Riechzellen entschlüsselt werden. Diese Neuronen leiten die Informationen wiederum direkt an den Bulbus olfactorius, eine Vorderhirnregion, in der die meisten Gerüche verarbeitet werden, weiter. Die erste größere Weiterverarbeitung des olfaktorischen Inputs findet im Bulbus olfactorius statt, wo diese durch die Interaktion verschiedener Neuronentypen, die in verschiedenen Schichten voneinander abgetrennt sind, vermittelt wird. Der Bulbus olfactorius ist eng verbunden mit höheren Verarbeitungsregionen, an die er die zuvor bearbeiteten Informationen weiterleitet. Umgekehrt innervieren unterschiedliche kortikale Regionen über zentrifugale Fasern den Bulbus und regulieren so dessen Aktivität. Die direkte Verbindung zwischen Bulbus olfactorius und dem Verhalten zugeordneten Regionen lässt vermuten, dass die Verschaltungen im Bulbus olfactorius direkt mit dem Verhalten verknüpft sind. Unterschiedliche Verhaltenzustände können verschiedenen Aktivitätsmustern im Bulbus olfactorius zugeordnet werden, welche sich als osszilatorische Aktivität in unterschiedlichen Frequenzen darstellen. Bis jetzt wurden die genauen Mechanismen und Netzwerke, die die Osszilationen bestimmen, noch nicht völlig verstanden. Die Forschung am olfaktorischen System verbunden mit Osszilationen wurde zum Teil an akuten Präparaten und/oder an anästhesierten Tieren *in vivo* durchgeführt.

In dieser Arbeit habe ich neue Alternativen für gängige experimentelle Vorgehensweisen erforscht. Dies war begründet durch die Notwendigkeit eine intakte und funktionierende olfaktorische Bahn aufrechtzuerhalten, ohne Anästhesie zu nutzen. Das zuvor beschriebene semi-intakte Präparat schien eine gute Alternative

zum *in vivo* Präparat zu sein. Trotzdem wurde bisher keines bei Nagetieren beschrieben, welches ein Atemwegssystem wie *in vivo* aufrechterhält. Dementsprechend wurde in dieser Arbeit ein neuartiges semi-intaktes Präparat einer Ratte entwickelt, bei dem Geruchs- und Atemwegssystem gut erhalten bleiben.

Dieses Präparat umgeht viele Probleme anderer Vorgehensweisen, besitzt aber trotz allem eigene Einschränkungen. Die Vorteile scheinen jedoch zu überwiegen und ich konnte in dieser Arbeit die Tauglichkeit des Präparats durch die Anwendung in der aktuellen olfaktorischen Forschung verifizieren. Direkte nasale Stimulationen mit unterschiedlichen Geruchsstoffen riefen olfaktorische Reaktionen im Bulbus olfactorius hervor und lösten spontane und durch Geruch hervorgerufene Oszillationen aus. Überdies war die Erhaltung von trigeminalen Afferenzen, die die nasale Schleimhaut innervieren, entscheidend, um zu erforschen wie der Geruchssinn mit der Atmung in Abwesenheit von Regionen des Mittelhirns welche bei chirurgischen Eingriffen entfernt wurden, interagiert. Bisher konnte ich aufzeigen, dass die sogenannten trigeminalen Geruchsstoffe das Atemwegssystem regulieren. Außerdem löste Stimulierung mit diesen Geruchsstoffen mutmaßliches Schnuppern in verschiedenen Frequenzen aus.

Es ist bekannt, dass synaptische Plastizität auf der Ebene des Bulbus olfactorius in direkter Beziehung zur oszillatorischen Aktivität steht. Folglich habe ich für die Zielsetzung dieser Arbeit an einem Nebenprojekt mitgearbeitet, in dem wir in akuten Präparaten des Bulbus olfactorius zeigen, dass unterschiedliche elektrische Stimulationsparadigmen, die schnelle und langsame Oszillationen imitieren, neuronale Plastizität hervorrufen.

Zusammenfassend kann gesagt werden, dass ich in dieser Arbeit die erfolgreiche Entwicklung einer neuen experimentellen Technik präsentiere. Diese erlaubt durch Geruch hervorgerufene Reaktionen, oszillatorische Aktivitäten und deren Interaktion mit dem Atemwegssystem und andere olfaktorische Funktionen auf unterschiedlichen Ebenen zu studieren. Schlussendlich zeige ich, dass oszillatorische Aktivitäten die neuronale Plastizität im Bulbus olfactorius antreiben.

Abstract

The sense of olfaction is vital for the survival of many animals in different ways. In contrast to humans, some groups of mammals rely on it in their daily life to perceive their environment in order to search for food, to communicate, detect predators or to find mates. This information arrives to an individual as an odor composed by different types of chemicals. In land mammals the detection of these chemicals cannot be understood without respiration, where inspiration of air provides oxygen to the body to survive but at the same time serves as an odor sampling mechanism of the surrounding. In this respect, the respiration transports odorants to olfactory detection tissues/epithelia where the chemicals are detected by specialized olfactory neurons. In turn, these neurons relay this information directly to the olfactory bulb, a forebrain area where the processing of odors is mediated by the interaction of different types of neurons which are spatially distributed in different layers. The olfactory bulb is densely connected with higher processing areas to where it relays the information previously processed. In turn, different cortical areas project back centrifugal fibers to the bulb, modulating its activity. The direct connection between olfactory bulb and behavior-related areas suggests that the wiring in the olfactory bulb is directly linked to behavior. Different behavioral states relate to different activity patterns in the olfactory bulb, which are reflected as oscillatory activity at different frequencies. So far, the exact mechanisms and networks ruling oscillations are still not fully understood. Research in the olfactory field related to oscillations has been performed to some extent in acute slices and/or in anaesthetized animals *in vivo*.

Within this thesis I explored new alternatives to more popular experimental approaches. This was motivated by the necessity of maintaining an intact and functional olfactory pathway while not using anesthesia. Previously described semi intact preparations seemed to be a good alternative for *in vivo* preparations. However, none was described in rats that maintained an *in vivo*-like olfactory network. Thus, in this thesis a novel semi intact preparation of the rat was developed with well-preserved olfactory and respiratory networks. This preparation circumvents many issues from other approaches but it also has its own limitations. However, the advantages seem to exceed the limitations, and within this thesis I could verify the suitability of this preparation to be used in the current olfactory research. Direct nasal stimulation using different odorants evoked olfactory responses in the olfactory bulb and elicited spontane-

ous and odor-evoked oscillations. Moreover, preservation of trigeminal afferents innervating the nasal mucosa was crucial to investigate how olfaction interacts with respiration in the absence of midbrain areas which were removed during surgical procedures. So far, I could demonstrate that so-called trigeminal odorants modulate respiratory networks. Besides, stimulation with these odorants triggered putative sniffs at different frequencies.

Synaptic plasticity at the level of the olfactory bulb is known to be directly related to oscillatory activity. Thus, for the purpose of this thesis, I participated actively in a side project in which we demonstrate in olfactory bulb acute slices that different electrical stimulation paradigms mimicking fast and slow oscillatory components elicits synaptic plasticity.

Conclusively, in this thesis I present the successful development of a new experimental technique. This new technique allows to study olfactory function at different levels, odor-evoked responses, oscillatory activity and how it interacts with respiratory networks. Finally, I show that oscillatory activity can drive neural plasticity in the olfactory bulb.

1. **INTRODUCTION**

1.1. The importance of the sense of smell

Olfaction is an active process which enables animals to get information of the air-borne chemical environment. Some vertebrates, like rodents, critically rely on their olfactory sense for their survival. This sense is known to be crucial for diverse behaviors such as tracking sources of food, mating, detecting predators or social communication among others (Doty 1986; Keverne 2004; Restrepo, Arellano et al. 2004). In turn, olfaction in humans did not get that much attention in the last century compared to research on other sensory systems. Nowadays, it might be accepted that humans do not essentially rely on the sense of smell for the daily life. However, olfactory dysfunction can precede different disorders and might have a direct impact on life quality (Hummel, Landis et al. 2011). Nevertheless, in the last decades olfaction gained more attention since it is a good model to investigate how external sensory information is coded in the brain from the molecular to the network level. Impairment of olfactory function could indicate early stages of certain neurodegenerative diseases (Hummel, Landis et al. 2011; Doty and Kamath 2014; Godoy, Voegels et al. 2015), which makes olfactory research a field of interest for different medical studies. Thus, much effort has been performed to study the olfactory network architecture, its properties and interactions and to understand how odor information is processed and coded in the OB. The study of the different cell layers forming the OB uncovered different cell types and properties as well as different cellular-regulatory mechanisms revealing a complex and dynamic network, based on the interaction between mainly glutamatergic and GABAergic neurons (Egger and Urban 2006; Urban and Arevian 2009; Nunes and Kuner 2015). Besides, the OB is broadly connected to many other brain regions. Thus, odor stimuli entail information which will be processed in the OB and will afterwards be relayed in different olfactory-related brain areas modulating the behavioral output.

Odors are chemically very diverse and they travel downwind in mixtures as small packages of volatile molecules. Odorants are basically small organic molecules of less than 400 Da which differ in size, shape, functional groups and charge. Different chemical classes form odorant molecules such as alcohols, aldehydes, ketones and

esters; chemicals with aromatic, alicyclic, polycyclic or heterocyclic ring structures; and innumerable substituted chemicals of each of these types, as well as combinations of them (Gaillard, Rouquier et al. 2004). Its detection depends on their concentration and on the volatility of the chemical although not all the volatile molecules are detected. Notably, despite humans have only a small epithelial area and low sensitivity to odorants (Galizia and Lledo 2013) it is reported to be able to discriminate over a trillion of odorants (Bushdid, Magnasco et al. 2014), although this statement is likely to be imprecise and still under debate (Meister 2015).

1.2. Organization of the olfactory system

Chemosensory stimuli are very diverse, which detection influence our behavior. Therefore, two major systems are in charge for detecting and transducing these sensory inputs in vertebrates. On the one hand, the main olfactory system processes mostly volatile molecules in the MOB. Their detection occurs at the level of the olfactory epithelium by olfactory sensory neurons (OSNs). Receptors located on the surface of the cilia of the OSNs bind odor molecules and send the signal to the main olfactory bulb (MOB). Within the OB interactions between glutamatergic mitral and tufted cells with inhibitory granule cells (GCs) process most of the olfactory stimuli. Mitral (MC) and tufted (TC) cells project to different cortical areas propagating this input onto cortico-limbic networks. In turn, feedback projections from cortical areas synapse mostly on GCs shaping odor responses from MCs and TCs. On the other hand, the accessory olfactory system detects pheromones via the vomeronasal organ. The vomeronasal organ is a bilateral tubular structure that is enclosed in a cartilaginous capsule. It is located at the base of the nasal septum and it connects to the nasal cavity via a narrow duct. Vomeronasal sensory neurons project their axons to few glomeruli in the accessory olfactory bulb. Pheromone responses mediate many behaviors that range from aggression, sexual behavior to endocrine changes (Meredith 1991; Halpern and Martinez-Marcos 2003; Ackels, von der Weid et al. 2014).

There are further other olfactory subsystems which respond to chemosensory cues. The Grueneberg Ganglion is a cluster of sensory neurons located on the rostral part of the nasal cavities that project directly to the MOB. These neurons are thought to play a key role in thermosensation as well as constituting a detector for alarm pheromones since the activation of the Grueneberg Ganglion induces freezing behavior (Brechbuhl, Klaey et al. 2008). Projections to the OB provide directly social relevant chemical information suggesting a role for interactions between individuals (Munger, Leinders-Zufall et al. 2010). In the ventral side of the nasal septum, there is the septal organ of masera, another olfactory subsystem. It is formed by sensory neurons which project directly to the MOB and are thought to be important for mechanosensation (Grosmaitre, Santarelli et al. 2007).

The interactions between the principal olfactory systems in combination with the different olfactory subsystems might provide an optimal perception of the surrounding

for most vertebrates. Because sensory information coming from the different systems and subsystems might be synergetic at the level of the OB, it might provide a fast and accurate behavioral output which might be crucial for the animal´s development and survival.

1.3. <u>Olfactory perception: from detection to processing</u>

In most vertebrates, the olfactory system samples the chemical environment rhythmically, detecting and processing different odors. It provides information that is retained in small volatile molecules often mixed with other molecules. The detection of odors is localized in the nasal epithelium by specialized OSNs while the processing stage occurs at different levels in the MOB and in higher olfactory-related cortical areas. In the next sections, a description of the different olfactory processing stages is revealing in detail different cell types distributed in different layers and their connections within the OB and with other brain areas.

1.3.1. <u>Olfactory sensory neurons (OSNs)</u>

Olfactory sensory neurons (OSNs) are specialized neurons with a dual function being responsible for detection and transduction of odor and mechanical stimuli (Grosmaitre, Santarelli et al. 2007). They are located in the MOE and are surrounded by the Bowman´s gland, basal and supporting cells. OSNs have cilia that innervate the mucus of the olfactory epithelium. With each inspiration, volatile molecules get in contact with the cilia of the OSNs, binding specifically to olfactory receptors (ORs) expressed on the surface of the cilia. Beside the olfactory receptors, there are other G-protein coupled receptors known to exist in vertebrates such trace amine-associated receptors (TAARs) (Borowsky, Adham et al. 2001; Liberles and Buck 2006) and formyl peptide receptors (Riviere, Challet et al. 2009). Additionally there are two more gene families coding for receptors detecting pheromones in the vomeronasal organ (f*or more details see section "Accessory olfactory bulb"*). ORs represent the biggest family in the nasal epithelium (1000 genes coding for ORs in rodents with 370 functional ones in humans; (Mombaerts 2001)), followed by TAARs (15 genes in mice and 6 in humans (Liberles and Buck 2006; Johnson, Tsai et al.

2012) and FPRs (7 genes in rodents; (Monahan and Lomvardas 2015)). Each OSN that expresses one single type of OR from the whole repertoire project its axons through the lamina propia and the cribriform plate onto one or two glomeruli in the MOB (Mombaerts, Wang et al. 1996). ORs bind epitopes, an integral part of the molecule that can be present in different types of odors. The combinatorial activation of different ORs provides a representation of a certain odor, which is the odor perception at this early stage (Malnic, Hirono et al. 1999). The repertoire of ORs is well distributed in different zones in the olfactory epithelium along the rostral-dorsal axis and they are different in number across species depending on the number of genes coding for them.

At the level of OSNs, odor molecules are transformed into electrical signals which will be processed in the OB. When volatile molecules bind receptors, it activates a specific G-protein named G_{olf}. This results in an increase of cyclic adenine monophosphate (cAMP) via activation of adenyl cyclase III (ACIII). Consequently, cAMP opens cyclic nucleotide gated channels (CNGC) allowing the entrance of Na^+ and Ca^{2+} ions. The influx of Ca^{2+} ions also activates Ca^{2+} activated chloride channels (CaCC) leading to Cl^- ion efflux. The overall result is the generation of an action potential which will be relayed to the main olfactory bulb.

1.3.2. Main olfactory bulb (MOB)

The main olfactory bulb is a multi-layered neural network where olfactory sensory inputs are processed as well as different centrifugal inputs. Located in the rostral part of the forebrain, it receives inputs directly from the OSNs (Vassar, Chao et al. 1994). The OSNs expressing the same receptors, project their axons onto one or few glomeruli (Mombaerts, Wang et al. 1996), the first complex processing structures in the OB. Different cell types are distinguished depending on their morphology and localization in different layers in the OB. The main layers I will focus on in this thesis are the glomerular layer, the external plexiform layer, the mitral cell layer and the granule cell layer. In the next sections I describe first all these layers anatomically, give detail of the physiology of the most numerous synapses at the level of the olfactory bulb and overview the response dynamics of the main cell types involved in olfactory processing.

1.3.2.1. Glomerular layer (GL)

The glomerular layer is formed by glomeruli, neuropil structures located on the superficial layer of the olfactory bulb where presynaptic axons of OSNs synapse with apical dendrites of glutamatergic mitral and tufted cells (De Saint Jan, Hirnet et al. 2009; Najac, De Saint Jan et al. 2011; Gire, Franks et al. 2012). Glomeruli are surrounded by juxtaglomerular cells, which includes GABAergic periglomerular cells (PGC), superficial short axon cells (sSACs) and external tufted cells (eTC). These cells differ in number, size, morphology, innervation pattern of glomeruli and each group can be divided into different subtypes (Pinching and Powell 1971; Parrish-Aungst, Shipley et al. 2007; Kosaka and Kosaka 2011; Nagayama, Homma et al. 2014). While eTCs are glutamatergic, PGCs and sSACs are GABAergic although they can also release dopamine. Once the input arrived to the glomerular layer, it propagates downstream to tufted cells (TCs) in the external plexiform layer (EPL) and to mitral cells (MCs) in the mitral cell layer (MCL) disynaptically or even monosynaptically directly from OSNs (De Saint Jan, Hirnet et al. 2009; Najac, De Saint Jan et al. 2011).

1.3.2.2. External plexiform layer (EPL) and mitral cell layer (MCL)

Tufted (TC) and mitral cells (MC) are the main glutamatergic neurons in the OB. With similar morphological and to some extent biophysical properties, a detailed description of these two types of neurons and their interactions is needed to understand their crucial functions during odor processing.

TCs are classified in two subgroups depending on their location in the OB and anatomical differences (depending on the presence or absence of secondary dendrites). Middle and internal TCs project secondary dendrites to different areas in the EPL while a small portion of TCs have no secondary dendrites (Orona, Rainer et al. 1984).

Medial to the EPL there are MCs located in the MCL, which have larger somata compared to TCs and most of them extend secondary dendrites into the EPL. They are classified into different subtypes depending on their projection to intermediate or deeper layers of the EPL (Mori, Kishi et al. 1983; Orona, Rainer et al. 1984).

Within the EPL there are different types of interneurons, mostly GABAergic, that interact mostly with projection neurons. These neurons are partially classified depending on their expression of different calcium-binding proteins such paralbumin (PV), calbindin (CB), calretinin (CR) and neurocalcin (Brinon, Martinez-Guijarro et al. 1999) and further are classified by their morphology and connectivity as Van Gehuchten cells and multipolar type cells. Van Gehuchten short-axon cells are interneurons that have some features in common with somatostatin-immunoreactive cells. Both are in the same size range and are located throughout the EPL (Schneider and Macrides 1978) with a more localized presence of somatostatine-immunoreactive cells (~95%) in the intermediate-deep EPL (Lepousez, Csaba et al. 2010). Multipolar type cells are classified depending on their morphology, exact location and dendritic extension, being (1) inner horizontal cells, (2) large short axon cells and (3) other types. These three different types of cells have different morphology, spatial distribution and synapse with distinct cell types throughout the OB (Schneider and Macrides 1978; Kosaka, Heizmann et al. 1994; Brinon, Arevalo et al. 1998; Lepousez, Csaba et al. 2010).

1.3.2.3. Granule cell layer (GCL)

The most abundant cell types in the OB are the granule cells (GCs), inhibitory axonless interneurons that release gamma - aminobutyric acid (GABA). They have small cell bodies (6-8 µm) (Price and Powell 1970) and although they are mostly located in the GCL, they could also be found in the IPL and in the MCL (Nagayama, Homma et al. 2014). Granule cells are classified in three different groups depending on if they project their dendrites to any depth of the EPL (type I), only to deeper layer of the EPL (type II) or to the superficial layer of the EPL (type III) (Mori, Kishi et al. 1983), targeting mostly MCs and TCs. A recent study reported two new types of granule cells. They were observed to be generated in the subventricular zone (SVZ) and migrate to the GCL (Merkle, Fuentealba et al. 2014). The first new type projects their dendrites exclusively to the GCL (type IV GC) while the other new one has somata lacking basal dendrites and being restricted to the MCL (type-V GC). Other types of GABAergic interneurons in the GCL are deep short-axon cells (dSAC) which have larger cell bodies compared to GCs. They synapse onto GCs although they also interact with other cell types depending on which layer they project into. They are

classified into three different groups based on their location and morphology. DSACs are located at the frontier between the GCL and IPL, with their dendrites being confined within the IPL, but their axons project to the GL. Other dSACs (11-15 µm), are located in the medial GCL. They have dendrites that project widely across the MCL, IPL and GCL, while their axons extend mostly to the EPL. The last type of dSACs (10-20 µm) is located in the GCL and its dendrites project as well to the MCL, IPL and GCL but their axons extend to the GCL and some to the olfactory cortex (Schneider and Macrides 1978; Eyre, Antal et al. 2008; Eyre, Kerti et al. 2009; Nagayama, Homma et al. 2014).

1.3.3. Reciprocal dendrodendritic synapse between mitral cell and granule cells

Granule cells are the most numerous neurons in the vertebrate olfactory bulb (Egger and Urban 2006). Interactions of GCs with MCs are known to be critical in the processing of odor information. The MC-GC synapse is dendrodendritic and reciprocal, being glutamatergic from MC to GC and GABAergic from GC to MC. In MCs, the release of glutamate is typically mediated by action potentials (APs) (Xiong and Chen 2002) which depolarize its dendrites and mediate the opening of high-threshold voltage-dependent calcium channels (VDCC). Glutamate released in the synaptic cleft binds to NMDA and AMPA receptors in GC spines which contribute to the excitation of the GC (Isaacson and Strowbridge 1998; Sassoe-Pognetto and Ottersen 2000). Since glutamate binds both receptors, excitability of the GC spine occurs in two phases, where first AMPA receptors mediate fast depolarizations of the spines followed by NMDA receptor activation being responsible for long lasting depolarizations in the GC spine (Schoppa, Kinzie et al. 1998; Isaacson 1999; Isaacson and Murphy 2001; Egger, Svoboda et al. 2005; Egger and Urban 2006). The outcome of this interaction can lead to three different scenarios (Egger, Svoboda et al. 2003) in which (1) excitation of a GC spine by glutamate promotes the release of GABA back to the MC (Isaacson and Strowbridge 1998) even without the generation of an AP (Jahr and Nicoll 1980; Jahr and Nicoll 1982). (2) activation of a GC spine excites proximal spines on the same GC due to subthreshold activity between spines, leading in consequence to potential inhibition of an adjacent MC (Jahr and Nicoll 1982; Woolf, Shepherd et al. 1991). The last scenario (3) would be a mechanism of global lateral inhibition where a strong suprathreshold activation of the GC leads to the generation

8

of an AP which could propagate throughout the dendritic tree causing global lateral inhibition to all connected MCs (Chen, Xiong et al. 2000). Thus, GCs modulate MC activity by different inhibition mechanisms suggesting that their contribution might be crucial for shaping odor responses.

GCs activation does not only depend on MCs. There are plenty of centrifugal inputs and different neuromodulatory projections coming from higher cortical areas which may contribute to the excitation of GCs. As stated above, MC-GC synapses are the most predominant connections in the OB and their interactions generate oscillatory activity at different frequencies that can lead to different mechanisms of synaptic plasticity. Both oscillatory and synaptic plasticity are complex topics and in order to get a better understanding I will provide a more detailed description for both neural mechanisms in the next sections (see 1.5).
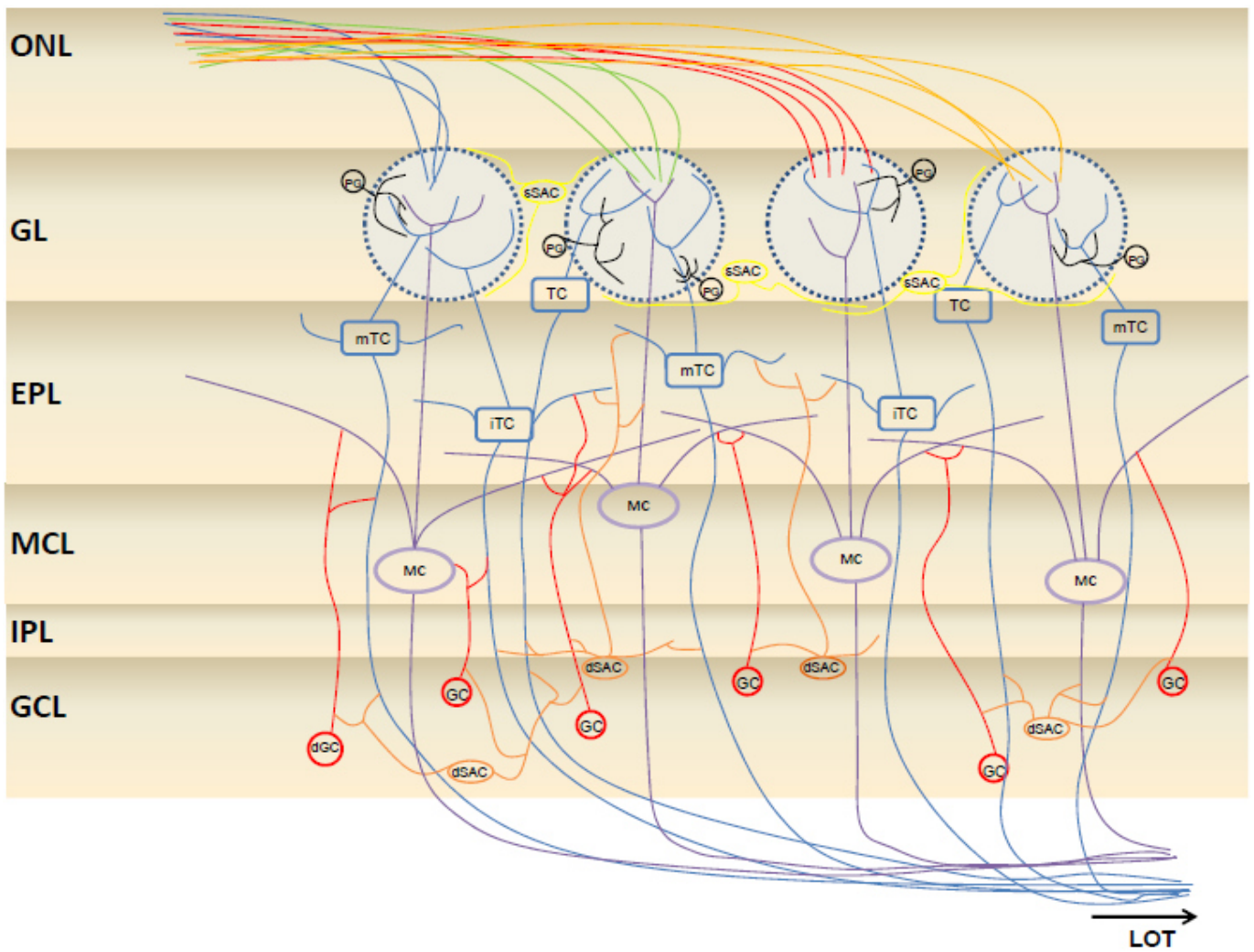
Figure 1. Representation of the olfactory bulb circuitry.
The olfactory bulb is divided in different layers: olfactory nerve layer (ONL), glomerular layer (GL), external plexiform layer (EPL), mitral cell layer (MLC), internal plexiform layer (IPL) and granule cell layer (GCL). In each layer there are different types of neurons. In the GL there are different cell types like periglomerular cells (PG), superficial short-axon cells (dSACs) and tufted cells (TC). In the EPL there are internal (iTC) and medial tufted cells (mTC) as well as projections of the lateral dendrites of mitral cells (MCs). In the MCL there are glutamatergic mitral cells (MCs). In the GCL there are inhibitory granule cells (GC) and deep short axon cells (dSACs), which project onto different layers as the EPL, MCL, IPL and GCL. LOT stands for lateral olfactory tract.

1.3.4. Odor - evoked responses in the MOB

Olfactory information transduced by OSNs is relayed in the glomerular layer, the first level of olfactory processing. At that stage, presynaptic OSN axons synapse with juxtaglomerular cells as well as apical dendrites of TCs and MCs (Imai 2014). Inhibitory periglomerular neurons and SACs modulate TC and MC activity at this synapse and different centrifugal fibers target these interneurons (Ma and Luo 2012). Odor presentation elicits sniffing behavior which, combined with the flow rate, is known to have an impact on the dynamics of glomerular responses (Esclassan, Courtiol et al. 2012) and how this information is relayed to the main glutamatergic neurons in the OB.

As mentioned in the last sections, TCs and MCs share some morphological properties (more detailed in Nagayama et al 2014). Apically, they both receive monoglomerular input since they project dendrites to one glomerulus but still they show different response properties. Moreover, there is evidence that an "olfactory column" in the ipsilateral bulb might target the contralateral bulb forming symmetric odor representations (Imai and Sakano 2008; Yan, Tan et al. 2008). Both TCs and MCs project to higher cortical areas. It has been hypothesized that they could engage in different processes since TCs project specifically to the olfactory tubercle (OT) and anterior olfactory nucleus (AON) while MCs project their axons more broadly to many more olfactory areas (Igarashi, Ieki et al. 2012; Kay 2014). Distributed in different layers, they have different spatio-temporal patterns of activity during basal states or in response to odor stimuli (Kollo, Schmaltz et al. 2014). During resting states both MCs and TCs show activity locked to respiration (Macrides and Chorover 1972; Onoda and Mori 1980). More specifically, TCs fire action potentials during inspiratory periods while MCs show more delayed activity in the transition period between inspiration to expiration. During odor presentation, TCs and MCs maintain respiratory synchronization with increasing odor concentration. TCs show shorter onset latency and respond to lower concentrations than MCs. Thus, MCs and TCs display a complex pattern of cell activity depending on excitatory and inhibitory network input activity (Wellis, Scott et al. 1989; Laurent 1999).

These interactions are mediated by AMPA and NMDA receptors, with NMDARs being of special importance to mediate dendrodendritic inhibition (Isaacson and Strowbridge 1998; Chen, Xiong et al. 2000). Granule cells are known to have key

11

roles in bulbar activity patterns since they modulate glutamatergic neuronal activity synchronizing their temporal patterns (Friedrich and Laurent 2001; Nusser, Kay et al. 2001) and sharpening OB network activity. So far, the function of GCs regarding MCs is well studied at different levels (Wellis and Kauer 1993; Yokoi, Mori et al. 1995; Egger, Svoboda et al. 2003; Egger and Stroh 2009; Abraham, Egger et al. 2010). Nevertheless, many open questions remain, especially how the network is regulated and how it affects odor discrimination. Most studies concerning GC dynamics (as well as MCs) have been performed *in vitro* using acute slices or *in vivo* preparations under anesthesia (Isaacson and Strowbridge 1998; Schoppa, Kinzie et al. 1998; Cang and Isaacson 2003; Egger, Svoboda et al. 2003; Egger, Svoboda et al. 2005; Egger and Urban 2006; Egger and Stroh 2009; Cazakoff, Lau et al. 2014). Studies using awake animals revealed another scenario. In contrast to what is observed in anesthetized animals, GCs are spontaneously more active and responsive to odors making MC odor responses more sparse and temporally dynamic (Rinberg, Koulakov et al. 2006; Kato, Chu et al. 2012; Cazakoff, Lau et al. 2014), probably because a more active GC network might facilitate more lateral interactions between MCs. Moreover, repeated odor presentation can lead to experience-dependent plasticity at the level of mitral cells which is odor specific and recovers gradually over time and can be repeatable with different odors (Kato, Chu et al. 2012). This is in line with what is observed in studies on oscillatory activity and how oscillations evolve after odor learning. Thus, temporal dynamics of the spatially different distributed OB neurons across layers are state-dependent. Their odor-evoked responses depend on their interaction where excitatory and inhibitory neurons process olfactory information which can lead to synaptic plasticity mechanisms and generate oscillatory activity at different frequencies.

1.3.5. <u>Accessory olfactory bulb (AOB)</u>

Communication between individuals is crucial for the survival of the population. Pheromones are chemical substances secreted from the body which can be perceived by another individual of the same species (Wyatt 2003). They are found in many fluids ranging from saliva to vaginal secretions and are known to play an important role in aggression and reproduction. Pheromones are detected by G-protein coupled receptor neurons in the vomeronasal organ (VNO) (Berghard and Buck 1996). Located in the nasal septum, the VNO is a tubular structure enclosed in a cartilaginous capsule that connects to the oral cavities through the narrow duct. Responses of vomeronasal sensory neurons (VSNs) depend on a vascular pumping mechanism of the stimuli into the lumen of the VNO. Once the stimuli are pumped in the VNO, it binds to receptor neurons. So far, two major types of receptor neurons have been identified in the VNO which are thought to detect different types of stimuli. On one hand, there are V1Rs located in the apical layer of the VNO which respond to small volatile chemosignals such as testosterone molecules present in mouse urine. On the other hand, VNO neurons expressing V2Rs are located in the basal layer of the VNO and respond to a wide variety of stimuli such as mouse urine proteins (MUPs), major histocompatibility complex (MHC) peptides and exocrine-gland secretion peptides (ESPs) (Brennan 2010). The VNO neural pathway has a similar architecture as the MOB in terms of OSN projections. VSNs project their axons exclusively to glomerular neuropil in the anterior or posterior AOB depending on their expression of V1Rs or V2Rs, respectively. This input synapses onto mitral cell apical dendrites which in turn project their axons to different cortical regions such the medial amygdala (MeA), posteromedial amygdala (PMCoA), bed nucleus of the stria terminalis (BNST) and bed nucleus of the accessory olfactory tract (BNAOT) reaching at last hypothalamic areas (Gutierrez-Castellanos, Pardo-Bellver et al. 2014). Bulbar and cortical processing of pheromone detection provides behavioral and endocrine outputs that are important for interaction between individuals. So far, the behavior from an individual depends on their environment. Volatile molecules and pheromones provide sensory cues regarding basic needs like feeding, reproduction or aggression behaviors necessary for survival.

1.3.6. Cortico-bulbar feedback projections

Different cortical networks receive direct input from glutamatergic mitral and tufted cells. In turn, there are centrifugal inputs reaching the olfactory bulb which are in their majority glutamatergic and arise mostly from the anterior olfactory nucleus (AON), piriform cortex (PCx) and the entorhinal cortex (ECx). Moreover, it also receives GABAergic, neuromodulatory and hormonal inputs thought to be important during different olfactory behaviors (Apicella, Yuan et al. 2010; Boyd, Sturgill et al. 2012; Ma and Luo 2012; Nunez-Parra, Maurer et al. 2013; Rothermel and Wachowiak 2014; Otazu, Chae et al. 2015). Centrifugal inputs are state-dependent (Boyd, Kato et al. 2015) and are thought to shape sensory processing in the olfactory bulb.

AON feedback projections represent a major source of cortical input to the OB. The AON receives inputs from the OB, but also send projections to olfactory and non-olfactory areas including the anterior piriform cortex, olfactory tubercle, ECx and periamygdaloid cortex from which it also receives feedback projections (Brunjes, Illig et al. 2005; Rothermel and Wachowiak 2014). The AON neural architecture is organized in different zones depending on different cell types and is classified as (1) pars externa, (2) pars medialis and (3) pars ventroposterior, lateralis and dorsalis. Most glutamatergic fibers project to the ipsilateral bulb (pars medialis) and in a minority to the contralateral bulb (pars externa) (Reyher, Schwerdtfeger et al. 1988) showing differences in the distribution of AON fibers (Davis and Macrides 1981; Schoenfeld and Macrides 1984; Shipley and Adamek 1984). AON fibers synapse mostly on interneurons in the granule cell layer and more sparsely in the glomerular layer modulating MC activity disynaptically. Nevertheless, they also synapse monosynaptically on MCs, depolarizing them (Markopoulos, Rokni et al. 2012). Sensory input activates AON feedback projections to both bulbs rapidly, although this activation might be also influenced by interactions with other neuromodulatory centers.

Centrifugal inputs from the PCx, mostly from pyramidal cells in layer II and layer III (Davis and Macrides 1981), also target mainly inhibitory GCs. Moreover, they contact dSACs which inhibit at the same time GCs. Electrical or optogenetic activation of cortico-bulbar projections targeting PG cells and sSACs modulate M/T cells indirectly, suppressing their activity (Nakashima, Mori et al. 1978; Boyd, Sturgill et al. 2012). Still the impact of their activation across layers is unknown since mitral and tufted cells project differently to many cortical areas. So far, top-down inputs from the PCx

are spontaneously active and show exclusively enhanced or suppressed responses to odor presentation, with a small percentage of fibers showing both types of responses independent of the odor concentration (Otazu, Chae et al. 2015).

Sensory information processed in the OB is also modulated by different neuromodulatory systems including serotonergic, cholinergic and noradrenergic projections innervating the OB. Serotonergic projections originating in the dorsal and medial raphe nuclei are known to densely innervate the OB (McLean and Shipley 1987; Steinfeld, Herb et al. 2015; Brunert, Tsuno et al. 2016). They project to inhibitory interneurons in the glomerular layer as well as glutamatergic M/T cells (Liu, Aungst et al. 2012; Schmidt and Strowbridge 2014; Brill, Shao et al. 2016; Kapoor, Provost et al. 2016). The exact mechanism of sensory input modulation by serotonergic fibers is still not fully understood. Nevertheless, activation of serotonergic centrifugal projections suppresses OSNs and activates GABAergic populations in the glomerular layer (Brunert, Tsuno et al. 2016). Besides, it can excite ETCs and it can suppress or enhance odor responses in MCs (Kapoor, Provost et al. 2016). Cholinergic fibers arising from the basal forebrain also modulate OB activity (Devore and Linster 2012). They act on nicotinic and muscarinic receptors in the glomerular and granule cell layers (Heimer, Zahm et al. 1990; Castillo, Carleton et al. 1999; Pressler, Inoue et al. 2007). While nicotinic receptors are found in glomerular and mitral cell layers, muscarinic receptors are found mostly in the granule cell layer showing a distributed segregation across layers. Cholinergic inputs enhance inhibition on periglomerular and mitral cells which affects temporal dynamics of MCs odor responses. The OB integrates as well noradrenergic projections (40%) from the locus coeruleus. These fibers are known to be dense in the granule and internal plexiform layer, being sparse in the glomerular layer (McLean, Shipley et al. 1989). There are three major noradrenaline receptors which are expressed in different bulbar layers. The result of noradrenergic modulation is an enhancement of network excitability at the level of the mitral cells (Devore and Linster 2012). Thus, it is clear that neuromodulation of the olfactory network by serotonin, choline and noradrenaline has a direct impact on sensory perception. While serotonin has diverse effects on early olfactory processing (Kapoor, Provost et al. 2016) and is implicated in reward behavior, choline and noradrenaline are involved in odor discrimination and modulation of signal-to-noise ratio, respectively (Escanilla, Alperin et al. 2012). Moreover, activation of both α and β NE receptors play an important role for discrimination between similar odors (Doucette,

Milder et al. 2007). Granule cells represent the biggest population in the OB and they receive dense cholinergic and noradrenergic fibers which activate them and consequently modulate M/T cells activity. Besides, there are also GABAergic projections arising from the horizontal limb of the diagonal band of Broca (HDB) and magnocellular preoptic area (MCPO) projecting preferentially to the granule cell layer (Gaykema, Luiten et al. 1990; Gracia-Llanes, Crespo et al. 2010). These fibers inhibit granule cells and it has been shown that they have a direct impact on odor discrimination (Nunez-Parra, Maurer et al. 2013).

1.4. <u>Oscillatory activity in the olfactory bulb</u>

 The OB is a complex and dynamic neuronal network. The main OB neurons display neural activity at different frequency bands in the presence or absence of an odor and their activity is correlated to the respiratory rhythm in a basal state. At the single cell level, different neurons in the OB show firing patterns locked to respiration (Cazakoff, Lau et al. 2014). At the population level, different types of measurements such as the electroencephalogram (EEG) or local field potentials (LFPs) revealed the presence of neural oscillatory activity known to be dependent on the behavioral state and to be different across species (Boudreau 1962; Bressler and Freeman 1980; Gelperin and Tank 1990; Kleinfeld, Delaney et al. 1994; Laurent and Davidowitz 1994; Dorries and Kauer 2000; Lam, Cohen et al. 2000; Friedrich and Laurent 2001; Hall and Delaney 2001). Reminiscent of other brain areas, these phenomena reflect synchronized activity from a large population of neurons. Generally they arise from feedback connections between neurons that result in the synchronization of their firing patterns. However, they can also occur in a subthreshold regime which is known to be sufficient to sustain bulbar oscillatory activity (Bathellier, Lagier et al. 2006). Nevertheless, in response to sensory stimuli, changes in the oscillatory activity are reflected as changes in frequency, amplitude or phase resetting. Within the OB, interactions between main glutamatergic cells (MCs and TCs) with GABAergic GCs form a large network that is known to be essential for olfactory processing. A main feature of this network is the presence of slow and fast oscillatory activity. At the level of mitral cells, interactions between different types of oscillations create a phenomenon called theta-gamma coupling which is thought to be crucial for olfactory coding.

Oscillatory activity can be classified in different classes depending on the frequency of the oscillations. The classification I describe below is standard for rodents and might be different for other species. Nevertheless, it is possible that within the literature this classification for oscillations in the rat olfactory bulb might differ a bit in nomenclature. In general, bulbar oscillations are classified in slow oscillatory activity (delta and theta frequencies) and in fast oscillations (beta and gamma frequencies).

1.4.1. Slow oscillatory activity

1.4.1.1 Delta (δ) oscillations

Delta rhythms, also called ultra-slow waves, oscillate at a frequency between 0.5 - 2 Hz and they are considered as a physiological signature for the deepest sleeping states (Fontanini, Spano et al. 2003; Jessberger, Zhong et al. 2016). They are most likely the least studied oscillations in the olfactory bulb since activity at higher frequencies was considered more important in the last decades. So far, their exact function and which specific networks are involved in generating them are still unknown. Nevertheless, it is thought that more superficial layers in the OB are responsible for their generation (Fourcaud-Trocme, Courtiol et al. 2014). They are a biomarker for deep sleeping states where they are locked to respiration maintaining a basal level of activity in the olfactory bulb and consequently in higher cortical areas (Fontanini, Spano et al. 2003). Interestingly, delta activity has been reported to be important for processes such as memory consolidation in the neocortex during slow-wave sleeping states when the breathing rate is relatively slow in contrast to the awake state (Fontanini, Spano et al. 2003; Tsuno, Kashiwadani et al. 2008; Barnes and Wilson 2014). Rodents are mostly olfactory animals and the fact that the olfactory bulb and neocortex showed synchronized activity at this frequency during sleeping states indicates that olfaction might have had an important role during neocortical evolution (Kaas 2005). Besides, there is evidence that suggest that olfactory cortical areas generate top-down inputs to the olfactory bulb to synchronize activity at this frequency (Manabe, Kusumoto-Yoshida et al. 2011), potentially to maintain uninterrupted different cognitive processes during sleeping states. Nevertheless, odor presentation during sleep enhances slow wave activity and reactivates memories while maintaining synchronized activity (Perl, Arzi et al. 2016).

1.4.1.2. Theta (θ) oscillations

Bulbar theta oscillations refer to activity between 4-12Hz and they are also called respiratory oscillations since it has been observed that they follow the respiratory rhythm. As bulbar theta waves are the signature for respiration, changes in the behavioral state might change the respiratory theta rhythm. These changes might affect the way in which this information is carried by other brain areas which receive input from the OB. Nevertheless, during active sampling behaviors, e.g. sniffing, it is still unknown if there is coherence between theta and all sniffing frequencies. It is known that waves at a theta frequency coexist with fast oscillatory activity during normal respiration. At the beginning of one theta wave, which corresponds to the inspiratory phase, there is a slight increase in frequency thought to be caused by glutamatergic tufted cells. At the transition point from inspiration to expiration, it governs activity at a gamma frequency corresponding to the firing of mitral cells followed by the expiration phase in which activity at a beta frequency is predominant (Buonviso, Amat et al. 2003). The circuits involved in its generation have been under debate for many years, since theta rhythm in both olfactory bulb and hippocampal networks matched under some behavioral states (Colgin 2013). In fact, this frequency band is called theta rhythm in the OB similar to the brain area that this frequency oscillation was first observed, the hippocampus. So far, it has been recently shown that theta waves generated in the olfactory bulb closely match in frequency the oscillations observed in the hippocampus. However, a hippocampal theta rhythm independent from respiration is thought to influence activity in the olfactory bulb (Nguyen Chi, Muller et al. 2016). Within the olfactory bulb, glomeruli networks receiving direct input from OSN have been shown to be crucial for theta generation which seems to be confined to this layer (Fourcaud-Trocme, Courtiol et al. 2014). Nevertheless, in this thesis I show evidence that the OB might have all the necessary intrinsic machinery to generate theta rhythms without a respiration-like pattern (for more details see Perez de los Cobos Pallares et al, 2015), similar to what has been demonstrated in hippocampal acute slices (Colgin 2013).

The respiratory rhythm, which is reflected in glomerular activity, is not exclusively dependent on the input stimulus. There are centrifugal inputs from respiratory networks in the brainstem and different neuromodulators that modulate activity in OB neurons (Castillo, Carleton et al. 1999; Devore and Linster 2012; de Almeida, Idiart et

al. 2013; Schmidt and Strowbridge 2014). Moreover, since diverse behavioral states relate to different respiratory rates, inputs at these frequencies might favor synaptic plasticity in the olfactory bulb and it could serve as a model for sensory coupling in multisensory processing (Kay 2005).
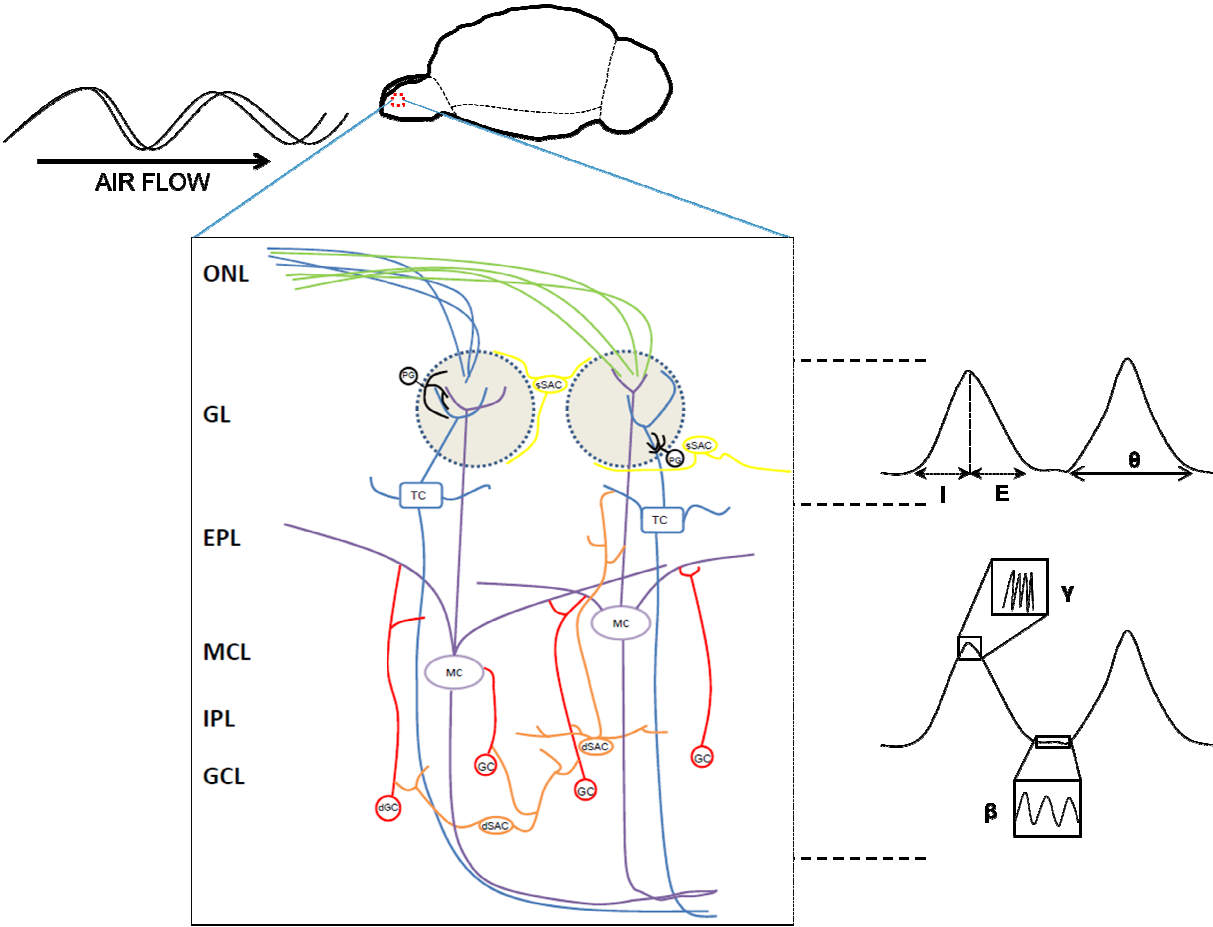
Figure 2. Representation of theta (θ) oscillatory activity in the rat olfactory bulb local field potential.
Bulbar theta oscillations are locked to the respiratory rhythm, where the glomerular circuitry is known to play a key role in their generation. Within the same theta oscillation, it is observed activity at higher frequencies at the transition point between inspiration to exhalation (γ) and during exhalation (β) mediated by deeper layers in the bulb.

1.4.2. <u>Fast oscillations</u>

1.4.2.1. <u>Beta (β) oscillations</u>

Discovered primarily in the early 1990´s in the hippocampus, beta waves oscillating between 15 - 35 Hz have been mostly described in the motor and olfactory systems. They have been observed in the OB and PCx in response to highly volatile molecules as well as during associative learning in odor discrimination tasks (Vanderwolf 1992; Kay 2005; Kay and Beshel 2010; Martin and Ravel 2014). Little is known concerning the circuits involved in their generation. Nevertheless, there is evidence suggesting that beta waves rely on intact loops between the olfactory bulb and higher cortical areas (Neville and Haberly 2003; Martin, Gervais et al. 2006). This statement is based on some studies in which isolation of the OB from the rest of the brain abolishes these oscillations, in contrast to what is observed for gamma oscillatory activity. Within the OB, some studies showed evidence of the implication of different layers in the OB (Fourcaud-Trocme, Courtiol et al. 2014) in generating activity at this frequency range. Interactions between the OB and centrifugal inputs from cortical areas might be crucial for their generation although the exact mechanisms are not fully understood. There are some studies suggesting a network phenomenon in which oscillations at higher frequencies are transformed into waves at a beta frequency (Olufsen, Whittington et al. 2003; Traub, Bibbig et al. 2004). Whereas the functional role of these oscillations is still unknown, there is coherence at this frequency between different olfactory brain areas during odor presentation, suggesting that they might favor temporal coordination of sensory information across brain areas (Varela, Lachaux et al. 2001; Siegel, Donner et al. 2012; Martin and Ravel 2014).

1.4.2.2. Gamma (γ) oscillations

Waves between 40 and 120 Hz are probably the most studied oscillatory events at the level of the olfactory bulb. During eupneic respiratory patterns, they appear at the transition between inspiration and exhalation and although this phase relationship is quite robust, the amplitude and frequency can vary. Gamma oscillations have been classified in two subgroups depending on the frequency, being gamma 1 (60-120 Hz) and gamma 2 (40-60 Hz; also called low-gamma) (Bressler 1988; Kay 2003; Manabe and Mori 2013; Mori, Manabe et al. 2013) which relates to different behaviors (Kay, Beshel et al. 2009). Several studies have shown the importance of the reciprocal dendrodendritic synapse between mitral and granule cells to generate activity at this frequency (Buzsaki and Wang 2012; Fourcaud-Trocme, Courtiol et al. 2014). More specifically, GCs seemed to have a key role since inactivation of the granule cell layer reduced significantly the generation of gamma oscillations (Kay 2014). In contrast to beta oscillations, cutting top-down inputs to the OB causes an increase of gamma activity (Neville and Haberly 2003). Centrifugal input from the piriform cortex contacts mostly GABAergic granule cells, which might interfere with reciprocal connections between mitral and granule cells (Kay, Beshel et al. 2009) desynchronizing local activity. Since gamma oscillations have been observed in bulbar acute slices and also in an OB isolated from the rest of the brain (Buzsaki and Wang 2012), activity at a gamma frequency is suggested to be a local phenomenon. Nevertheless, in vivo recordings show periods of coherence with other higher cortical areas (Kay 2014) and some studies suggest that OB inputs tune the piriform cortex into a proper excitatory state to produce activity at this frequency (Mori, Manabe et al. 2013). So far, the same effect has been observed in the entorhinal cortex (Ahrens and Freeman 2001). Within the OB, the exact circuits generating low-gamma frequencies (gamma 2) are still not fully known.

There are two hypotheses which potentially might give an explanation concerning the generation source of gamma 2. The first one is based on studies with beta3 knockout mice which lack functional GABA-A receptors on olfactory bulb granule cells (Nusser, Kay et al. 2001). These knockout mice show no low - gamma activity, suggesting that local inhibitory circuits might be responsible. The second one claims that TCs and MCs might be responsible for fast and slow gamma activity respectively. This is in line with the observed gamma in the respiratory cycle. TCs fire action potentials early

in the respiratory cycle generating high frequency gamma oscillations while MCs fire action potentials later generating low - gamma frequency activity (Mori, Manabe et al. 2013). Since the main two glutamatergic neurons in the OB project their axons differently to higher cortical areas, this raises the question if gamma and low gamma might code for different odor computation processes. Different behaviors have been related to gamma oscillations. Most described states include fine odor discrimination, exploration or odor association (Kay 2003). Interestingly, in the latter it is shown that when an odor association is learned, new patterns of oscillatory activity associated to the odor appeared and evolved slowly over time into a new pattern as the subject gained more experience (Freeman and Schneider 1982; Di Prisco and Freeman 1985). Based on the observation of lower gamma frequencies during interbreath periods, gamma 2 relates to motionless and grooming behaviors (Kay 2003).
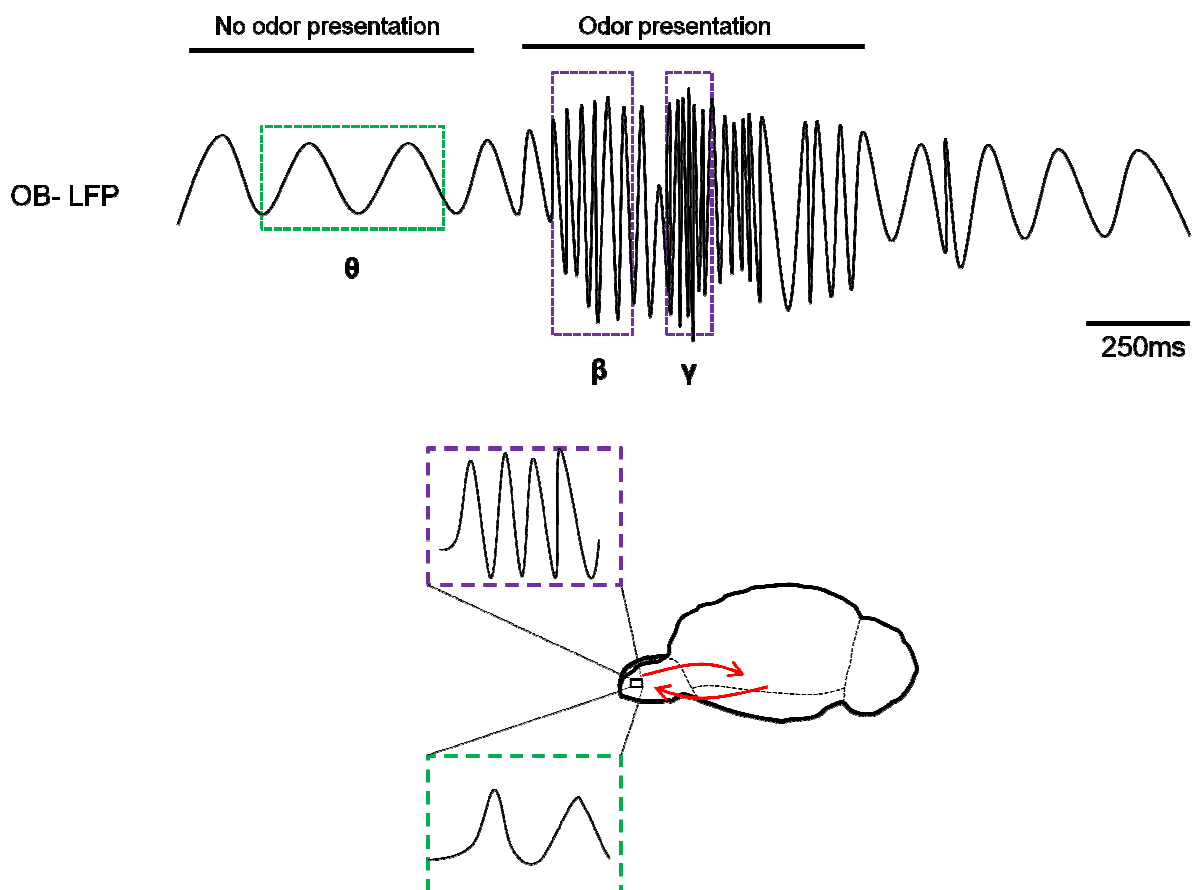

Figure 3. Representation of fast oscillatory activity in the rat olfactory bulb.
Olfactory bulb local field potentials (OB-LFP) reveal activity at a low frequency during respiration in the absence of sensory input (green insets). During odor presentation, oscillatory activity at higher frequencies is predominant at beta (β) and gamma frequencies (γ) (purple insets).

	Nomenclature	Frequency (Hz)	Circuits involved in their generation	Function	Behavioural output
Slow oscillations	Delta	0.5 - 2	Glomeruli networks are thought to be involved	Marker for sleeping states Locked to respiration during sleep Mantainance of cognitive processes during sleep	Slow- wave sleep
	Theta	4 - 12	Interaction between neurons in the glomerular layer	Follow respiration in the awake state. Synchronization with hippocampus.	Resting states Sniffing behaviours Odor learning and memory
Fast oscillations	Beta	15 - 35	Loop networks between the OB and cortical areas Dendrodendritic synapses in the OB	Related to odor responses Temporal coordination of sensory stimulus across brain areas	Odor discrimination Learning association processes
	Gamma Gamma 1 Gamma 2	60 - 120 40 - 60	Local networks in the OB Importance of granule cell layer MC - GC synapse	Related to odor responses Temporal coordination of sensory stimulus across brain areas	Odor discrimination Exploration Odor association Alert Grooming

Table 1. Summarized standard classification of the oscillatory activity in the olfactory bulb.

1.5. Oscillatory activity and synaptic plasticity

As described above, different physiological states show oscillations at different frequencies but also underlie neural plasticity mechanisms. At the level of the olfactory bulb, reciprocal dendrodendritic synapses between MCs and GCs are crucial for odor processing which involves the generation of oscillatory activity. These MC-GC synapses integrate fast and slow components of signaling (Isaacson and Strowbridge 1998), coupling activity at a theta and gamma frequency (theta-gamma coupling) which might be crucial for olfactory coding. Being the most abundant connections in the bulb, they experience changes in their structure, membrane excitability and synapse efficiency leading to neural plasticity, which is related to different processes such as odor memory (Sailor, Valley et al. 2016). Thus, the relation between bulbar oscillatory activity and neural plasticity seems evident. Oscillatory activity in the OB is reminiscent of what is observed in the hippocampus (HPC), where waves at a theta frequency appear during odor-memory tasks and are coherent with the ones observed in the OB. Theta burst stimulation in the HPC is known to elicit long-term potentiation and there is also data suggesting similar plasticity mechanisms in the OB.

In the OB, the synapses from the MC to a GC are glutamatergic while they are GABAergic from the GC to the MC. Glutamate release activates NMDARs and AMPARs. Importantly, the blockade of NMDARs abolishes neural plasticity at this synapse, suggesting the important role of NMDARs to elicit plasticity. Besides, centrifugal inputs from cortical areas and different neuromodulators targeting MCs and GCs might contribute to establish plasticity at this synapse (Pandipati, Gire et al. 2010; Eckmeier and Shea 2014).

1.6. <u>Physiology of respiration</u>

Respiration is an autonomic process controlled by a complex network in the brain. Neural networks located in the pons and medulla oblongata are so-called central pattern generators and their interactions ensure an eupneic respiratory pattern maintaining a proper oxygenation of the body.

1.6.1. <u>Organization of respiratory networks</u>

Respiration is needed for life since it is the first and the last process in a living animal. No matter the situation, respiratory activity links sensory information to motor output. Therefore respiration adapts to most situations showing a big malleability of its neural activity revealing a neural network flexible for physiological and behavioral integration. Breathing is a primal homeostatic process and the neural circuits underlying this function must be stable to be responsible for different challenges affecting O_2, CO_2 and pH levels in the body depending on the individual needs (Feldman, Mitchell et al. 2003; Feldman and Del Negro 2006). Respiratory movements occur automatically in which different muscles are involved. Skeletal muscles are known to be largely related to respiration although the autonomic control of respiration is coupled to smooth muscles. The physical act of respiration is based on inspiratory and expiratory periods. However, the respiratory motor cycle is traditionally divided in three different phases starting with an inspiration (I), followed by a post-inspiration (E1) and finished by a late expiration (E2) (Richter and Spyer 2001). As stated before, different muscles coordinate these phases. So-called pump muscles like the diaphragm and external intercostal muscles control inspiration while others, e.g. abdominal and internal intercostals muscles control expiration (Bianchi and Gestreau 2009). Brainstem motorneurons innervating the oro-pharyngeal area and its respective nerves control these muscles. Some of the cranial nerves are implicated during inspiration to dilate the pharynx (glossopharyngeal nerve, IX CN) or to prevent tongue protrusion (hypoglossal nerve, XII CN). During expiration, constriction of the pharynx is driven by the recurrent laryngeal nerve, a branch of the vagus nerve (X CN). The trigeminal nerve (V CN) is also related to respiration since it innervates most of the face controlling muscles that are also involved in breathing. Most of the

CNs arise from the brainstem where, as described above, some of them control respiration-related muscles.

Respiratory networks located in the brainstem play a key role in breathing control. Neural networks located in the medulla oblongata and the pons constitutes two respiratory centers and their interactions form a functional respiratory network. Medullary respiratory networks are formed by the dorsal respiratory group (DRG) in the nucleus of the solitary tract (NTS) region and the ventral respiratory group (VRG) located in the ventro-lateral medulla which is closely associated with the nucleus ambiguous (NA) (Ballanyi, Onimaru et al. 1999; Bianchi and Gestreau 2009). Moreover, another important respiratory-related area is the pontine respiratory group (PRG) located in the dorso-lateral pons. The PRG consists of a network of neurons distributed in the Kölliker-Fuse (KF) nucleus and the medial parabrachial nucleus. The VRC has the largest mass of respiratory neurons (Alheid, Gray et al. 2002) and is thought to be responsible for rhythm generation. Divided in different "compartments", they are distributed from rostral to caudal in the retropezoid nucleus, the Bötzinger Complex (BötC), the preBötzinger Complex (preBötC), the rostral VRG (rVRG) and the caudal VRG (cVRG) (Alheid, Gray et al. 2002; Feldman and D.R. 2003; Feldman, Mitchell et al. 2003). The neurons forming the last four different groups serve different functions in respiration. The BötC and the cVRG have a population of neurons mostly active during expiration while neurons in the rVRG are predominant in inspiratory periods. The preBötC is formed by a neural population exhibiting inspiratory and expiratory activity thought to be needed for rhythm generation. Therefore, putative neurons in the preBötC are thought to be responsible for the generation of basic respiratory rhythms (Smith, Ellenberger et al. 1991; Ramirez and Richter 1996; Sun, Goodchild et al. 1998; Koshiya and Smith 1999; Guyenet and Wang 2001). Different types of studies support this statement (Schwarzacher, Smith et al. 1995; Alheid, Gray et al. 2002; Wang, Germanson et al. 2002). Besides, rhythmic activity observed in medullary slices including the PreBötC is abolished upon application of CNQX (an AMPA receptor antagonist) (Smith, Ellenberger et al. 1991). More evidence supporting this is that different subsets of neurons in the PreBötzC expressing Neurokinin-1 receptor (NK1R) were identified in *in vitro* and *in vivo* studies to be critical for generation of rhythmic activity (Gray, Rekling et al. 1999; Gray, Janczewski et al. 2001; Guyenet and Wang 2001).

In pontine respiratory networks, the PRG is thought to mediate the total duration of the post-inspiratory phase (Dutschmann and Herbert 2006; Smith, Abdala et al. 2007). Interactions with the DRG and VRG, more specifically from the KF nucleus, are thought to mediate apneic responses associated with protective breath holds such as the diving reflex (Dutschmann and Herbert 1996) coordinating respiratory muscles during respiratory and non-respiratory behaviors (Bianchi and Gestreau 2009). The trigeminal nerve (V CN) is known to be involved in protective responses. Activation of nasal trigeminal afferents (ethmoidal nerve) innervating the nasal mucosa might interact with the PRG to favor these protective responses. Neurons in the parabrachial region are thought to determine respiratory phase transition(Cohen 1971; Cohen and Shaw 2004).

In different scenarios, the respiratory networks need to adapt to a certain situation. Neuroplasticity in respiratory networks could be elicited under several conditions such as hypoxia, abnormal O_2 levels, hypercapnia, sensory denervation, neural injury or conditioning (Millhorn and Eldridge 1986; Baker, Fuller et al. 2001; Gallego, Nsegbe et al. 2001; Carroll 2003; Forster 2003). Serotonergic, dopaminergic or noradrenergic neuromodulation plays an important role in order to maintain neural plasticity in respiratory networks (Mitchell and Johnson 2003) and thus maintain a normal function during diseases, environmental changes or normal development.

Taken together, normal breathing activity depends on excitatory and inhibitory interactions between different regions in the brainstem. These regions of the brainstem receive diverse neuromodulatory inputs under different situations which might favor neural plasticity in respiratory networks. The final outcome of this complex interaction is to maintain proper levels of oxygen in the body to ensure the survival of the animal. Breathing depends directly on information provided by different O_2, CO_2 and pH-sensitive chemoreceptors. While O_2-sensitive chemoreceptors are totally external to the brain located in the carotid bodies, CO_2 and pH-sensitive chemoreceptors, so-called central chemoreceptors, are located both in the carotid bodies and also in major sites within the lower brain (Coates, Li et al. 1993; Bernard, Li et al. 1996; Nattie 1999; Nattie 2000; Ballantyne and Scheid 2001).

1.6.2. Trigeminal-mediated modulation of respiratory networks

Preservation of nasal trigeminal afferents has been crucial in this thesis to study interactions between olfaction and respiration in the absence of midbrain networks. The trigeminal nerve (V cranial nerve) is a sensory motor nerve and it rises in the pons bilaterally forming the trigeminal ganglion. At this point, it splits up into three different nerves: maxillary, mandibulary and ophthalmic nerve. Each one covers different regions across the face. The maxillary and ophthalmic are purely sensory while the mandibulary has sensory and motor functions. The ophthalmic is a sensory nerve that ramifies in the frontal, lacrimal and nasocilliary nerve. The latter branches in the infratrochlear and the anterior ethmoidal nerve. The anterior ethmoidal nerve projects some fibers into the nasal septum providing trigeminal sensation during sensory stimulation (more details in Perez de los Cobos Pallarés et al., 2016; result section).The trigeminal nerve innervates most of the face. Therefore there are trigeminal receptors (TRs) at the main entrances to the body, the nostrils and the mouth (Silver and Maruniak 1981) as well as provides non-visual sensory innervation of the eye (Guzman-Aranguez, Gasull et al. 2014). TRs detect extreme temperatures and potential noxious molecules that can harm the body and prevent us to smell or ingest them. The repertoire of receptors varies from vanillioid receptor 1 (TRPV1), purinergic receptors (P2X), acid-sensing ion channels (ASIC) (also found in mouse OB M/T neurons, see (Li, Liu et al. 2014) and nicotinic acetylcholine receptors (nAChR) (Alimohammadi and Silver 2000; Ichikawa and Sugimoto 2002; Dinh, Groneberg et al. 2003; Silver, Clapp et al. 2006). Nasal trigeminal receptors detect a wide range of chemicals. Some molecules can activate both olfactory and trigeminal receptors in parallel, with the detection threshold for the latter being lower compared to ORs. Thus, potential noxious molecules detected by TRs, relay this information directly onto respiratory networks in order to safeguard the upper ways. Besides detection of harmful molecules, the nasal trigeminal pathway triggers a protective breath hold in mammals when fluid enters the nostrils due to the diving reflex.

1.7. Interaction between odor sensing and respiration

Respiration is an autonomic function known to be coupled to olfaction. Because odorants cannot be detected without movement of air into the nostrils, breathing at different frequencies is crucial for odor sensing (Wachowiak 2011). In the absence of sensory input, nasal airflow itself modulates olfactory bulb activity (Westecker 1970; Delaney and Hall 1996; Rojas-Libano, Frederick et al. 2014) and drives neurons in higher cortical areas such as the hippocampus at the same frequency as in the OB (Nguyen Chi, Muller et al. 2016). Coherence between respiration and olfactory bulb activity has been shown in many LFP recordings (Adrian 1942; Eeckman and Freeman 1990; Buonviso, Amat et al. 2003; Kay 2005; Buonviso, Amat et al. 2006; Rojas-Libano, Frederick et al. 2014). In fact, respiration modulates OB neurons activity having strong effects on olfactory dynamics. Mitral and tufted cells have a temporal firing pattern locked to the inspiration and to the transition period between inspiration and expiration, respectively (Buonviso, Amat et al. 2003). Granule cell activity is also coupled to respiration in the anesthetized state (Ravel, Caille et al. 1987) although in the awake state they are broadly tuned and asynchronous to respiration (Cazakoff, Lau et al. 2014). During odor sampling, rodents exhibit different sniffing behaviors based on changes in frequency and flow rate which is thought to have a direct impact on response dynamics (Courtiol, Amat et al. 2011; Esclassan, Courtiol et al. 2012). Moreover, increases in frequency during sniffing is correlated to increases of the odorant concentration during odor-detection tasks (Youngentob, Mozell et al. 1987), but not when performing an odor-discrimination task (Wesson, Verhagen et al. 2009) since it is known that rodents might be able to accurately discriminate different odor stimuli with a single sniff (Kepecs, Uchida et al. 2006).

1.8. Semi intact preparations

Rodents, as olfactory animals, are excellent animal models to investigate how olfactory neuronal networks function, from the molecular to the neural network level. So far, in the last century research in olfaction has been restricted to two main different approaches. On the one hand, *in vitro* acute slices have been widely used in electrophysiological studies despite of their reduced connectivity, and lack the possibility of natural odor stimulation. On the other hand, *in vivo* studies have own ethical concerns, the access to the bulb is limited to the dorsal side and they are restricted by the use of anesthesia and its effects on cell properties (Kato, Chu et al. 2012; Li, Zhang et al. 2012).

Semi intact preparations represent a potential good alternative for research that circumvents many of these problems. Within this thesis, I present a novel semi-intact preparation based on previously described perfused preparations in order to study olfaction combined with respiration. To understand how this preparation was developed and its innovative features, it is necessary to describe the most representative developments of other *en bloc* and *in situ* preparations in the last 35 years. Briefly, in the 1980s, the workgroup of M. Sugimori (Llinas, Yarom et al. 1981; Llinas and Muhlethaler 1988) used an isolated and perfused mammalian brain in vitro for the first time to study electrical activity of brainstem networks. Since then, different types of preparations have been developed. E.g. in the mid 1990s, a frog preparation with a functionally intact olfactory pathway was used to study odor-evoked oscillatory activity (Delaney and Hall 1996). At around the same time, a working heart-brainstem preparation of the mouse was developed to study synaptic and cellular mechanisms within the medulla that regulate cardio-respiratory activity (Paton 1996). This development is crucial for the characterization of eupneic inspiratory events recorded via the phrenic nerve which is different compared to other events, e.g. gasping. Later, in the 2000s, the first whole brain preparation in mammals (guinea-pig) with an intact olfactory pathway was developed (Ishikawa, Sato et al. 2007). Few years later, we developed the first perfused nose-olfactory bulb brainstem preparation (NOBBP) of the rat.

The innovation of this preparation is that it is the first semi intact preparation developed in rat (as described in Paton 1996) which, in the absence of cortico-limbic networks, maintains an *in vivo*-like intact olfactory pathway. Furthermore, preservation of

the respiratory network allows to study interactions between odor sensing and respiration simultaneously. New features characterizing this preparation in contrast to previous described preparations are for instance the removal of different organs such as the lungs or the heart to avoid mechanical and electrical artifacts. Last, the stability of this preparation is monitored based on the characterization of spontaneous inspiratory activity and the ability of recording odor-evoked responses over time with direct nasal stimulation. The reappearance of spontaneous inspiratory activity is achieved by tuning different variables like the perfusion flow rate of the preparation. This challenging process is defined by the age and size of the animal as well as the physiological performance of the preparation.

2. Aims of the thesis

Research in olfactory neuronal processing is mostly restricted to *in vivo* or *in vitro* acute slices preparations. Nevertheless, in the last decade, awake head - fixed animal preparations became more popular. Within this thesis I present a new *in vitro* technique that represents a good alternative to study bulbar networks at the first stage of olfactory processing. The difficulties shown within *in vitro* and *in vivo* approaches led to one of the main aims of this thesis: to develop and stablish a semi-intact preparation based on previous described preparations (Aim 1). The novelty of this preparation is that in the absence of the midbrain, it has an intact olfactory pathway as well as a preserved respiratory brainstem. The lack of use of anesthesia, the fast performance of the surgery, and the stability of the preparation makes it a good alternative for research in the olfactory field. The preservation of the olfactory bulb (OB) and the brainstem (BS) allow for simultaneous recordings of OB activity and inspiratory activity via the phrenic nerve. Evidence of the stability and functionality of the preparation to record odor-evoked field potentials and multi-unit activity as well as to study bulbar oscillatory activity is reflected in the publication *Pérez de los Cobos Pallarés et al., 2015*.

This preparation allows to study oscillatory activity in the olfactory bulb (Aim 2), showing spontaneous slow frequency activity during baseline and high frequency activity during odor presentation (*Pérez de los Cobos Pallarés et al., 2015).*

As olfaction and respiration are directly coupled, I was also interested in investigating interactions between odor sensing and respiration (Aim 3). Modulation of respiration has been thought to depend on cortico-limbic networks. Preservation of nasal trigeminal afferents irrigating the nasal mucosa allowed to investigate these interactions in the absence of cortico-limbic networks. The trigeminal nerve (V cranial nerve) has receptors in the nasal mucosa that connect directly to the brainstem, where it interacts with respiratory networks. Inspiratory recordings from the phrenic nerve reflected trigeminal modulation of respiratory networks during odor presentation. Faster phrenic bursts compared to eupneic inspiration, similar to putative sniffing, shed light on a potential influence of the trigeminal pathway on the generation of sniffing-like behaviors (Perez de Los Cobos Pallares, Bautista et al. 2016).

Oscillatory and synaptic plasticity events are correlated. Thus, in a side project I demonstrated in olfactory bulb acute slices that electrical inputs combining fast and slow components, as occurring in oscillatory activity, can lead to bulbar neural plasticity. For this study, different stimulation paradigms were tested, such single sniff or theta-gamma coupling (Chatterjee et al 2016).

3. List of publications

3.1. <u>An arterially perfused nose-olfactory bulb preparation of the rat.</u>

F.P.d.l.C.P., D.S., D.F., M.D., and V.E. conception and design of research; F.P.d.l.C.P. and M.D. performed experiments; F.P.d.l.C.P., M.D., and V.E. analyzed data; F.P.d.l.C.P., M.D., and V.E. interpreted results of experiments; F.P.d.l.C.P., M.D., and V.E. prepared figures; F.P.d.l.C.P., M.D., and V.E. drafted manuscript; F.P.d.l.C.P., D.F., M.D., and V.E. edited and revised manuscript; F.P.d.l.C.P., M.D., and V.E. approved final version of manuscript.

An arterially perfused nose-olfactory bulb preparation of the rat

Fernando Pérez de los Cobos Pallarés,[1,2] Davor Stanić,[3] David Farmer,[3] Mathias Dutschmann,[3] and Veronica Egger[1,2]

[1]*Systems Neurobiology, Department of Biology II, Ludwigs-Maximilians-Universität München, Martinsried, Germany;*
[2]*Neurophysiology, Zoological Institute, Regensburg University, Regensburg, Germany; and* [3]*Florey Institute of Neuroscience and Mental Health, University of Melbourne Victoria, Melbourne, Victoria, Australia*

Pérez de los Cobos Pallarés F, Stanić D, Farmer D, Dutschmann M, Egger V. An arterially perfused nose-olfactory bulb preparation of the rat. *J Neurophysiol* 114: 2033–2042, 2015. First published June 24, 2015; doi:10.1152/jn.01048.2014.—A main feature of the mammalian olfactory bulb network is the presence of various rhythmic activities, in particular, gamma, beta, and theta oscillations, with the latter coupled to the respiratory rhythm. Interactions between those oscillations as well as the spatial distribution of network activation are likely to determine olfactory coding. Here, we describe a novel semi-intact perfused nose-olfactory bulb-brain stem preparation in rats with both a preserved olfactory epithelium and brain stem, which could be particularly suitable for the study of oscillatory activity and spatial odor mapping within the olfactory bulb, in particular, in hitherto inaccessible locations. In the perfused olfactory bulb, we observed robust spontaneous oscillations, mostly in the theta range. Odor application resulted in an increase in oscillatory power in higher frequency ranges, stimulus-locked local field potentials, and excitation or inhibition of individual bulbar neurons, similar to odor responses reported from in vivo recordings. Thus our method constitutes the first viable in situ preparation of a mammalian system that uses airborne odor stimuli and preserves these characteristic features of odor processing. This preparation will allow the use of highly invasive experimental procedures and the application of techniques such as patch-clamp recording, high-resolution imaging, and optogenetics within the entire olfactory bulb.

neural oscillation; theta rhythm; olfactory bulb; odor coding; brain stem

IN MAMMALS, ODORANTS INTERACT with receptors on the cilia of olfactory sensory neurons located in the olfactory epithelium. All olfactory sensory neurons that express the same olfactory receptor have axonal projections onto one or several specific glomeruli in the olfactory bulb (Mombaerts et al. 1996). Here, the axons connect directly or disynaptically to glutamatergic mitral and tufted cells (Gire et al. 2012; Najac et al. 2011) for which axons in turn project into higher structures such as the olfactory cortex. The first steps of odor processing in the olfactory bulb are performed within at least two elaborate networks that involve complex synaptic interactions between *1*) mitral and tufted cell apical dendritic tufts and diverse subtypes of periglomerular neurons within the glomerular layer and *2*) mitral and tufted cell lateral dendrites with inhibitory granule cells within the external plexiform layer (Aungst et al. 2003; Shepherd and Greer 1990).

A main feature of these networks is the presence of oscillatory activity, in both the fast gamma and slow theta range, with the latter known to be coupled to the respiratory rhythm (e.g., Adrian 1950; Bressler 1987; Buonviso et al. 1992; Chaput and Holley 1980; Freeman and Schneider 1982; Macrides and Chorover 1972; Margrie et al. 2001; Onoda and Mori 1980; Rubin and Katz 1999; Spors and Grinvald 2002). Whereas the origin of theta oscillations is more associated with the glomerular layer network (e.g., Fukunaga et al. 2014; Schoppa and Westbrook 2001; Wachowiak and Shipley 2006), faster oscillations emerge from local dendrodendritic interactions between mitral cells and granule cells in the case of gamma oscillations (Fukunaga et al. 2014; Lagier et al. 2004; Schoppa 2006). Top-down inputs to the external plexiform layer drive beta oscillations (Chabaud et al. 2000; Fourcaud-Trocmé et al. 2014; Neville and Haberly 2003). During odor sensing, slow and fast oscillations can interact within individual mitral cells, a phenomenon called theta-gamma coupling that also occurs in hippocampal networks (Buzsáki and Draguhn 2004; Lisman 2005). This interaction governs the spiking activity of mitral cells and is thought to be crucial for olfactory coding (e.g., Cang and Isaacson 2003; Margrie and Schaefer 2003).

These mechanisms of network odor processing are difficult to investigate in vivo due to movement artifacts, limitation of access to the dorsal side of the olfactory bulb, and interference with anesthesia (e.g., Kato et al. 2012; Li et al. 2012). To address these issues, in situ isolated and perfused whole brain preparations have been used since early in the 1980s, when whole brain preparations of guinea pigs and frogs were developed to study olfactory networks (Alonso et al. 1990; de Curtis et al. 1991; Delaney and Hall 1996; Ishikawa et al. 2007; Llinás et al. 1981; Mühlethaler et al. 1993). Because of ethical issues associated with whole brain approaches in vitro as well as experimental limitations (e.g., tissue hypoxia), such preparations did not become popular. Alternative in vitro techniques such as acute brain slices offer only limited possibilities to investigate oscillatory activity due to the severe reduction of network connectivity and of course do not allow for physiological stimulation. Oscillations in bulb slices are dampened after a few cycles when triggered by electrical stimulation of the sensory afferents (Carlson et al. 2000; Friedman and Strowbridge 2003; Lagier et al. 2004; Schoppa and Westbrook 2001) or require pharmacological stimulation such as perfusion with NMDA to persist (Schoppa and Westbrook 2001).

Here, we present a novel in situ technique that circumvents these problems. Our method is based on established techniques for studying autonomic brain-stem function (Paton 1996). We demonstrate that in this preparation the olfactory bulb can be

reliably perfused via the ophthalmic artery and thus kept viable, allowing for detection of odor responses and oscillatory activity. Potential applications of the preparation include investigations of rhythmic neuronal activity and interactions between odor sensing and respiration. Odor mapping within a large spatial range is also possible due to the accessibility of wide parts of the bulbar surface. Since the preparation is decerebrated, there are fewer ethical concerns compared with in vivo or whole brain approaches. This technique thus complements established in vivo and in vitro methods.

METHODS

All experiments were approved in accordance with the stipulations of the German law governing animal welfare (Tierschutzgesetz). Figure 1A shows a schematic representation of the preparation and experimental setup.

The perfused olfactory bulb-brain stem preparation. As described previously (Paton 1996), juvenile Wistar rats (*postnatal days 17–21*) were deeply anesthetized with isoflurane (1-chloro-2,2,2-trifluoro-ethyl difluoromethyl ether; Abbott, Wiesbaden, Germany). As soon as the animal failed to respond to tail pinch, it was transected caudal to the diaphragm and transferred into an ice-cooled chamber filled with artificial cerebrospinal fluid (ACSF; in mM: 1.25 $MgSO_4 \cdot 7HO_2$, 1.25 KH_2PO_4, 3 KCl, 125 NaCl, 25 $NaHCO_3$, 2.5 $CaCl_2 \cdot 2H_2O$, 10 D-glucose). The lower body was discarded. The animal was decerebrated at the precollicular level, and the skull was opened. The forebrain was entirely removed by suction, leaving intact solely the olfactory bulb. To ensure the anatomic integrity of the olfactory bulb, remaining small adjacent fragments of the piriform cortex and the brain stem were left untouched. After removing both lungs, the dorsal left phrenic nerve was isolated from the pericardial sac and cut at the level of the diaphragm to record subsequently the respiratory (inspiratory) activity (Paton 1996). To prevent mechanical and electrical artifacts, the heart was removed after previous ligation of the major ascending arteries with suture (for details, see Dutschmann et al. 2009). The descending aorta was then isolated from the spinal cord. Next, the preparation was transferred to the recording chamber, and the descending aorta was cannulated (ø 0.8×38 mm; B. Braun Melsungen). The preparation was perfused via the aorta with ACSF containing 1.25% Ficoll PM 70 (sucrose-polymer; Sigma) to provide oncotic
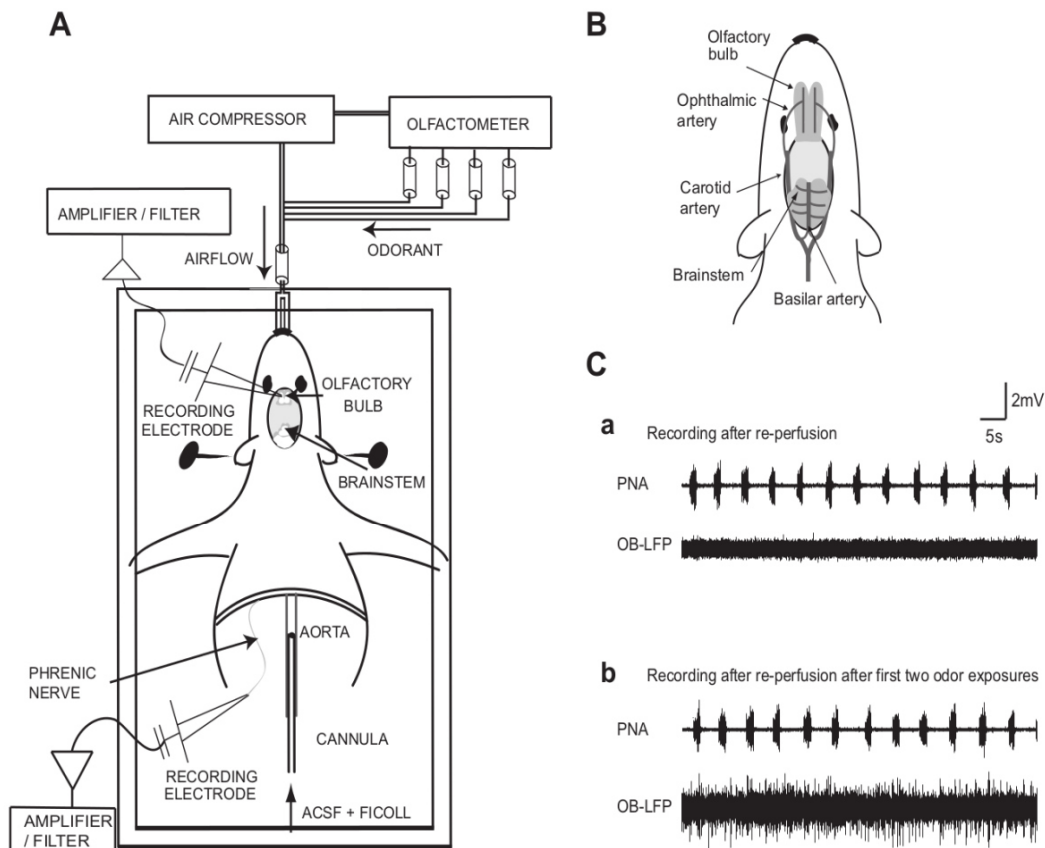

Fig. 1. Schematic depiction of the perfused nose-olfactory bulb-brain stem preparation and "resuscitation" of network activity. *A*: the entire preparation was perfused via the cannulated descending aorta. Odor application was performed via a computer-controlled olfactometer, whereas odor-evoked LFPs or multiunit activity (MUA) were recorded from the olfactory bulb. In parallel, the activity of the respiratory brain stem was monitored via phrenic nerve activity (PNA) recording. ACSF, artificial cerebrospinal fluid. *B*: the diagram shows the main blood vessels that supply the olfactory bulb and the brain stem. The perfusion of the preparation allows for the oxygenation of the olfactory bulb via the intact ophthalmic artery, whereas the brain stem is oxygenated via the basilar artery. *C*: sensory activation of the olfactory network in the initial phase. Representative experiment. *a*: Thirty minutes after the start of the arterial perfusion of the olfactory bulb-brain stem preparation: a stable and rhythmic PNA was observed, however, little or no spontaneous activity was present within olfactory bulb local field potentials (OB-LFP) at this stage. *b*: On 2 successive odor applications (20 s each), spontaneous activity emerged in the OB-LFP, whereas PNA remained stable (recorded 50 min after start of perfusion).

37

pressure during experiments using a peristaltic pump (Watson-Marlow 520S). Its flow rate ranged from 23 to 28 ml/min and was adjusted according to the age and size of the animal, and perfusion pressure was maintained at 70–90 mmHg (Paton 1996). The perfusate was continuously gassed with carbogen (95% O_2-5% CO_2) and warmed to a temperature of 30°C. To ensure optimal perfusion of the brain stem and olfactory bulb, major arteries and veins were ligated with suture as they enter or exit the heart. The phrenic nerve was aspirated with

a suction electrode. Whereas the olfactory bulb was oxygenated via the ophthalmic artery, the brain stem was oxygenated via the basilar artery, both via cannulation of the aorta (see Fig. 1, *A* and *B*). Adjacent fragments of the piriform cortex are likely to have suffered from hypoxia since the branches of the middle brain artery supplying the anterior part of the piriform cortex (the corticostriate artery) were also removed by suction (Scremin 2004). Thus any cortical feedback to the olfactory bulb is highly unlikely to have occurred.

After a few minutes of perfusion, respiratory movements appeared, and spontaneous, rhythmic activity in the phrenic nerve was observed. The neuromuscular blocker vecuronium bromide (0.3 μg/ml; Sigma) was added to the perfusate to prevent movement artifacts. The viability of the preparation was determined by observation of a pattern of phrenic nerve discharge resembling eupnoea (Dutschmann et al. 2000; Paton 1996; see below).

Odor application. Preparations were stimulated with several non-diluted fragrant oils (menthol, JHP Rödler, Ulm, Germany; lavender and rose, TAOASIS, Bielefeld, Germany) using a four-channel, computer-controlled olfactometer that produced a constant forward airflow of 70 ml/min during each stimulus delivery only and otherwise applied backward suction with the same (then negative) pressure (KNOSYS Olfactometers). Exposure of the olfactory epithelium to odorants was achieved via cannulation of the nasal cavities using a custom-made set of small adaptors for the nostrils (1- to 3-mm diameter range). The duration of odor stimulation was variable (5–40 s).

Recording phrenic nerve activity, local field potentials, and multiunits in the olfactory bulb. The phrenic nerve activity (PNA) was recorded via suction electrodes with a silver wire (ESW-F20P; Warner Instruments), digitized, and displayed via a PowerLab 26T data acquisition device (ADInstruments). For recording of olfactory bulb activity, we used glass microelectrodes filled with 2 M NaCl. For local field potential (LFP) recordings, the electrode tips were adjusted to an electrical resistance of 0.5–2 MΩ. For multiunit recordings, the electrode resistance was 6–10 MΩ. Recordings were usually performed in the deeper layers of the dorsal olfactory bulb, well below the glomerular layer. Phrenic nerve and olfactory bulb activity was sampled at 10 kHz, amplified, and band-pass filtered (PNA: low pass 5 kHz, high pass 100 Hz; olfactory bulb activity: low pass 3 kHz, high pass 300 Hz; DP-311 Differential Amplifier; Warner Instruments).

Data analysis. For the analysis and offline filtering of raw data, we used LabChart software (version 7.2; ADInstruments). Integration of PNA and olfactory bulb activity was performed with a decay time constant of 100 ms. For Fourier analysis of the frequency domains of spontaneous olfactory bulb oscillations, we used IGOR software (WaveMetrics). From each preparation, LFP data were filtered and analyzed within a randomly selected time window of 50–60 s. If the resulting peaks in the Fourier transform of an interval were at least twofold in amplitude above background level, the power amplitudes were measured and normalized to the largest peak, resulting in a set of main frequencies and their relative powers. These frequency peak
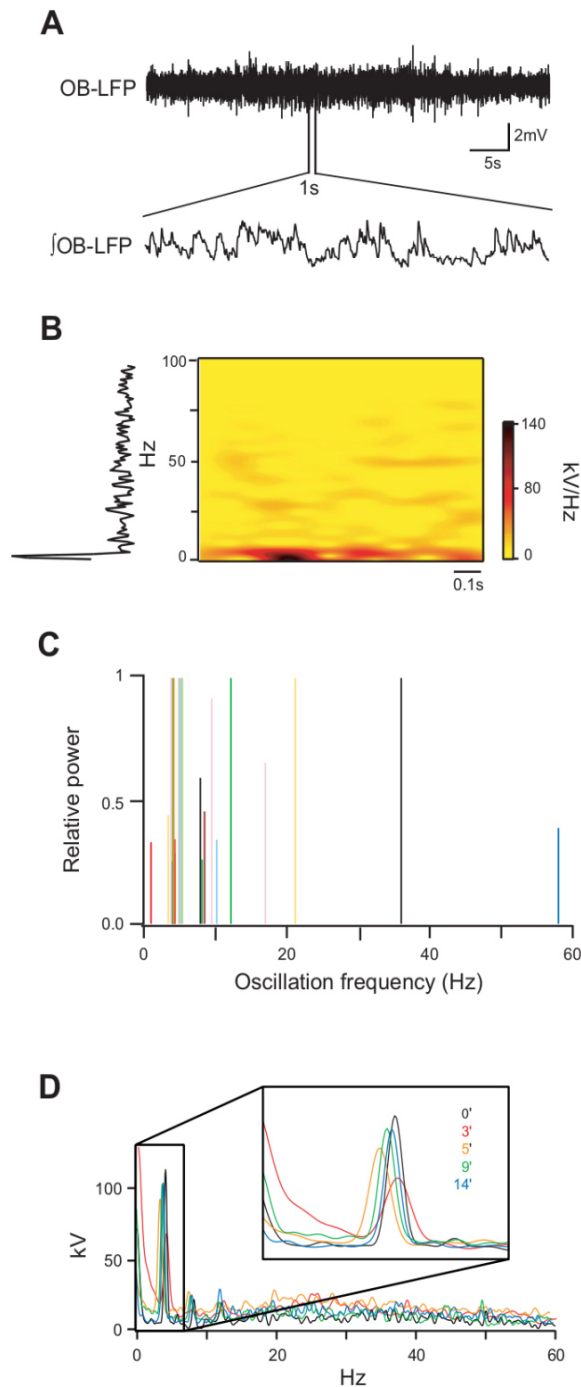

Fig. 2. Slow oscillatory activity recorded in the olfactory bulb mitral and granule cell layers. *A*: representative experiment. The upper trace shows OB-LFP during baseline in an individual experiment, and the lower trace shows the integrated OB-LFP in a short time interval. *B*: representative sonogram calculated from the integrated OB-LFP shown in the bottom of *A*. The Fourier transform of the entire trace is shown in vertical direction on the left side. *C*: cumulative distribution of main spectral peaks collected from individual Fourier analyses of spontaneous olfactory bulb oscillations recorded in 10 preparations. Peak amplitudes of the 10 Fourier spectra sampled from the individual experiments were thresholded and normalized to the largest peak (see METHODS). A different color was assigned to each experiment. Mean frequency 13 $\pm$ 15 Hz, median 7 Hz (n = 22 components $\geq$ 1 Hz). *D*: stationarity analysis within a single preparation in the presence of slow spontaneous oscillations. Five random time windows 20 s each, time of recording in minutes indicated in *inset*, total analyzed duration 15 min.

38

data sets from each preparation were then collated and graphed (Fig. 2C). We also performed stationarity analysis to determine the variability of peak frequencies within each experiment using time windows of 20 s, randomly selected from a recording period of 15 min (Fig. 2D).

To perform time-frequency analysis, we also used IGOR software. Sonograms were plotted from filtered raw data using the Gabor method. A spectrum was generated from every 10 data points with a frequency resolution of 10 Hz. The resulting sonogram was optimized using the IGOR Image Processor.

Spike sorting was performed using ADInstruments software (LabChart 7.4, additional module Spike Histogram; Fig. 5). Raw data were filtered using a median filter with a box width of 11 points. All spikes with amplitudes above a threshold of 0.25 mV from baseline were included for analysis. Detected action potentials were associated with putative individual neurons depending on their overall shape parameters, including slope, amplitude, and width.

RESULTS

In the present study, we demonstrate that the olfactory bulb of the decorticated and precollicularly decerebrated preparation (Fig. 1A) can be arterially perfused via the descending aorta and the carotid arteries that branch into the ophthalmic artery (Fig. 1B). The ophthalmic artery provides the main blood supply for the olfactory bulb (Green 1955). Thus the anatomic integrity of olfactory axons innervating the perfused olfactory bulb allows for studies of odor processing in situ.
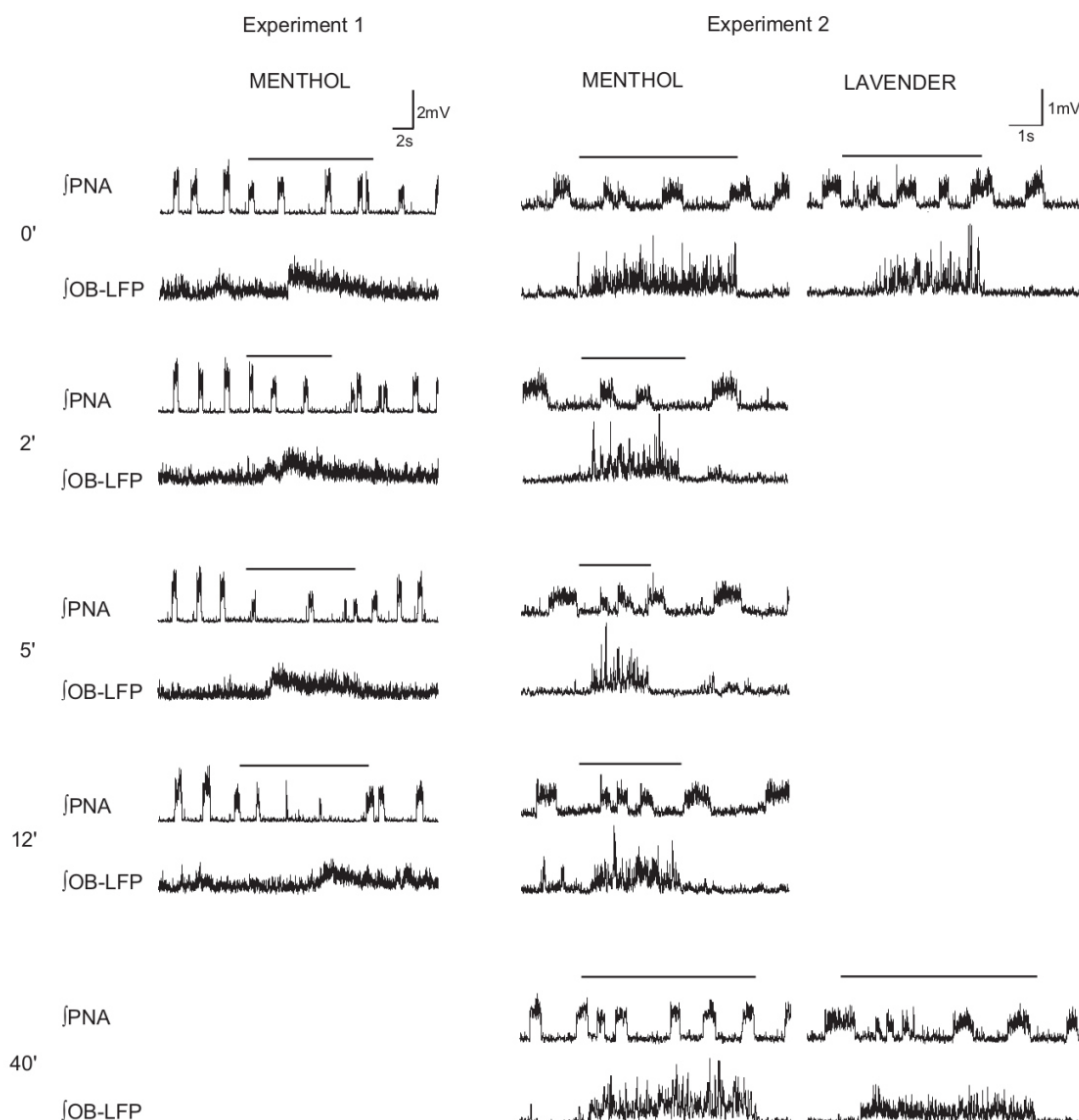
Fig. 3. Intertrial stability of odor-evoked LFPs in the olfactory bulb in situ. Evoked LFPs on stimulation of the olfactory epithelium with menthol and lavender from 2 different preparations at different time points as indicated on the very left side (in minutes). The upper traces show the ongoing integrated PNA during odor exposure, and the lower traces the simultaneously recorded integrated olfactory bulb field potentials. The duration of odor stimulation is indicated by the horizontal bars above the traces. Note that the duration of stimulation was different across recordings.

General methodology. After the surgical procedures, the olfactory bulb-brain stem preparation was reperfused, and perfusion pressure and flow rates were adjusted to generate an eupnea-like discharge pattern (ramping discharge of 1-s duration) of PNA at a frequency range of 13–20 bursts per minute (average rate 16 ± 3 bursts per minute, $n = 9$ preparations). This activity indicates the successful resuscitation of the respiratory pattern generator and shows that the brain-stem circuitry is sufficiently perfused (Dutschmann et al. 2000; Paton 1996; Wilson et al. 2001). LFP recordings obtained from deeper layers of the olfactory bulb 10–15 min after successful resuscitation of the brain-stem circuits showed negligible spontaneous oscillatory or tonic activity (Fig. 1C). However, a profound increase in activity levels was observed after 1–2 extended exposures (duration 10–20 s) to olfactometer output containing any type of odor from our odor set (menthol, rose, and lavender) or plain room air.

In some preparations, the initial adjustment of brain-stem perfusion failed, and thus the rhythmic PNA could not be recorded. Stimulus-locked LFPs in the olfactory bulb could still be evoked by exposure to odor in these preparations ($n = 12$ preparations, data not shown). However, none of these preparations showed the increase in spontaneous activity after sensory stimulation described above. Moreover, none of them showed the spontaneous oscillations in the theta range described below. These observations suggest that the restoration of spontaneous, rhythmic PNA is a key indicator of proper network function also within the perfused olfactory bulb preparation.

Spontaneous oscillatory activity of the olfactory bulb in situ. Spontaneous oscillatory activity in the perfused olfactory bulb in situ was investigated in 10 preparations, with the LFP recordings located at least as deep as the mitral cell layer. We consistently observed ongoing spontaneous oscillations (Fig. 2, A and B). Fourier analysis of the frequency range of oscillatory olfactory bulb activity (Fig. 2, B and C; see METHODS) revealed distinct peaks between 4 and 10 Hz in all of these preparations except for 1; in 3 preparations, there were also pronounced spontaneous oscillations at higher frequencies (20–60 Hz). The stability of theta oscillations was evident from stationarity analysis of the oscillatory activity at different time intervals within the same preparation that showed closely overlapping peaks in the Fourier analysis (Fig. 2D). Changes in perfusate temperature from 30°C up to physiological levels (36°C) or down to 25°C caused increases and decreases in the frequencies of both PNA and olfactory bulb theta activity, respectively ($n = 3$ preparations, data not shown) but did not suppress oscillatory activity.

Odor-evoked LFPs and oscillatory activity. LFP recordings in the deeper layers of the perfused olfactory bulb revealed robust responses to menthol, lavender, and rose oil applied via a four-channel, computer-controlled olfactometer. In $n = 21$ preparations, odor application triggered stimulus-locked and reproducible LFPs, as exemplified in Fig. 3. In total, we recorded $n = 189$ evoked LFP responses (menthol $n = 108$; lavender $n = 41$; roses $n = 40$).

The probability of obtaining an odor-evoked response in a given preparation with functional PNA was 76% (evaluated across $n = 10$ preparations).

The recordings shown in Fig. 3 also demonstrate that odor responses at a given location were not only reproducible from one recording to the next, but also stable over an extended

period of time (40 min). In some preparations, odor responses were detectable for up to 4 h (data not shown).

In accordance with the literature (Buonviso et al. 2003; Martin and Ravel 2014), spectral analysis of LFPs in the perfused olfactory bulb showed a marked increase in power at frequencies between 1 and 100 Hz during odor stimulation compared with baseline (example shown in Fig. 4, A and B), which was observed for each of 12 analyzed odor responses (from $n = 10$ different preparations).

Odor-evoked single-cell responses. Multiunit activity (MUA) recordings were obtained at the level of the mitral cell layer or below (depth ≥ 500 μm) and thus most likely reflect mitral

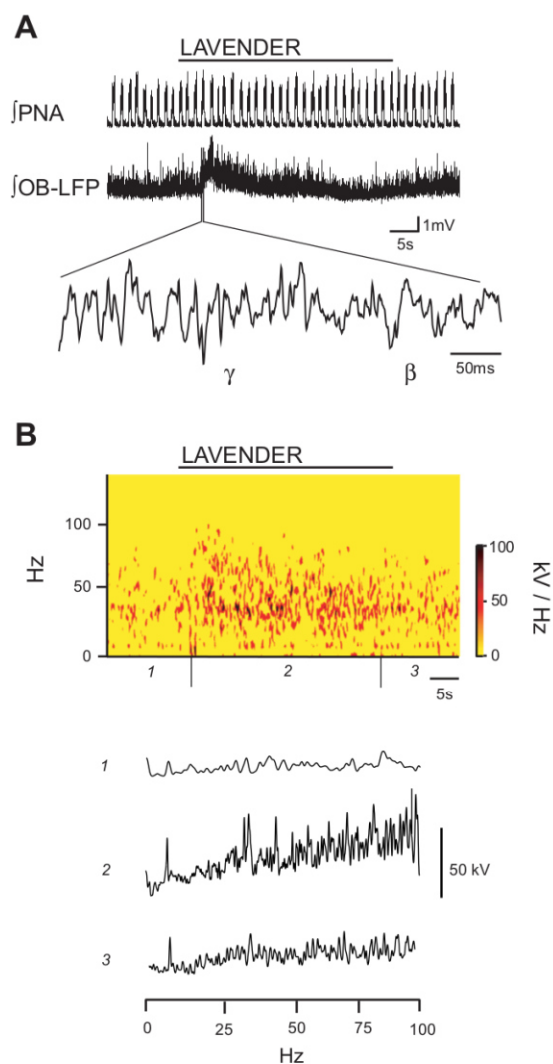
Fig. 4. Odor-evoked responses exhibit oscillatory activity at higher frequencies. A: representative experiment. Odor stimulation triggering responses in the olfactory bulb show oscillatory activity in the beta and gamma frequency ranges. B: sonogram calculated from A. Below, the Fourier analyses for the intervals before stimulation (1), during odor stimulation (2), and afterward (3) are shown.

and/or granule cell activity. Reponses to odor stimulation could be reliably detected in most preparations tested ($n = 122$ responses in 10 preparations). The MUA recordings clearly displayed different response types of individual neurons to odor application. Most MUA recordings revealed a strong stimulus-locked excitation of neurons that were silent during baseline ($n = 84$ recordings; see Fig. 5, *A* and *B*), whereas other tonically active units showed stimulus-dependent inhibition ($n = 38$ recordings; see Fig. 5*C*). Both types of responses

were observed for all odorants. Spike sorting analysis also revealed OFF responses of individual neurons in one of these recording sites with an onset right after odor application and a duration of a few seconds (Fig. 5*B*). Other neurons became tonically active after or during odor stimulation (e.g., Fig. 5*A*).

Control experiments: trigeminal stimulation and room air stimulation. Previous studies showed that stimulation of trigeminal afferents (i.e., the ethmoidal nerve) of the nasal mucosa can trigger profound reflex responses such as the
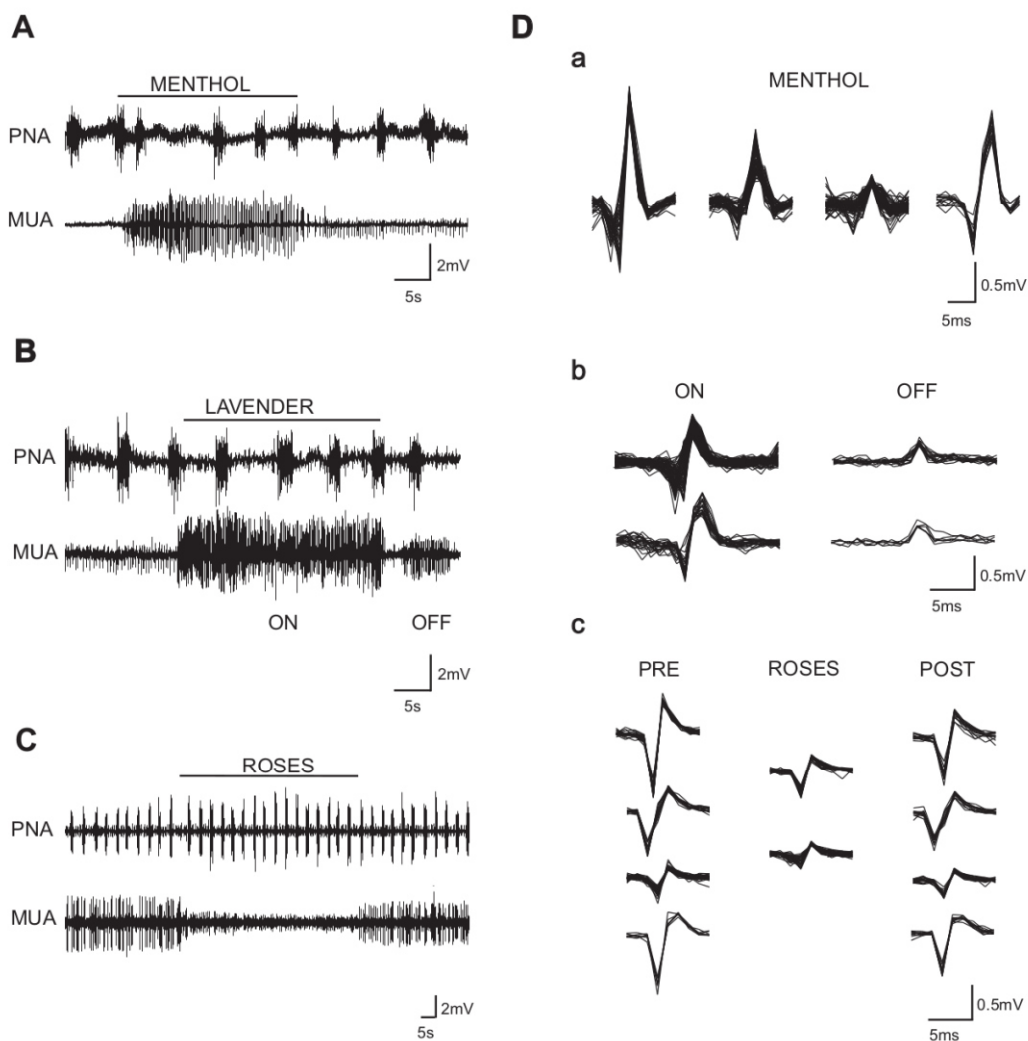

Fig. 5. Multiunit recordings of evoked olfactory bulb neuron responses. MUA recordings were obtained for various odorants (menthol, lavender, and roses); data shown are from 2 different preparations. Please note the transient response of PNA to the trigeminal odor menthol in *A*. *A* and *B*: evoked excitatory responses of neurons that were silent before stimulation; responses to both odorants in the same location. The recordings show excitation of several individual neurons. In *A*, a unit with small action potential amplitude remained active after menthol exposure. *B*: after the end of exposure to lavender, a unit became spontaneously active for ~5 s. This could also be explained as an OFF response (see DISCUSSION). Repetitive odor stimulation yielded similar responses at this site ($n = 9$). *C*: evoked inhibition of neuronal activity at a different recording site. Note that the dominant tonically firing neurons showed clear odor-evoked inhibition. The low amplitude activity detectable in both PNA and MUA reflects activity from the atria of the heart that was not entirely silenced in this experiment. *D*: identified different neurons are involved in odor-evoked (ON) and OFF responses. *a*: Spike sorting analysis (see METHODS) of the odor response shown in *A* yields 4 different active units. *b*: Two putative units were involved in the odor response shown in *B*. After stimulation, 2 different neurons were activated for a limited time, corresponding to an OFF response. *c*: Units that were active during baseline in *C* (PRE) were inhibited during odor presentation (ROSES). After odor presentation (POST), those units were active again. Two different putative units became active during odor presentation.

41

diving response in the perfused brain-stem preparation (Dutschmann and Paton 2002a,b). The integrity of the sensory trigeminal pathways allowed us to conduct control experiments to prove the odor selectivity of the olfactory bulb-brain stem preparation. Irrigation of the nasal mucosa with cold saline in $n = 7$ preparations triggered a reflex apnea characteristic of the diving response (Fig. 6A; see Dutschmann and Paton 2002a for details). This stimulus never evoked any response in LFP recordings from the perfused olfactory bulb.

Another important test for odor specificity of the responses was the application of room air via the olfactometer, which never evoked any marked LFP responses in the deeper olfactory bulb, i.e., comparable with the odor responses shown in Fig. 3 (Fig. 6B; $n = 64$ tests, $n = 16$ preparations). Thus this test also excludes mechanical recording artifacts due to the switching of flow direction through the nostrils. However, the application of room air was observed to cause a slight increase in the power of the spontaneous theta oscillations described above (in 4 out of 5 tested preparations).

DISCUSSION

In situ perfused olfactory bulb-brain stem preparation. The olfactory bulb-brain stem preparation is an adaptation of the working heart-brain stem preparation of rat (see Dutschmann et al. 2000; Paton 1996; Paton et al. 1999). This specialized technique was originally designed to study autonomic brain-stem function in situ, e.g., autonomic reflexes, mechanisms of sympathetic-respiratory coupling, and hierarchical organization of the central pattern generator for breathing. In the current study, respiratory activity generated by the brain-stem circuits is not coupled to olfactory bulb activity because of the precollicular decerebration. However, it remains an important indicator of the viability of the preparation itself. An active respiratory network implies that the perfusion pressure and flow are sufficient to ensure the oxygenation of the olfactory

A

nasal irrigation (0.1 ml cold saline)

∫PNA

∫OB-LFP

2mV
10s

B

AIR

∫PNA

∫OB-LFP

2mV
10s

Fig. 6. Representative control experiments for odor specificity. *A*: trigeminal stimulation of the nasal mucosa with water did not evoke any LFP in the olfactory bulb but triggered the anticipated protective diving breath hold illustrated by the transient cessation of PNA. *B*: application of room air did not elicit OB-LFP and had no obvious effect on PNA.

bulb. This type of monitoring allowed us to maintain a viable olfactory bulb preparation for up to 4 h.

Similar to previous observations in the respiratory brain-stem preparation (Dutschmann et al. 2000), we observed that the bulbar network required prolonged sensory input to trigger its reactivation. We speculate that this "rebooting" may be necessary because the olfactory network activity collapsed in the absence of rhythmic airflow or other sensory stimulation during the early stages of the preparation. Interestingly, both delivery of air and odorant were sufficient for rebooting, although delivery of air alone did not result in marked LFPs. However, there was a slight increase in theta power during delivery of air. This observation suggests that there is a pathway providing weak input on stimulation with air that contributes to the reactivation of bulbar networks, perhaps mediated by mechanoreceptive stimulation of olfactory sensory neurons due to the positive pressure exerted by the airflow (Grosmaitre et al. 2007) or by olfactory stimulation with low concentrations of odorants present in the room air. In any case, we observed that this reactivation is an important prerequisite for proper network function.

Oscillatory activity. In the perfused olfactory bulb preparation, we have consistently observed spontaneous LFP oscillations within a frequency band of 4–10 Hz, corresponding to the theta range. Almost all analyzed recordings showed a major oscillatory component ~4 Hz, whereas a smaller subset of preparations also displayed faster frequency components within beta and gamma bands. Thus the perfused olfactory bulb maintains oscillatory network activity, similar to what has been reported from in vivo recordings (for review, see Kay 2014) and from other semi-intact approaches in other species (Delaney and Hall 1996; Ishikawa et al. 2007).

Hippocampal theta oscillations can synchronize with the olfactory bulb oscillations, most likely via respiration coupling mediated by septal neurons (Tsanov et al. 2014) and could be required for forms of odor learning (e.g., Colgin 2013; Kay 2005; Macrides et al. 1982). Since the arterially perfused olfactory bulb preparation lacks central and respiration-coupled inputs, we conclude that the olfactory bulb network itself generates intrinsic theta oscillations that can couple to external inputs (such as respiration and hippocampal activity) as has been also found by others (e.g., Fukunaga et al. 2014; Schoppa and Westbrook 2001; Sobel and Tank 1993). Thus the in situ preparation could be used to verify whether bulbar intrinsic oscillations may contribute to odor-induced bulbar plasticity in the absence of the hippocampus. Moreover, the specific contribution of slow bulbar conductances to the intrinsic theta rhythm generation can now be explored in detail; for example, we have proposed that the activation of T-type voltage-dependent Ca^{2+} channels, NMDA receptors, TRPC channels, and their interactions might allow olfactory bulb granule cells to couple to ongoing theta activity (Egger et al. 2003, 2005; Egger 2008; Stroh et al. 2012).

Odor-evoked responses. Despite the lack of information on glomerular mapping and the small odor set in our experiments, there was a high probability for the detection of odor-evoked responses, probably due to the use of undiluted essential oils (corresponding to mixtures of various components), which cause widespread activation of bulbar networks (e.g., Meister and Bonhoeffer 2001). Using multiunit recordings from presumptive mitral and granule cells in the perfused olfactory
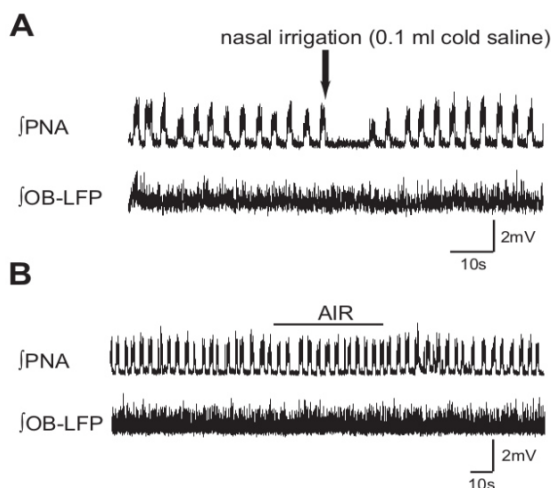
bulb, we have demonstrated persistent excitatory as well as inhibitory responses to stimulation with essential oils (see Fig. 5). These basic response types are also known from in vivo recordings of responses to both olfactory stimuli and optogenetically activated glomeruli (e.g., Bathellier et al. 2008; Buonviso et al. 1992; Cang and Isaacson 2003; Davison and Katz 2007; Haddad et al. 2013; Meredith 1986). Some neurons became tonically active following odor stimulation, whereas others showed a bout of increased activity immediately after odor stimulation (Fig. 5B). The latter effect might be explained by mitral cell and/or granule cell OFF responses (Debarbieux et al. 2003; Kato et al. 2012).

In addition, we have consistently observed an increase in oscillatory power in higher frequency bands during LFP odor responses (Fig. 4). This finding is well in line with observations in vivo, where stimulus-locked oscillations in the gamma range have been associated with dendrodendritic interactions between mitral and granule cells during odor processing (e.g., Eeckman and Freeman 1990; Fukunaga et al. 2014; Mori et al. 1977; Nusser et al. 2001). The presence of both spontaneous slow and evoked fast oscillations therefore proves that intrinsic bulbar neuronal network interactions within the perfused preparation are preserved. Since beta oscillations are of central origin (Chabaud et al. 2000; Fourcaud-Trocmé et al. 2014; Neville and Haberly 2003), it remains to be elucidated whether any faster oscillations observed here belong to the gamma type.

Taken together, the proofs of principle provided in our study show that the bulbar neuronal networks for initial odor processing are most likely fully functional in situ. Thus the in situ perfused olfactory bulb provides a solid experimental platform for the investigation of fundamental mechanisms of odor processing in the absence of central inputs. This preparation might thus help to dissect out the contribution of purely local odor processing by the olfactory bulb from central influences (e.g., Boyd et al. 2012; Rothermel and Wachowiak 2014) to odor representations.

Perspectives. The observed stability of odor-evoked LFP responses in situ over an extended time is in line with proper, constant oxygenation of the olfactory bulb and thus with sufficient perfusion. Thus the perfused preparation is suitable for the application of pharmacological and other time-consuming experimental paradigms in studies of olfactory processing.

In patch-clamp studies of cardiorespiratory function, various different spatial access routes were realized via a dorsal, lateral, or ventral exposure of the perfused brain stem preparation (Dutschmann and Paton 2003; Moraes et al. 2014b; Paton et al. 1999). Arterially perfused preparations were also demonstrated to facilitate the use of optical technologies such as voltage-sensitive dye imaging (Potts and Paton 2006) and optogenetics (Moraes et al. 2014a). Likewise, the perfused olfactory bulb preparation will allow for highly invasive approaches to investigate the network function of olfactory processing within the entire olfactory bulb. For example, a hemihead preparation of the mouse was used to explore mirror mapping in the olfactory bulb and olfactory sensory axonal responses to glomerular odor application (Lodovichi et al. 2003; Maritan et al. 2009) but so far without implementation of direct nasal olfactory stimulation.

Moreover, the perfused preparation might also be extended to neonatal rats, since they have a functional olfactory system (Wilson and Sullivan 1994), as well as to older

animals (Paton 1996) and thus could be useful for studies of sensory development.

In the current study, slow bulbar oscillations were generated in the absence of respiratory-like airflow. However, a more physiological stimulation technique could be realized via the "sniff playback" device developed by Cheung et al. (2009). In any case, the presence of both spontaneous slow theta oscillations and fast cellular responses in the mitral and granule cell layer of the olfactory bulb will enable investigations of neuronal synchronization to ongoing rhythmic activity, a widely studied topic in various brain areas.

In conclusion, the perfused olfactory bulb preparation is a valuable and complementary tool to decipher mechanisms of spatiotemporal olfactory coding further.

DISCLOSURES

No conflicts of interest, financial or otherwise, are declared by the author(s).

AUTHOR CONTRIBUTIONS

F.P.d.l.C.P., D.S., D.F., M.D., and V.E. conception and design of research; F.P.d.l.C.P. and M.D. performed experiments; F.P.d.l.C.P., M.D., and V.E. analyzed data; F.P.d.l.C.P., M.D., and V.E. interpreted results of experiments; F.P.d.l.C.P., M.D., and V.E. prepared figures; F.P.d.l.C.P., M.D., and V.E. drafted manuscript; F.P.d.l.C.P., D.F., M.D., and V.E. edited and revised manuscript; F.P.d.l.C.P., M.D., and V.E. approved final version of manuscript.

REFERENCES

Adrian ED. The electrical activity of the mammalian olfactory bulb. *Electroencephalogr Clin Neurophysiol* 2: 377–388, 1950.

Alonso A, de Curtis M, Llinás R. Postsynaptic Hebbian and non-Hebbian long-term potentiation of synaptic efficacy in the entorhinal cortex in slices and in the isolated adult guinea pig brain. *Proc Natl Acad Sci USA* 87: 9280–9284, 1990.

Aungst JL, Heyward PM, Puche AC, Karnup SV, Hayar A, Szabo G, Shipley MT. Centre-surround inhibition among olfactory bulb glomeruli. *Nature* 426: 623–629, 2003.

Bathellier B, Buhl DL, Accolla R, Carleton A. Dynamic ensemble odor coding in the mammalian olfactory bulb: sensory information at different timescales. *Neuron* 57: 586–598, 2008.

Boyd AM, Sturgill JF, Poo C, Isaacson JS. Cortical feedback control of olfactory circuits. *Neuron* 76: 1161–1174, 2012.

Bressler SL. Relation of olfactory bulb and cortex. I. Spatial variation of bulbocortical interdependence. *Brain Res* 409: 294–302, 1987.

Buonviso N, Amat C, Litaudon P, Roux S, Royet JP, Farget V, Sicard G. Rhythm sequence through the olfactory bulb layers during the time window of a respiratory cycle. *Eur J Neurosci* 17: 1811–1819, 2003.

Buonviso N, Chaput MA, Berthommier F. Temporal pattern analyses in pairs of neighboring mitral cells. *J Neurophysiol* 68: 417–424, 1992.

Buzsáki G, Draguhn A. Neural oscillations in cortical networks. *Science* 304: 1926–1929, 2004.

Cang J, Isaacson JS. In vivo whole-cell recording of odor-evoked synaptic transmission in the rat olfactory bulb. *J Neurosci* 23: 4108–4116, 2003.

Carey RM, Wachowiak M. Effect of sniffing on the temporal structure of mitral/tufted cell output from the olfactory bulb. *J Neurosci* 31: 10615–10626, 2011.

Carlson GC, Shipley MT, Keller A. Long-lasting depolarizations in mitral cells of the rat olfactory bulb. *J Neurosci* 20: 2011–2021, 2000.

Chabaud P, Ravel N, Wilson DA, Mouly AM, Vigouroux M, Farget V. Exposure to behaviourally relevant odour reveals differential characteristics in rat central olfactory pathways as studied through oscillatory activities. *Chem Senses* 25: 561–573, 2000.

Chaput M, Holley A. Single unit responses of olfactory bulb neurons to odour presentation in awake rabbits. *J Physiol (Paris)* 76: 551–558, 1980.

Cheung MC, Carey RM, Wachowiak M. A method for generating natural and user-defined sniffing pattern in anesthetized or reduced preparations. *Chem Senses* 34: 63–76, 2009.

Colgin LL. Mechanisms and functions of theta rythms. *Annu Rev Neurosci* 36: 295–312, 2013.

Davison IG, Katz LC. Sparse and selective odor coding by mitral/tufted neurons in the main olfactory bulb. *J Neurosci* 27: 2091–2101, 2007.

de Curtis M, Paré D, Llinás RR. The electrophysiology of the olfactory-hippocampal circuit in the isolated and perfused adult mammalian brain in vitro. *Hippocampus* 1: 341–354, 1991.

Debarbieux F, Audinat E, Charpak S. Action potential propagation in dendrites of rat mitral cells in vivo. *J Neurosci* 23: 5553–5560, 2003.

Delaney KR, Hall BJ. An in vitro preparation of frog nose and brain for the study of odour-evoked oscillatory activity. *J Neurosci Methods* 68: 193–202, 1996.

Dutschmann M, Mörschel M, Rybak IA, Dick TE. Learning to breathe: control of the inspiratory-expiratory phase transition shifts from sensory- to central-dominated during postnatal development in rats. *J Physiol* 587: 4931–4948, 2009.

Dutschmann M, Paton JF. Influence of nasotrigeminal afferents on medullary respiratory neurones and upper airway patency in the rat. *Pflügers Arch* 444: 227–235, 2002a.

Dutschmann M, Paton JF. Trigeminal reflex regulation of the glottis depends on central glycinergic inhibition in the rat. *Am J Physiol Regul Integr Comp Physiol* 282: R999–R1005, 2002b.

Dutschmann M, Paton JF. Whole cell recordings from respiratory neurones in an arterially perfused in situ neonatal rat preparation. *Exp Physiol* 88: 725–732, 2003.

Dutschmann M, Wilson RJ, Paton JF. Respiratory activity in neonatal rats. *Auton Neurosci* 84: 19–29, 2000.

Eeckman FH, Freeman WJ. Correlations between unit firing and EEG in the rat olfactory system. *Brain Res* 528: 238–244, 1990.

Egger V. Synaptic spikes in olfactory bulb granule cells cause long-lasting depolarization and calcium entry. *Eur J Neurosci* 27: 2066–2075, 2008.

Egger V, Svoboda K, Mainen ZF. Dendrodendritic synaptic signaling in olfactory bulb granule cells: local spine boost and global low-threshold spike. *J Neurosci* 25: 3521–3530, 2005.

Egger V, Svoboda K, Mainen ZF. Mechanisms of lateral inhibition in the olfactory bulb: efficiency and modulation of spike-evoked calcium influx into granule cells. *J Neurosci* 23: 7551–7559, 2003.

Fourcaud-Trocmé N, Courtiol E, Buonviso N. Two distinct olfactory bulb sublaminar networks involved in gamma and beta oscillation generation: a CSD study in the anesthetized rat. *Front Neural Circuits* 8: 88, 2014.

Freeman WJ, Schneider W. Changes in spatial patterns of rabbit olfactory EEG with conditioning to odors. *Psychophysiology* 19: 44–56, 1982.

Friedman D, Strowbridge BW. Both electrical and chemical synapses mediate fast network oscillations in the olfactory bulb. *J Neurophysiol* 89: 2601–2610, 2003.

Fukunaga I, Herb JT, Kollo M, Boyden ES, Shaefer AT. Independent control of gamma and theta activity by distinct interneuron networks in the olfactory bulb. *Nat Neurosci* 17: 1208–1216, 2014.

Gire DH, Franks KM, Zak JD, Tanaka KF, Whitesell JD, Mulligan AA, Hen R, Schoppa NE. Mitral cells in the olfactory bulb are mainly excited through a multistep signaling path. *J Neurosci* 32: 2964–2975, 2012.

Green EC. *Anatomy of the Rat.* New York: Hafner, 1955.

Grosmaitre X, Santarelli LC, Tan J, Luo M, Ma M. Dual functions of mammalian olfactory sensory neurons as odor detectors and mechanical sensors. *Nat Neurosci* 10: 348–354, 2007.

Haddad R, Lanjuin A, Madisen L, Zeng H, Murthy VN, Uchida N. Olfactory cortical neurons read out a relative time code in the olfactory bulb. *Nat Neurosci* 16: 949–957, 2013.

Ishikawa T, Sato T, Shimizu A, Tsutsui K, de Curtis M, Iijima T. Odor-driven activity in the olfactory cortex of an in vitro isolated guinea pig whole brain with olfactory epithelium. *J Neurophysiol* 97: 670–679, 2007.

Kato HK, Chu MW, Isaacson JS, Komiyama T. Dynamic sensory representations in the olfactory bulb: modulation by wakefulness and experience. *Neuron* 76: 962–975, 2012.

Kay LM. Circuit oscillations in odor perception and memory. *Prog Brain Res* 208: 223–251, 2014.

Kay LM. Theta oscillations and sensorimotor performance. *Proc Natl Acad Sci USA* 102: 3863–3868, 2005.

Lagier S, Carleton A, Lledo PM. Interplay between local GABAergic interneurons and relay neurons generates gamma oscillations in the rat olfactory bulb. *J Neurosci* 24: 4382–4392, 2004.

Li A, Zhang L, Liu M, Gong L, Liu Q, Xu F. Effects of different anesthetics on oscillations in the rat olfactory bulb. *J Am Assoc Lab Anim Sci* 51: 458–463, 2012.

Lisman J. The theta/gamma discrete phase code occurring during the hippocampal phase precession may be a more general brain coding scheme. *Hippocampus* 15: 913–922, 2005.

Llinás R, Yarom Y, Sugimori M. Isolated mammalian brain in vitro: new technique for analysis of electrical activity of neural circuit function. *Fed Proc* 40: 2240–2245, 1981.

Lodovichi C, Belluscio L, Katz LC. Functional topography of connections linking mirror-symmetric maps in the mouse olfactory bulb. *Neuron* 38: 265–276, 2003.

Macrides F, Chorover SL. Olfactory bulb units: activity correlated with inhalation cycles and odor quality. *Science* 175: 84–87, 1972.

Macrides F, Eichenbaum HB, Forbes WB. Temporal relationship between sniffing and the limbic theta rhythm during odor discrimination reversal learning. *J Neurosci* 2: 1705–1717, 1982.

Margrie TW, Sakmann B, Urban NN. Action potential propagation in mitral cell lateral dendrites is decremental and controls recurrent and lateral inhibition in the mammalian olfactory bulb. *Proc Natl Acad Sci USA* 98: 319–324, 2001.

Margrie TW, Schaefer AT. Theta oscillation coupled spike latencies yield computational vigour in a mammalian sensory system. *J Physiol* 546: 363–374, 2003.

Maritan M, Monaco G, Zamparo I, Zaccolo M, Pozzan T, Lodovichi C. Odorant receptors at the growth cone are coupled to localized cAMP and Ca^{2+} increases. *Proc Natl Acad Sci USA* 106: 3537–3542, 2009.

Martin C, Ravel N. Beta and gamma oscillatory activities associated with memory tasks: different rythms for different functional networks? *Front Behav Neurosci* 8: 218, 2014.

Meister M, Bonhoeffer T. Tuning and topography in an odor map on the rat olfactory bulb. *J Neurosci* 21: 1351–1360, 2001.

Meredith M. Patterned response to odor in mammalian olfactory bulb: the influence of intensity. *J Neurophysiol* 56: 572–597, 1986.

Mombaerts P, Wang F, Dulac C, Chao SK, Nemes A, Mendelsohn M, Edmondson J, Axel R. Visualizing an olfactory sensory map. *Cell* 87: 675–686, 1996.

Moraes DJ, Abdala AP, Machado BH, Paton JF. Functional connectivity between Bötzinger complex glycinergic neurons and parafacial late-expiratory neurons for expiratory and sympathetic control. *FASEB J* 28, *Suppl* 1: 712–17, 2014a.

Moraes DJ, Machado BH, Paton JF. Specific respiratory neuron types have increased excitability that drive presympathetic neurones in neurogenic hypertension. *Hypertension* 63: 1309–1318, 2014b.

Mori K, Kogure S, Takagi S. Alternating responses of olfactory bulb neurons to repetitive lateral olfactory tract stimulation. *Brain Res* 133: 150–155, 1977.

Mühlethaler M, de Curtis M, Walton K, Llinás R. The isolated and perfused brain of the guinea-pig in vitro. *Eur J Neurosci* 5: 915–926, 1993.

Najac M, De Saint Jan D, Reguero L, Grandes P, Charpak S. Monosynaptic and polysynaptic feed-forward inputs to mitral cells from olfactory sensory neurons. *J Neurosci* 31: 8722–8729, 2011.

Neville KR, Haberly LB. Beta and gamma oscillations in the olfactory system of the urethane-anesthetized rat. *J Neurophysiol* 90: 3921–3930, 2003.

Nusser Z, Kay LM, Laurent G, Homanics GE, Mody I. Disruption of $GABA_A$ receptors on GABAergic interneurons leads to increase oscillatory power in the olfactory bulb network. *J Neurophysiol* 86: 2823–2833, 2001.

Onoda N, Mori K. Depth distribution of temporal firing patterns in olfactory bulb related to air-intake cycles. *J Neurophysiol* 44: 29–39, 1980.

44

Paton JF. A working heart-brainstem preparation of the mouse. *J Neurosci Methods* 65: 63–68, 1996.

Paton JF, Li YW, Kasparov S. Reflex response and convergence of pharyngoesophageal and peripheral chemoreceptors in the nucleus of the solitary tract. *Neuroscience* 93: 143–154, 1999.

Potts JT, Paton JF. Optical imaging of medullary ventral respiratory network during eupnea and gasping in situ. *Eur J Neurosci* 23: 3025–3033, 2006.

Rothermel M, Wachowiak M. Functional imaging of cortical feedback projections to the olfactory bulb. *Front Neural Circuits* 8: 73, 2014.

Rubin BD, Katz LC. Optical imaging of odorant representations in the mammalian olfactory bulb. *Neuron* 23: 499–511, 1999.

Schoppa NE. Synchronization of olfactory bulb mitral cells by precisely timed inhibitory inputs. *Neuron* 49: 271–283, 2006.

Schoppa NE, Westbrook GL. Glomerulus-specific synchronization of mitral cells in the olfactory bulb. *Neuron* 31: 639–651, 2001.

Scremin OU. Cerebral vascular system. In: *The Rat Nervous System* (3rd ed.), edited by Paxinos G. San Diego, CA: Elsevier Academic Press, 2004, p. 922–963.

Shepherd GM, Greer CA. *The Synaptic Organization of the Brain*, edited by Shepherd GM. New York: Oxford Univ. Press, 1990, p. 317–345.

Sobel EC, Tank DW. Timing of odor stimulation does not alter patterning of olfactory bulb unit activity in freely breathing rats. *J Neurophysiol* 69: 1331–1337, 1993.

Spors H, Grinvald A. Spatio-temporal dynamics of odor representations in the mammalian olfactory bulb. *Neuron* 347: 301–315, 2002.

Stroh O, Freichel M, Kretz O, Birnbaumer L, Hartmann J, Egger V. NMDA-receptor dependent synaptic activation of TRPC channels in the olfactory bulb. *J Neurosci* 32: 5737–5746, 2012.

Teicher MH, Blass EM. First suckling response of the newborn albino rat: the roles of olfaction and amniotic fluid. *Science* 198: 635–636, 1977.

Tsanov M, Chah E, Reilly R, O'Mara SM. Respiratory cycle entrainment of septal neurons mediates the fast coupling of sniffing rate and hippocampal theta rhythm. *Eur J Neurosci* 39: 957–974, 2014.

Wachowiak M, Shipley MT. Coding and synaptic processing of sensory information in the glomerular layer of the olfactory bulb. *Semin Cell Dev Biol* 17: 411–423, 2006.

Wilson DA, Sullivan RM. Neurobiology of associative learning in the neonate: early olfactory learning. *Behav Neural Biol* 61: 1–18, 1994.

Wilson RJ, Remmers JE, Paton JF. Brain stem PO_2 and pH of the working heart-brain stem preparation during vascular perfusion with aqueous medium. *Am J Physiol Regul Integr Comp Physiol* 281: R528–R538, 2001.

45

3.2. <u>Brainstem-mediated sniffing and respiratory modulation during odor stimulation.</u>

46

Brainstem-mediated sniffing and respiratory modulation during odor stimulation.

47

Fernando Pérez de los Cobos Pallares[1], Tara G. Bautista[2], Davor Stanić[2], Veronica Egger[1], Mathias Dutschmann[2]

1   Zoological Institute, University of Regensburg, D-93040 Regensburg.
2   Florey Institute of Neuroscience and Mental Health, Gate 11 Royal Parade, 3052 University of Melbourne Victoria, Australia.

Running head: Respiratory brainstem response to trigeminal odors

Corresponding authors:

Fernando Pérez de los Cobos Pallares, Zoological Institute, University of Regensburg, email: Fernando.Perez@biologie.uni-regensburg.de
OR
Mathias Dutschmann, Florey Institute of Neuroscience and Mental Health, email: mathias.dutschmann@florey.edu.au

Abstract

The trigeminal and olfactory systems interact during sensory processing of odor. Here, we investigate odor-evoked modulations of brainstem respiratory networks in a decerebrated perfused brainstem preparation of rat with intact olfactory bulbs. Intranasal application of non-trigeminal odors (rose) did not evoke respiratory modulation in absence of cortico-limbic circuits. Conversely, trigeminal odors such as menthol or lavender evoked robust respiratory modulations via direct activation of preserved brainstem circuits. Trigeminal odors consistently triggered short phrenic nerve bursts (fictive sniff), and the strong trigeminal odor menthol also triggered a slowing of phrenic nerve frequency. Phrenic and vagal nerve recordings reveal that fictive sniffs transiently interrupted odor evoked tonic postinspiratory vagal discharge. This motor pattern is significantly different from normal (eupneic) respiratory activity. In conclusion, we show for the first time the direct involvement of brainstem circuits in primary odor processing to evoke protective sniffs and respiratory modulation in the complete absence of forebrain commands.

1. Introduction

The processing of odorants within the main olfactory epithelium involves two primary and anatomically distinct neural systems. The first 'classic' olfactory pathway consists of axonal projections from the olfactory sensory neurons of the nasal epithelium into the glomeruli of the olfactory bulb. Within the glomeruli, the sensory input is forwarded to the mitral and tufted cells, which in turn widely project to forebrain structures such as the piriform cortex, hippocampus and amygdala (Doty, 2001; Firestein, 2001). The second 'naso-trigeminal brainstem' pathway is associated with the trigeminal system (Hummel et al., 2002; Brand, 2006). The anterior ethmoidal and infraorbital nerves, both of which are branches of the ophthalmic division of the trigeminal nerve, also innervate the nasal mucosa. Contrary to the forebrain projection of the olfactory system, the trigeminal sensory fibers project to spinal trigeminal nuclei such as the sub-nucleus caudalis and the sub-nucleus interpolaris (Anton and Peppel, 1991; Anton et al., 1991), which are located in the caudal brainstem.

Most odorants have the ability to co-activate both systems. This was demonstrated by simultaneous electrophysiological recording of olfactory and trigeminal sensory fibers of the nasal epithelium, which revealed a trigeminal response following exposure to a variety of odors that predominantly stimulated olfactory receptors (Beidler and Tucker, 1956). Thus, sensory processing of odors appears to involve the interplay between the top-down cortico-limbic olfactory system and a bottom-up trigeminal brainstem pathway. Both systems contribute to the processing and perception of smell via converging multi-synaptic projections to somatosensory cortico-thalamic, and limbic brain areas.

While, both systems contribute to sensory perception of odorants, the trigeminal pathway may serve additional functions (Hummel et al., 2002). The trigeminal system also safeguards the lower airways (lungs) to prevent inhalation of potentially noxious substances via protective reflexes, including a protective breath-hold or sneeze (Widdicombe, 1996). The latter underpins the tight association of olfaction and breathing. Respiratory modulation of olfactory bulb activity is well established and may involve peripheral sensory feedback from nasal airflow, as well as ascending modulation of olfactory bulb activity via the primary respiratory networks of the brainstem (Buonviso et al., 2006; Kepeces et al., 2006; Wachowiak, 2011).

The tight interaction between breathing and olfaction is seen in several olfactory behaviors, for example fast sniffing to enhance odor detection during active sensing in

the context of exploration or olfactory tasks (Wachowiak, 2011). The general view is that a switch from breathing to sniffing depends on behavioral forebrain (cortical and/or limbic) commands (Kepeces et al., 2006; Wachowiak, 2011), while the primary pattern generator for sniffing resides in close proximity to aspects of the respiratory pattern generator in the medulla oblongata (Moore et al., 2013; 2014). The modulation of brainstem respiratory cell activities during sniffing has been shown (Batsel and Lines, 1973; Du Pont, 1987). The precise source and anatomical pathways of the sniffing command that triggers the changes in respiratory neuron activity, however, are unknown so far; it might arise from either the trigeminal brainstem pathway or descending input from the cortico-limbic olfactory system, or both.

In the present study, we specifically address the potential contribution of the naso-trigeminal brainstem pathway to the mediation of respiratory modulations elicited by odorants; to this end we apply trigeminal and non-trigeminal odorants intra-nasally in an *in situ* perfused, decerebrated, olfactory-bulb-brainstem preparation (Pérez de los Cobos Pallarés et al., 2015). While this experimental approach can be used to study odor processing in the olfactory bulb (Pérez de los Cobos Pallarés et al., 2015), it also provides a unique opportunity for the investigation of trigeminally-mediated odor processing in the brainstem in the absence of confounding influences by the cortico-limbic systems. Previous work demonstrated that stimulation of the trigeminal ethmoidal nerve, or mechanical stimulation of the nasal mucosa (including its irrigation with cold water), reliably triggers cardio-respiratory reflexes such as the diving response in the *in situ* perfused brainstem preparation (Dutschmann and Paton, 2002a,b; Pérez de los Cobos Pallarés et al., 2015). Thus, the trigeminal innervation of the nasal cavity, including the primary sensory relay within the brainstem, remains intact under these experimental conditions. Since specific odorants stimulate the olfactory and the trigeminal system differentially (Doty et al., 1978), we analyzed respiratory responses to odors that are known to trigger a pure olfactory response (e.g. rose odor) vs. irritant odors such as menthol or lavender (linalool) that produce robust co-activation of the trigeminal system. The trigeminal odors menthol and lavender may act via TRP channels (Peer et al., 2002, Elsharif, 2015) expressed in the nasal mucosa (see Bessac and Jordt, 2008). For the remainder of the manuscript we refer to these odors as non-trigeminal and trigeminal odors, respectively.

We demonstrate that the brainstem alone can initiate short bursts of phrenic nerve activity that are evocative of fictive sniffing as well as subsequent respiratory depression, in the complete absence of the forebrain.

2. Material and Methods

2.1 Ethical approval

All experimental procedures were performed either in accordance with the Australian code of practice for the care and use of animals for scientific purposes or with the stipulations of the German law governing animal welfare (Tierschutzgesetz). The ethics committee of the Florey Institute approved the study design.

2.2. The perfused olfactory bulb brainstem preparation

As described previously (Paton 1996), juvenile *Sprague* Dawley rats (p17-21) were deeply anesthetized with isoflurane (1-Chloro-2,2,2-trifluoroethyl-difluoromethylether, Isoflurane, Forene®, Abbott GmbH & Co. KG, Wiesbaden, Germany). As soon as the animal failed to respond to a tail pinch, it was transected caudal to the diaphragm and transferred into an ice-cooled chamber filled with ACSF (mM: $1.25MgSO_47HO_2$, $1.25KH_2PO_4$, 3 KCL, 125 NaCL, 25 $NaHCO_3$, 2.5 $CaCl_2·2H_2O$, D-glucose 10*)*. The animal was decerebrated at the pre-collicular level functionally preserving the brainstem including the periaqueductal gray (Farmer et al., 2014) and the skull was opened. The forebrain was entirely removed by suction, leaving intact solely the olfactory bulb, small adjacent fragments of the piriform cortex and the brainstem (Pérez de los Cobos Pallarés et al., 2015). After removing the lungs, the phrenic nerve was isolated on the right hand side and was cut at the level of the diaphragm to subsequently record respiratory (inspiratory) activity (Paton, 1996). To prevent mechanical and electrical artifacts, the heart was removed after ligation of the aortic arch. Next, the preparation was transferred to the recording chamber, and the descending aorta was cannulated to perfuse (peristaltic pump: Watson-Marlow 520S, Massachusetts, USA) the preparation with ACSF containing 1.25% Ficoll PM70 (Sigma), to provide oncotic pressure during experiments. Flow rates were adjusted according to the age of the animal and perfusion pressure was maintained at 50-70 mmHg (Paton, 1996). The perfusate was continuously gassed with carbogen (95% O_2, 5% CO_2) and warmed to a temperature of 30 °C. The phrenic nerve was aspirated with a suction electrode. While the olfactory bulb was oxygenated via the ophthalmic artery, the brainstem was oxygenated via the basilar artery (for details see Pérez de los Cobos

Pallarés et al., 2015). Both arteries were simultaneously perfused via the cannulated aorta.

After a few minutes of perfusion, respiratory movements appeared, and spontaneous rhythmic activity in the phrenic nerve was observed. The neuromuscular blocker vecuronium bromide (Sigma; 0.3 µg ml^{-1}) was added to the perfusate to prevent movement artifacts.

2.3. Odor application

Preparations (n=12) were stimulated randomly with several non-diluted fragrant oils (menthol, JHP Rödler, Ulm, Germany; lavender and rose, TAOASIS GmbH, Bielefeld, Germany) using a four-channel computer controlled olfactometer, which produced a constant airflow of 70 cc/min (Knosys Olfactometers, Florida). Exposure of the olfactory epithelium to odorants (15-30 s) was achieved via cannulation of the nasal cavities, using a custom-made set of small adaptors for the nostrils (1-3 mm diameter range).

2.3. Recording phrenic nerve activity and field potentials and multi-units in the olfactory bulb

The phrenic nerve activity (PNA) was recorded via suction electrodes (DP-311 Differential Amplifier Warner Instruments, Connecticut, USA), digitized and displayed via a Powerlab 26T data acquisition device (ADInstruments, Australia) in all experiments. For recording of olfactory bulb activity (n=12 preparations) we used glass microelectrodes filled with 2 M NaCl. For field potential recordings, the electrode tips were adjusted to an electrical resistance of 0.5 - 2 MΩ. Recordings were usually performed in the deeper layers of the dorsal olfactory bulb, well below the glomerular layer. Phrenic nerve and olfactory bulb activity were sampled at 1 kHz, amplified and filtered (low pass 10 kHz; high pass 300 Hz).

In another subset of experiments (n=5 preparations), we recorded vagal nerve activity (VNA) to assess trigeminal odor-evoked respiratory changes in laryngeal motor activity (inspiratory abductor activity and postinspiratory abductor activity, see

Dutschmann and Paton 2002c). Integration of PNA, VNA and olfactory bulb activity was performed with a decay time constant of 100 ms.

2.4. Data analysis and statistics

For the analysis and offline filtering of raw data, we used LabChart software (version 7.2, ADInstruments). We analyzed basic respiratory parameters: namely total respiratory cycle length (T_{tot}) and inspiratory burst duration (T_i). We analyzed these respiratory parameters for 5 respiratory cycles prior to odor application and compared them to respiratory activity during odor exposure and to 5 respiratory cycles after termination of the sensory stimulus. Comparison of respiratory parameters before, during and after odor applications were performed using a two way ANOVA followed by a Fisher LSD post-hoc test (GraphPad-Prism). For statistical analysis of the T_i during eupnea (control) and odor stimulation, we used a two-tailed unequal variance t-test (Excel). Comparison of frequency and T_i before, during and after odor application within the same application groups were performed using an ANOVA for repeated measures followed by a Bonferroni post-hoc test (IBM SPSS Statistics 22). All data are expressed as mean ± standard error of the mean (SEM).

3. Results

We applied the strong trigeminal odor menthol, the mild trigeminal odor lavender, as well as the non-trigeminal odor rose to the nasal mucosa in a total of 12 *in situ* olfactory bulb-brainstem preparations. We used an olfactometer for all odor applications (for details see, Pérez de los Cobos Pallarés et al., 2015). We only analyzed odor applications that evoked a detectable local field potential in the olfactory bulb (Fig. 1) and thus verified the specificity of the odor stimulus (total n = 84 odor applications: rose n = 42, menthol n = 26, lavender n = 16).

3.1 Odor evoked respiratory modulation by trigeminal odorants in absence of the forebrain.

Rose odor (n = 42 applications in 11 preparations, Fig. 1A) evoked no significant changes of respiratory cycle length (T_{tot}) or inspiratory burst duration (T_i) between the control phase prior to odor application, (T_{tot} 3.72 ± 0.16 s; T_i 0.96 ± 0.24 s) during odor stimulation (T_{tot} 3.92 ± 0.20 s; T_i 0.96 ± 0.24 s) and during the post-stimulus rebound (T_{tot} 3.72 ± 0.17 s; T_i 0.98 ± 0.24 s). The lack of changes in respiratory frequency and inspiratory duration are summarized in Figure 2A.

In contrast, exposure of the nasal mucosa to the trigeminal odorants menthol and lavender consistently evoked significant changes in respiratory activity. An example of a respiratory response to menthol is illustrated in Fig. 1B. The most prominent response feature was the occurrence of 1-4 short duration PNA bursts during the initial 1-5 seconds after either menthol (Fig. 1B) or lavender application (not shown). At least one single short PNA burst was observed in all trigeminal odor applications. A total of n = 90 short PNA bursts (at least 50% reduction of baseline PNA burst duration) in response to 42 odor exposures were analyzed. These short PNA bursts had a mean duration of 0.29 ± 0.01 s and were significantly ($p < 0.0001$, paired Students t-test) shorter compared to normal respiratory PNA burst duration measured before odor application (1.00 ± 0.28 s). Due to the distinct PNA pattern and duration, we refer to these short bursts as fictive sniffs (see Fig. 1B, and discussion). In cases where odor application triggered multiple fictive sniffs (n = 21 stimulations with either menthol or lavender), the total duration of sniff cycles was significantly shorter compared to baseline breathing (sniff 0.80 ± 0.05 s vs. baseline 3.70 ± 0.14 s; $p < 0.001$, paired students t-test).
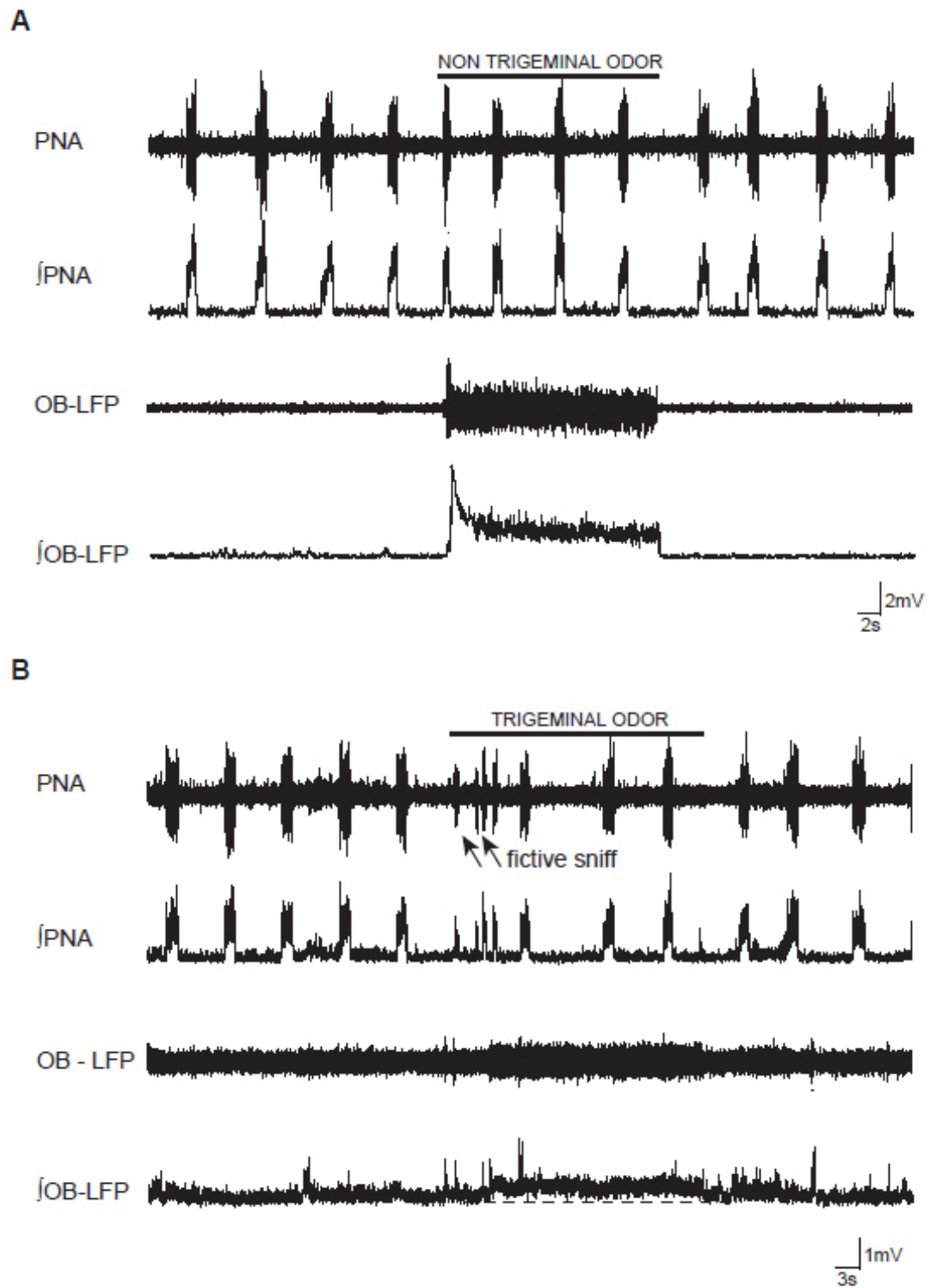
Figure 1. Respiratory modulation elicited by trigeminal and non-trigeminal odorants

(A) Direct stimulation with non-trigeminal odors (rose essential oil) administered to the olfactory epithelium did not elicit a significant respiratory response (n=42) as it is reflected in the PNA pattern (*upper trace)*. (Continue in the next page).

Responses of the olfactory bulb local field potentials (OB-LFP, *lower trace)* confirmed that the odor presented reached the nasal epithelium.

(B) Exposure of the nasal epithelium triggered to trigeminal odors (menthol or lavender essential oils, n=42) triggered field potentials in the olfactory bulb. Moreover, short-duration PNA bursts, so-called "fictive sniffs" were observed during odor presentation in the absence of midbrain areas.

Following the trigeminal odor-evoked fictive sniffs (Fig. 1B), normal (eupneic) PNA during odor application showed a respiratory depression as indicated by an increase in T_{tot} from 3.85 ± 0.24 s (baseline) to 5.15 ± 0.41 s ($p < 0.01$, ANOVA). T_i decreased from 0.98 ± 0.06 s (baseline) to 0.85 ± 0.05 s ($p < 0.01$). After termination of the trigeminal odor exposure, T_{tot} immediately returned to baseline values (3.75 ± 0.22 s), as well as T_i (1.00 ± 0.07 s). The overall changes in respiration are summarized in Figure 2B.

Further analysis revealed that respiratory depression was most pronounced during the application of the strong trigeminal odor menthol (n = 26; T_{tot} control 3.88 ± 0.30 s vs. stimulation 5.83 ± 0.68 s; $p<0.01$) while the mild trigeminal odor lavender (n = 16) triggered only a mild and insignificant increase in T_{tot} (3.80 ± 0.30 s vs. 4.07 ± 0.33 s, n.s.).

In summary, our data suggest that trigeminal odors can evoke respiratory patterns resembling fictive fast sniffing and subsequent respiratory depression in the complete absence of the cortico-limbic networks. In contrast, the non-trigeminal odor rose failed to trigger respiratory responses in absence of cortico-limbic systems. Since non-trigeminal and trigeminal odors were applied with identical experimental settings, the rose odor application can serve as an intrinsic control for odor evoked respiratory modulations. Only 3 out of 42 (7%) stimulations with rose odor evoked respiratory responses (see Fig. 2A) and were most likely caused by contamination of the olfactometer with previously used trigeminal odors. This data set excludes the possibility that respiratory changes were evoked by mechanical or other unspecific stimulation of the olfactory epithelium since stimulation with trigeminal odor consistently (100%) evoked respiratory responses (see Fig.2B). Finally, adequate odor stimulation was verified since all reported respiratory changes were associated with evoked or modulated field potentials of the olfactory bulb. Thus, the observed respiratory ef-

fects of trigeminal odors were triggered by the primary sensory processing of trigeminal odors within the brainstem circuits.
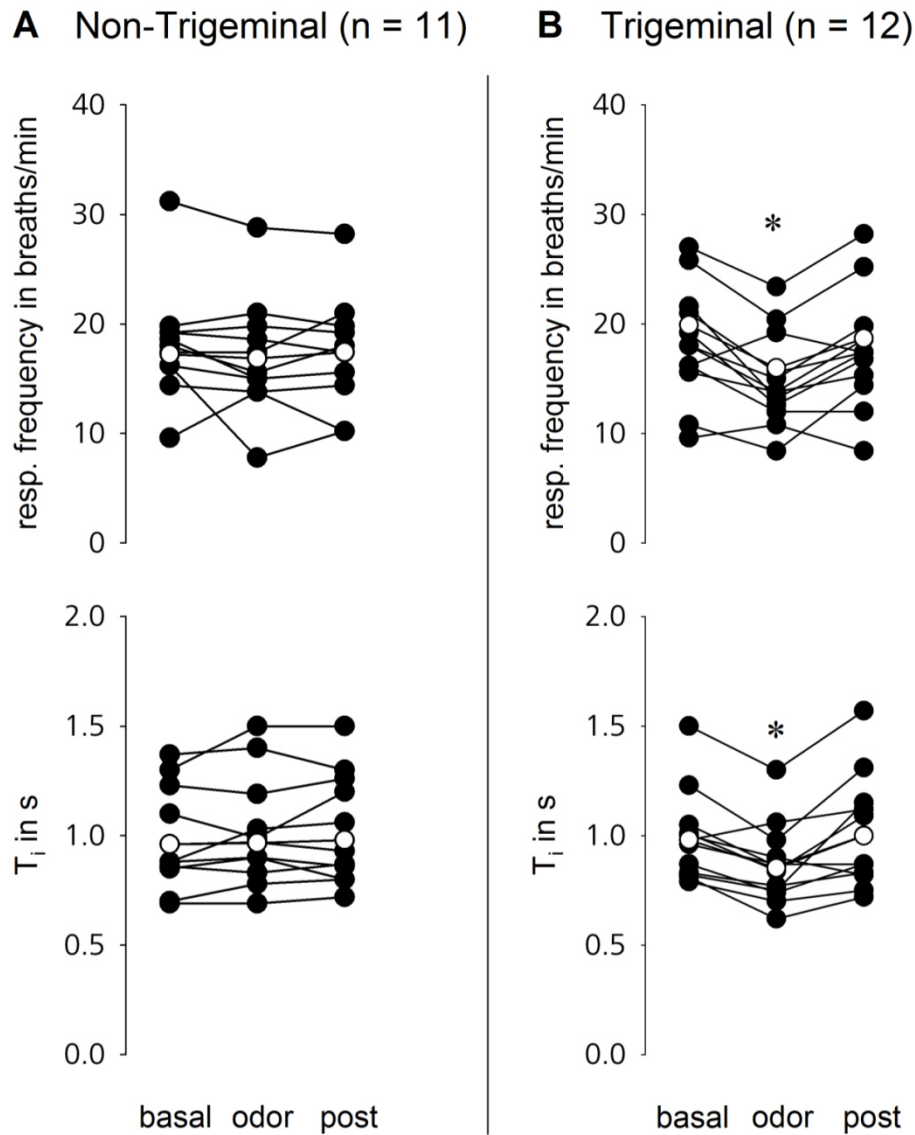
Figure 2: Summary of trigeminal odor evoked changes in baseline respiratory activity

Overall changes in respiratory frequency and duration of inspiration (T_i) before (before) during (odor), and after (post) non-trigeminal (A) and trigeminal (B) odor stimulation. Respiratory frequency and T_i are not modulated by non-trigeminal odor stimulation, but are decreased as a result of trigeminal odor stimulation (Frequency, $F_{(2,22)}=9.60$, $p<0.001$; T_i, $F_{(2,22)}=9.37$, $p<0.01$). Black line plots represent the means of several measurements within the same preparation. The white line plots represent the weighted mean of all preparations within the

respective odor application group, i.e. preparation means (black dots) consisting of several measurements are weighted corresponding to the number of incorporated measurements.

* p < 0.05 vs. before and post Using ANOVA for repeated measures followed by post-hoc comparison corrected with Bonferroni.

3.2 The respiratory motor pattern of fictive sniffs.

We further characterized the fictive sniff motor pattern by the simultaneous recording of VNA (vagal nerve activity, see Fig. 3) in an additional n = 5 preparations. The exposure of the nasal mucosa to menthol triggered fictive sniff responses in all preparations (Fig. 3B) as per our definition of fictive sniffs (short PNA bursts with decreased T_{tot}; see above). A total of 26 fictive sniff responses (at least n = 3 per preparation) could be analyzed. PNA burst duration during fictive sniffs was significantly shorter compared to normal baseline activity (0.30 ± 0.02 s vs. 0.90 ± 0.14 s; p < 0.001, paired t-test).

Parallel recording of VNA revealed that menthol elicited tonic vagal discharge during sniffing sequences. It has been proven experimentally in perfused brainstem preparations that postinspiratory VNA mediates laryngeal adduction (Dutschmann and Paton 2002a,b,c). Thus, the physiological function of this laryngeal constriction during sniffing might be to increase upper airway resistance in order to generate the high nasal airflow pressure (for further details see discussion). However, the robust postinspiratory discharge was transiently interrupted during the short PNA bursts that indicate fictive sniffs (Fig.3). This pattern was fundamentally different from the biphasic VNA during eupneic inspiration and postinspiration as observed before odor application (see Fig. 3B). Sniff-associated VNA was characterized by significantly reduced VNA during inspiration (simultaneous discharge of PNA and VNA), compared to the eupneic pattern that is associated with robust inspiratory VNA (see Fig. 3C).

After the initial fictive sniff response, the slowed respiration during the stimulation period was also associated with prolonged tonic postinspiratory discharge during the entire expiratory interval, however the peak amplitude of integrated postinspiratory VNA was reduced compared eupneic breaths at baseline (302 ± 21 vs 198 ± 44 µV/s, p<0.05)

A
olfactory bulbs
trigeminal nerve
colliculi
pontomedually brainstem

B
Menthol
(i) (ii)
PNA
200 µV
integ.
VNA
200 µV
integ.
OB- LFP
50 µV
integ.
10s

C
(i) (ii)
PNA
200 µV
integ.PNA
VNA
200 µV
integ. VNA
insp. postinsp.
0.5 s

D
n=5 prep.
integ. insp.
VNA (µV * 50 ms)
160
80
0
breath sniff
***

n=5 prep.
duration PNA (s)
1.0
0.5
0
breath sniff
**
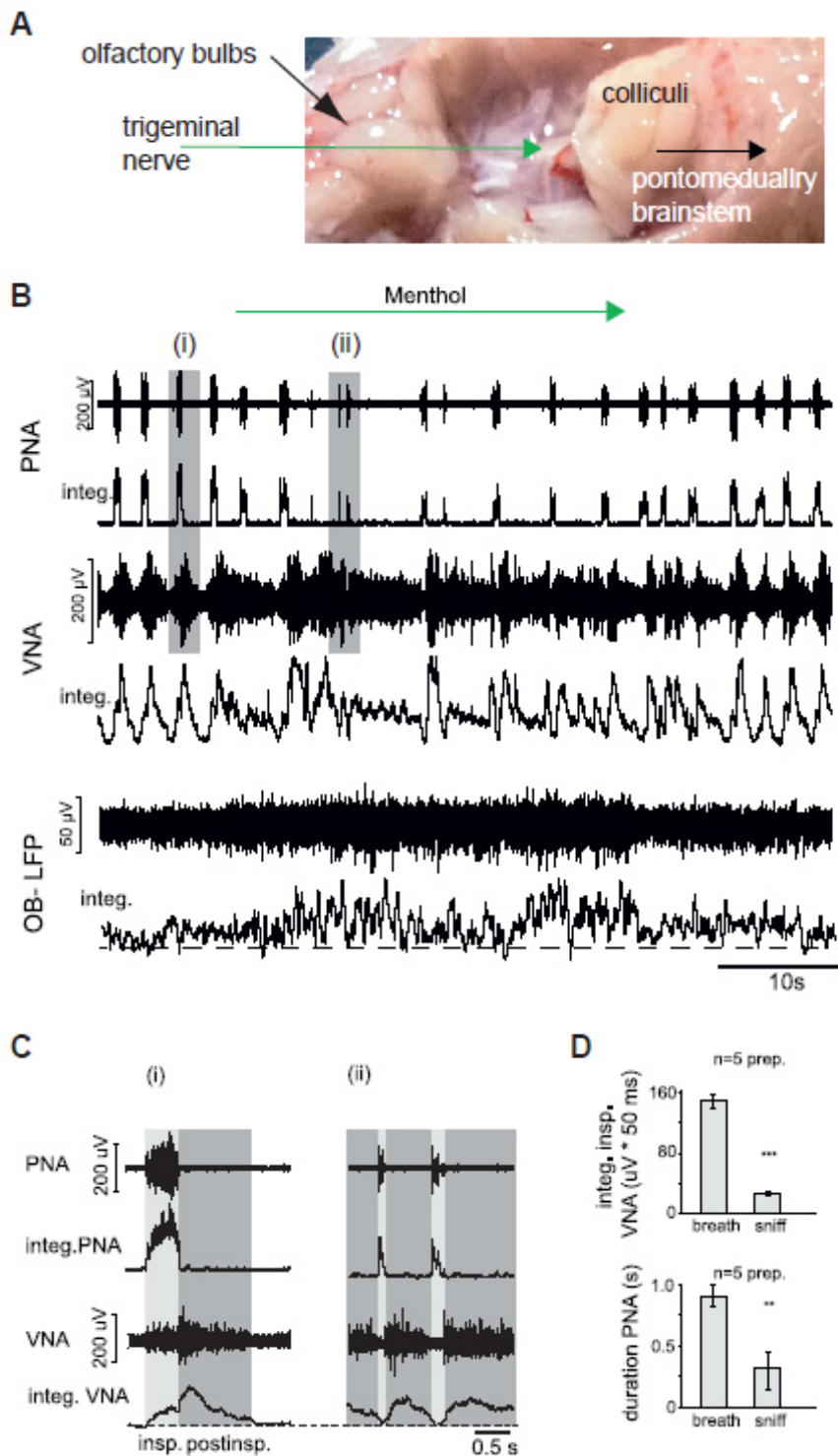
Figure 3. Simultaneous PNA, VNA and OB-LFP recordings during trigeminal odor stimulation .

(A) Photograph of the remaining brain areas in the semi-intact nose - olfactory bulb - brain-stem preparation. Observe that just the olfactory bulb, adjacent fragments to the bulb and the respiratory brainstem are anatomically intact. Since the midbrain is completely removed, there is not cortico-limbic modulation of respiratory activity (continue in the next page)

and all respiratory responses are directly modulated via the trigeminal pathway. (B) Representative experiment showing simultaneous recordings of the phrenic nerve activity (PNA), vagus nerve activity (VNA) and olfactory bulb local field potentials (OB-LFP) and corresponding integrated traces during trigeminal odor presentation (n=5 preparations). Exposure to menthol elicited a trigeminal response consisting of a change in the duration and amplitude of eupneic PNA bursts as well as the presence of fictive sniffing. Simultaneous recording of the VNA showed robust tonic activation during odor presentation. Grey boxes during baseline (i) and during odor presentation (ii) are magnified in (C). (i) Inspiratory (in phrenic and vagus nerves) and post-inspiratory (in vagus nerve) activity during baseline respiration (ii) Short-duration PNA bursts (fictive sniffing) in response to menthol. Note the difference of duration and amplitude of a normal burst of the PNA and VNA during baseline compared to stimulation. Note that VNA discharge is clearly interrupted during fictive sniffs. (D) Group data, sniff-associated VNA was significantly reduced in amplitude compared to eupneic VNA during inspiration (n= 5 preparations). Lower column bar graph: PNA burst during fictive sniffs showed a significant decrease in duration compared to baseline (p<0.001, paired t-test, n= 5 preparations)

4. Discussion

4.1   Respiratory responses to trigeminal odor.

The contribution of naso-trigeminal afferents to the modulation of primary cardio-respiratory networks of the brainstem is well established in the context of protective upper airway reflexes. Mechanical stimulation as well as irrigation and electrical stimulation of the anterior ethmoidal nerve can each trigger the diving response, which is characterized by breath-hold and bradycardia (Dutschmann and Paton 2002a; McCulloch et al., 1999; Panneton, 2013) or sneeze (Batsel and Lines, 1975; Wallois et al., 1995). The role of brainstem circuitries in the processing of trigeminal odorants was recognized decades ago (Allen, 1936; Adria, 1953), but remains poorly investigated compared to the perception and emotional significance of trigmeminal odors associated with activity in the cortico-limbic brain areas (Doty, 2001; Hummel et al., 2002; Iannilli et al., 2013; Jacquot et al., 2004). Although subconscious odor detection was proposed (Jacquot et al., 2004), the present study is the first to show the direct impact of trigeminal odor stimulation in a decerebrated, arterially perfused brainstem preparation. Our findings imply that trigeminal odors are perceived in the brainstem where they can trigger short sniffs and respiratory modulation.

4.2. Sniffing is not breathing: The respiratory motor pattern during brainstem mediated naso-trigeminally-evoked sniffing.

Sniffing is usually discussed in the context of exploratory and therefore conscious behavior (Ranade et al., 2013; Wesson et al., 2008). Sniffing is often described as breathing at elevated respiratory frequency that can be easily detected with thermo-couples or plethysmograph recordings of respiratory activity during olfactory tasks or in response to sensory-evoked arousal in behaving animals (Bondarenko et al., 2015; Canevali et al., 2013; Welker, 1964; Wesson et al., 2008, 2011; Wesson 2013).

The data obtained in the present study indicate that the motor pattern of sniffing is different from normal, eupneic breathing. The sniff-like motor pattern observed in the perfused brainstem preparation was characterized by significantly shorter inspiratory duration compared to eupneic respiratory activity. The short inspiratory burst duration

is in accordance with laryngeal-evoked reflex sniffs (Batsel and Lines, 1973; Tomori and Widdicombe, 1969), and with short duration diaphragm (100 ms) EMG bursts during odor sampling (Rojas-Libano and Kay, 2012). Furthermore, the eupneic respiratory motor pattern is defined by augmenting inspiratory activity in phrenic and vagal nerve recordings, followed by a distinct decrementing postinspiratory discharge during the early phase of expiration. The biphasic discharge of the vagal nerve is functionally linked to the dynamic regulation of upper airway patency (Dutschmann and Paton 2002c). The inspiratory discharge component reflects laryngeal abduction causing glottal dilation while the postinspiratory phase of the vagal discharge correlates with laryngeal adduction and ensuing transient glottal constriction. Contrary to this pattern, during fictive sniffs, the vagal nerve motor activity displayed tonic postinspiratory activity during the sniff-cycle interval that was transiently suspended during the short inspiratory bursts. Laryngeal adduction is also observed in humans during voluntary sniffing (Mukai, 1989) and was also suggested to occur during sensory-evoked sniffing in cat (Lawson et al., 1991).

The functional consequence of the present observations is that the glottis is mostly constricted during sniffing, except for the passive relaxation during the active inspiratory component of the sniff. At least three physiologically relevant implications ensue: (i) airway resistance needs to increase in order to generate the characteristic high nasal flow pressures during sniffing; (ii) restricted pulmonary inspiratory and particularly expiratory airflow would prevent excessive CO_2 exhalation during the high frequency sniffing, thus actively counteracting the rapid emergence of pathological hypocapnia (Gardner, 1996); and (iii) the limitation of inspiratory airflow would protect the lungs from the inhalation of larger amounts of potentially noxious substances (Dutschmann and Paton, 2002a; Panneton , 2013).

In addition to the observed laryngeal constriction, nasal resistance is actively modulated during sniffing. However, activity patterns of facial motor nerves innervating the intra-nasal musculature were not investigated in the present study.

4.4. The anatomical framework for the processing of naso-trigeminally-mediated olfaction.

Tracing studies have identified the primary terminal fields of the anterior ethmoidal and infraorbital nerves in the caudal nucleus of the sensory spinal-trigeminal tract (Sp5C, Jacquin and Rhoades, 1983; Panneton, 1991; Panneton et al., 2006). Additional terminal fields of the ethmoidal nerve are located in the nucleus of the solitary tract (NTS) and the pontine Kölliker-Fuse nucleus (KF, Panneton, 1991; Panneton et al., 2006). The second order projections of the caudal nucleus show a dense connectivity with the lateral ponto-medullary respiratory column (Panneton, 1991; Feil and Herbert, 1995). These pathways are consistently activated by nasal or ethmoidal nerve stimulation producing a sneeze or the diving response as shown in c-fos mapping studies (Dutschmann and Herbert, 1997; Jakus et al., 2004; McCulloch and Panneton, 1997; Wallois et al., 1995); however, no data are available for nasal stimulation with odorants.

4.5 Location and gating of a central pattern generator (CPG) for sniffing.

Our study shows that the sniff motor pattern is significantly different from the normal respiratory motor pattern. The differential motor patterns suggest that sniffing and eupneic breathing could be generated by separate CPGs. The existence of CPGs for specific oro-facial motor activities (e.g. swallowing, coughing and vocalizing) that functionally and anatomically partly overlap with the respiratory CPG is well accepted (Bianchi and Gestreau, 2009; Moore et al., 2014), but the anatomical location of the CPG for sniffing has not been explicitly identified. Since sniffing and whisking are highly coupled motor oscillations Moore et al., 2014; Welker, 1964), it is conceivable that the CPG for sniffing co-localizes with the recently identified CPG for whisking in the intermediate reticular formation dorso-medial to the pre-Bötzinger complex (Moore et al., 2013). While neither direct nor second order projections of the ethmoidal nerve appear to target this area (Panneton et al., 2006), the intermediate reticular formation is significantly activated after nasal stimulation with ammonia vapors (McCulloch and Panneton, 1997) and after naso-pharyngeal evoked sniff-like aspirations (Jakus et al., 2004).

The lack of direct trigeminal projections into the putative CPG for sniffing suggests that its activity is gated by other neural substrates that receive direct trigeminal input. A good candidate for the gating of the sniffing CPG could be the pontine KF nuclei, since they receive primary and secondary innervation from the naso-trigeminal system (Jacquin and Rhoades, 1983; Panneton, 1991; Panneton et al., 2006) and have a prominent role in the control of postinspiratory motor activity (Dutschmann and Herbert, 2006). Interestingly, KF-mediated modulation of postinspiratory motor output to the laryngeal constrictor muscles is already implicated in a large variety of oro-pharyngeal behaviors, including breath-hold during the ethmoidal nerve-mediated diving response (Dutschmann and Dick, 2012). The latter seems to be an important part of sniffing motor patterns as well. Further indirect evidence for a role of the KF in the gating of oro-facial motor CPGs is provided by a previous study that demonstrated KF-mediated gating of the medullary CPG for swallowing (Bautista and Dutschmann, 2014). Interestingly, both sniffing and swallowing are accompanied by high tonic postinspiratory drive towards laryngeal constrictor muscles. Thus, the initial modulation of airway resistance might be a prerequisite for the release of oro-facial motor CPGs.

Finally, the same brainstem pathways that convey nasal sensory information of the ethmoidal nerve could be activated via descending cortico-limbic projections. Evidence in support of this concept is provided by a recent study that showed a similar c-fos activation pattern in the ponto-medullary brainstem in naturally diving rats after transection of the ethmoidal nerves (McCulloch et al., 2016). These data suggest that the same brainstem circuits can be gated either by sensory protective reflex mechanisms (i.e. ethmoidal nerve stimulation) or behavioral commands arising from cortico-limbic systems after bilateral ethmoidal nerve transection (McCulloch et al., 2016). While, these data are restricted to the diving response so far, similar mechanisms may apply for the sniffing associated with odor perception.

Conclusions

The present study provides compelling evidence for brainstem-mediated processing of the trigeminal component of odorants that can trigger sub-consciously initiated fast sniffing and other respiratory modulations.

Acknowledgements

References

Adrian, E.D., 1953. Sensory messages and sensation; the response of the olfactory organ to different smells. Acta Physiol. Scand. 29(1), 5-14.

Allen, W.F., 1936. Studies on the level of anesthesia for the olfactory and trigeminal respiratory reflexes in dogs and rabbits. Am. J. Physiol. 115, 579-587.

Anton, F., Peppel, P., 1991. Central projections of trigeminal primary afferents innervating the nasal mucosa: a horseradish peroxidase study in the rat. Neurosci. 41(2-3), 617-628.

Anton, F., Peppel, P., Euchner, I., Handwerker, H.O., 1991. Controlled noxious chemical stimulation: responses of rat trigeminal brainstem neurones to CO_2 pulses applied to the nasal mucosa. Neurosci. Lett. 123, 208–211.

Batsel, H.L., Lines, A.J. Jr., 1973. Bulbar respiratory neurons participating in the sniff reflex in the cat. Exp. Neurol. 39, 469-481.

Batsel, H.L., Lines, A.J., 1975 Neural mechanisms of sneeze. Am. J. Physiol. 229(3), 770-776.

Bautista, T.G., Dutschmann, M., 2014. Ponto-medullary nuclei involved in the generation of sequential pharyngeal swallowing and concomitant protective laryngeal adduction in situ. J. Physiol. 592(12), 2605-2623.

Beidler, L.M., Tucker, D., 1956. Olfactory and trigeminal nerve responses to odors. Fed. Proceed. 15, 14.

Bessac, B.F., Jordt, S.E., 2008. Breathtaking TRP channels: TRPA1 and TRPV1 in airway chemosensation and reflex control. Physiology (Bethesda). 23, 360-70.

Bianchi, A.L., Gestreau, C., 2009. The brainstem respiratory network: an overview of a half century of research. Respir. Physiol. Neurobiol. 168(1-2), 4-12.

Bondarenko, E., Guimarães, D.D., Braga, V.A., Nalivaiko, E., 2015. Integrity of the dorsolateral periaqueductal grey is essential for the fight-or-flight response, but not the respiratory component of a defense reaction. Respir. Physiol. Neurobiol. doi: 10.1016/j.resp.2015.10.010.

Brand, G., 2006. Olfactory/trigeminal interactions in nasal chemoreception. Neurosci. Biobehav. Rev. 30(7), 908-917.

Buonviso, N., Amat, .C, Litaudon, P. 2006. Respiratory modulation of olfactory neurons in the rodent brain. Chem. Senses 31, 145–154.

Carnevali, L., Sgoifo, A., Trombini, M., Landgraf, R., Neumann, I.D., Nalivaiko, E., 2013. Different patterns of respiration in rat lines selectively bred for high or low anxiety. PLoS One. 8(5), e64519.

Doty, R.L., 2001. Olfaction. Annu Rev Psychol. 52:423-52.

Doty, R.L., Brugger, W.E., Jurs, P.C., Orndorff, M.A., Snyder, P.J., Lowry, L.D., 1978. Intranasal trigeminal stimulation from odorous volatiles: psychometric responses from anosmic and normal humans. Physiol. Behav. 20(2),175-185.

Du Pont., J.S., 1987. Firing patterns of bulbar respiratory neurones during sniffing in the conscious, non-paralyzed rabbit. Brain Res414, 163–168.

Dutschmann, M, Paton, J.F., 2002b Trigeminal reflex regulation of the glottis depends on central glycinergic inhibition in the rat. Am. J. Physiol. Regul. Integr. Comp. Physiol. 282(4), R999-R1005.

Dutschmann, M., Dick, T.E., 2012. Pontine mechanisms of respiratory control. Compr Physiol. 2(4), 2443-2469.

Dutschmann, M., Herbert, H., 1997. Fos expression in the rat parabrachial and Kölliker-Fuse nuclei after electrical stimulation of the trigeminal ethmoidal nerve and water stimulation of the nasal mucosa. Exp. Brain Res. 117(1), 97-110.

Dutschmann, M., Herbert, H., 2006. The Kölliker-Fuse nucleus gates the postinspiratory phase of the respiratory cycle to control inspiratory off-switch and upper airway resistance in rat. Eur. J. Neurosci. 24(4), 1071-1084.

Dutschmann, M., Paton, J,F., 2002a. Influence of nasotrigeminal afferents on medullary respiratory neurones and upper airway patency in the rat. Pflugers Arch. 444(1-2), 227-235.

Dutschmann, M., Paton, J.F., 2002c. Inhibitory synaptic mechanisms regulating upper airway patency. Respir. Physiol. Neurobiol. 2131(1-2), 57-63.

Elsharif, S.A., Banerjee, A., Buettner, A., 2015. Structure-odor relationships of linalool, linalyl acetate and their corresponding oxygenated derivatives. Front Chem. 3, 57.

Farmer, D.G., Bautista, T.G., Jones, S.E., Stanic, D., Dutschmann, M., 2014. The midbrain periaqueductal grey has no role in the generation of the respiratory motor pattern, but provides command function for the modulation of respiratory activity. Respir. Physiol. Neurobiol. 204, 14-20.

Feil, K., Herbert, H., 1995. Topographic organization of spinal and trigeminal somatosensory pathways to the rat parabrachial and Kölliker-Fuse nuclei. J. Comp. Neurol. 353(4), 506-528.

Firestein, S., 2001. How the olfactory system makes sense of scents. Nat. 413(6852), 211-218.

Gardner, W.N., 1996. The pathophysiology of hyperventilation disorders. Chest. 109(2), 516-534

Hummel, T., Livermore, A., 2002. Intranasal chemosensory function of the trigeminal nerve and aspects of its relation to olfaction. Int. Arch. Occup. Environ. Health. 75(5), 305-313.

Iannilli, E., Wiens, S., Arshamian, A., Seo, H.S., 2013. A spatiotemporal comparison between olfactory and trigeminal event-related potentials. Neuroimage 77, 254-261.

Jacquin, M.F., Rhoades, R.W., 1983. Central projections of the normal and 'regenerate' infraorbital nerve in adult rats subjected to neonatal unilateral infraorbital lesions: a transganglionic horseradish peroxidase study. Brain Res. 269(1), 137-144.

Jacquot, L., Monnin, J., Brand, G., 2004. Influence of nasal trigeminal stimuli on olfactory sensitivity. C. R. Biol. 327(4), 305-311.

Jacquot, L., Monnin, J., Brand, G., 2004. Unconscious odor detection could not be due to odor itself. Brain Res. 1002(1-2), 51-54.

Jakus, J., Halasová, E., Poliacek, I., Tomori, Z., Stránsky, A., 2004. Brainstem areas involved in the aspiration reflex: c-Fos study in anesthetized cats. Physiol. Res. 53(6), 703-17.

Kepecs, A., Uchida, N., Mainen, Z.F., 2006. The sniff as a unit of olfactory processing. Chem. Senses 31(2), 167-179.

Lawson, E.E., Richter. D.W., Czyzyk-Krzeska, M.F., Bischoff, A., Rudesill, R.C., 1991. Respiratory neuronal activity during apnea and other breathing patterns induced by laryngeal stimulation. J. Appl. Physiol. 70(6), 2742-2749.

McCulloch, P.F., Faber, K.M., Panneton, W.M., 1999. Electrical stimulation of the anterior ethmoidal nerve produces the diving response. Brain Res. 830(1),24-31.

McCulloch, P.F., Panneton, W.M., 1997. Fos immunohistochemical determination of brainstem neuronal activation in the muskrat after nasal stimulation. Neuroscience. 78(3), 913-925.

Mcculloch, P.F., Warren, E.A., DiNovo, K.M., 2016. Repetitive Diving in Trained Rats Still Increases Fos Production in Brainstem Neurons after Bilateral Sectioning of the Anterior Ethmoidal Nerve. Front. Physiol. 7:148.

Moore, J.D., Deschênes, M., Furuta, T., Huber, D., Smear, M.C., Demers, M., Kleinfeld, D., 2013. Hierarchy of orofacial rhythms revealed through whisking and breathing. Nat. 497(7448), 205-210.

Moore, J.D., Kleinfeld, D., Wang, F., 2014 How the brainstem controls orofacial behaviors comprised of rhythmic actions. Trends Neurosci. 37(7), 370-380.

Mukai, S., 1989 Vocal cord adduction while sniffing. Arch Otolaryngol Head Neck Surg. 115(11), 1362-1366.

Panneton, W.M., 1991. Primary afferent projections from the upper respiratory tract in the muskrat. J. Comp. Neurol. 308(1):51-65.

Panneton, W.M., 2013. The mammalian diving response: an enigmatic reflex to preserve life? Physiol. (Bethesda). 28(5), 284-297.

Panneton, W.M., Gan, Q., Juric, R., 2006. Brainstem projections from recipient zones of the anterior ethmoidal nerve in the medullary dorsal horn. Neuroscience. 141(2), 889-906.

Paton, J.F., 1996. A working heart-brainstem preparation of the mouse. J Neurosci. Methods. 65(1), 63-68.

Peier, A.M., Moqrich, A., Hergarden, A.C., Reeve, A.J., Andersson, D.A., Story, G.M., Earley, T.J., Dragoni, I., McIntyre, P., Bevan, S., Patapoutian, A., 2002. A TRP channel that senses cold stimuli and menthol. Cell 8;108(5), 705-15.

Pérez de los Cobos Pallarés, F., Stanic, D., Farmer, D., Dutschmann, M., Egger, V., 2015. An arterially perfused nose-olfactory bulb preparation of the rat. J. Neurophysiol. 114(3), 2033-2042.

Ranade, S., Hangya, B., Kepecs, A., 2013. Multiple modes of phase locking between sniffing and whisking during active exploration. J. Neurosci. 33(19), 8250-8256.

Rojas-Líbano, D., Kay, L.M., 2012. Interplay between sniffing and odorant sorptive properties in the rat. J. Neurosci. 32(44), 15577-15589.

Tomori, Z., Widdicombe, J.G., 1969. Muscular, bronchomotor and cardiovascular reflexes elicited by mechanical stimulation of the respiratory tract. J. Physiol. 200(1), 25-49.

Wachowiak, M., 2011. All in a sniff: olfaction as a model for active sensing. Neuron. 71(6), 962-673.

Wallois, F., Gros, F., Masmoudi, K., Larnicol, N., 1995. C-Fos-like immunoreactivity in the cat brainstem evoked by sneeze-inducing air puff stimulation of the nasal mucosa. Brain Res. 687(1-2), 143-154.

Welker, W.I., 1964. Analysis of Sniffing of the Albino Rat. Behaviour. 22 (3), 223 – 244.

Wesson, D.W., 2013. Sniffing behavior communicates social hierarchy. Curr Biol. 23(7):575-580.

Wesson, D.W., Donahou, T.N., Johnson, M.O., Wachowiak, M., 2008. Sniffing behavior of mice during performance in odor-guided tasks. Chem Sens. 33(7), 581-596.

Wesson, D.W., Donahou, T.N., Johnson, M.O., Wachowiak, M., 2008.Sniffing behavior of mice during performance in odor-guided tasks. Chem Senses. 33(7), 581-596.

Wesson, D.W., Varga-Wesson, A.G., Borkowski, A.H., Wilson, D.A., 2011. Respiratory and sniffing behaviors throughout adulthood and aging in mice. Behav. Brain Res. 223(1), 99-106.

Widdicombe. J.G., 1986. The physiology of the nose. Clin. Chest. Med. 17(2), 59-70.

3.3. Sniff-like patterned input results in long-term plasticity at the rat olfactory bulb mitral and tufted cell to granule cell synapse.

Research Article

Sniff-Like Patterned Input Results in Long-Term Plasticity at the Rat Olfactory Bulb Mitral and Tufted Cell to Granule Cell Synapse

Mahua Chatterjee,[1] Fernando Perez de los Cobos Pallares,[1,2] Alex Loebel,[1,3] Michael Lukas,[2] and Veronica Egger[1,2]

[1]*Department of Biology II, Ludwig-Maximilians-University, Grosshadernerstr. 2a, 82152 Martinsried, Germany*
[2]*Regensburg Center of Neuroscience, Regensburg University, Universitätsstr. 30, 93040 Regensburg, Germany*
[3]*Bernstein Center for Computational Neuroscience, Grosshadernerstr. 2a, 82152 Martinsried, Germany*

Correspondence should be addressed to Veronica Egger; veronica.egger@ur.de

During odor sensing the activity of principal neurons of the mammalian olfactory bulb, the mitral and tufted cells (MTCs), occurs in repetitive bursts that are synchronized to respiration, reminiscent of hippocampal theta-gamma coupling. Axonless granule cells (GCs) mediate self- and lateral inhibitory interactions between the excitatory MTCs via reciprocal dendrodendritic synapses. We have explored long-term plasticity at this synapse by using a theta burst stimulation (TBS) protocol and variations thereof. GCs were excited via glomerular stimulation in acute brain slices. We find that TBS induces exclusively long-term depression in the majority of experiments, whereas single bursts ("single-sniff paradigm") can elicit both long-term potentiation and depression. Statistical analysis predicts that the mechanism underlying this bidirectional plasticity involves the proportional addition or removal of presynaptic release sites. Gamma stimulation with the same number of APs as in TBS was less efficient in inducing plasticity. Both TBS- and "single-sniff paradigm"-induced plasticity depend on NMDA receptor activation. Since the onset of plasticity is very rapid and requires little extra activity, we propose that these forms of plasticity might play a role already during an ongoing search for odor sources. Our results imply that components of both short-term and long-term olfactory memory may be encoded at this synapse.

1. Introduction

Basal activity of the mammalian olfactory bulb is synchronized to breathing; during odor sensing the principal neurons of the olfactory bulb, the mitral and tufted cells (MTCs), are firing in repetitive bursts that are locked to the breathing rhythm [1–4]. This property is reminiscent of theta-gamma coupling in the hippocampus [5]. In the bulb, the fast component is by now known to be mostly driven by interactions between the excitatory MTCs and the inhibitory granule cells via a special type of microcircuit, a reciprocal synapse between the lateral dendrites of MTCs and the large GC spines that are also known as gemmules. The specific subtype of fast bulbar network oscillation—fast gamma, slow gamma, and/or beta—is related to the principal cell type and/or sublamina of the external plexiform layer involved, as well as the behavioral state of the animal which is reflected in different top-down interactions [6, 7]. MCs and TCs also differ with respect to the respiratory phase that their peaks of activity are locked to and the "burstiness" of their spiking [3, 8, 9].

With respect to a potential site for olfactory memory-related synaptic plasticity in mammals, MTCs project to the piriform cortex and numerous other higher olfactory areas, and subregions of the piriform cortex are involved in the synthesis and categorization of the odor percept, while conscious perception of odors most likely arises from the yet higher orbitofrontal cortex (reviewed in [10]). However,

it is known that odor recognition and discrimination, tasks that clearly involve aspects of memory, are to some extent already performed by olfactory bulb circuits, in particular by the reciprocal synapse mentioned above, since modification of GCs' postsynaptic receptors of the NMDA-, AMPA-, and GABA$_A$-type was shown to influence the speed of odor discrimination between highly overlapping mixtures and odor learning can be facilitated also by other interventions in GCs [11–14]. Thus, the MTC-GC synapse can decode stimulus properties and might serve as a locus of long-term plasticity.

Theta-gamma coupling in the form of theta burst stimulation (TBS) is known to induce long-term plasticity in the hippocampus, probably even more effectively than the classical high frequency stimulation (reviewed in [15]). As to TBS-induced plasticity at the MTC to GC synapse so far, a study by Ma et al. [16] observed LTD in granule cells following TBS in the external plexiform layer. We used a similar approach, yet based on glomerular stimulation which depolarizes individual glomeruli and thus consistently activates "sister mitral and tufted cells" that belong to the same glomerulus and the surrounding periglomerular circuitry. Compared to extracellular stimulation in the external plexiform layer, this paradigm should correspond to a more physiological situation with respect to activation of bulbar circuits during breathing since it stimulates the sensory input pathway instead of an accidental set of local synaptic connections.

We also applied variations of TBS, in particular a stimulation paradigm that attempts to mimic odor perception during just a single sniff. These investigations might prove illuminating in the context of natural odor sources in the wild because of two aspects. First, due to turbulent airflow odor molecule concentrations are unlikely to decline with distance from the odor source in a monotonic fashion; rather, patches of odor molecules separate from the original odor plume while drifting downwind. Thus odor detection is expected to be highly discontinuous (e.g., [17]), a notion that also increasingly influences studies on insect olfaction [18–21]. Second, it was observed that indeed rats can detect and discriminate odors within single sniffs [22, 23] and that they use casting techniques to track down patchy odor trails [24]. The single-sniff (or rather single-whiff-of-odor) scenario is thus likely to repeatedly occur within tens of seconds during the search for an odor source or during exploration of novel environments.

In summary, our study aims to determine whether plasticity at the MTC-GC synapse can be elicited by induction patterns based on coincident bulbar respiratory rhythmic activity and olfactory inputs.

2. Materials and Methods

2.1. Preparation of Brain Slices and Whole-Cell Recording. All experiments were carried out according to national and institutional guidelines, the rules laid down by the EC Council Directive (86/89/ECC) and German animal welfare. Animals were deeply anaesthetized with isoflurane and decapitated. Sagittal olfactory bulb brain slices were prepared of juvenile Wistar rats (thickness 300–350 μm; postnatal day (PND) 11–17). Neurons were visualized by infrared gradient-contrast illumination via an IR filter (Hoya, Tokyo, Japan) and patched with pipettes sized 6–8 MΩ. Somatic whole-cell patch-clamp recordings were performed with EPC-9 (HEKA, Lambrecht, Germany). Series resistances measured 10–40 MΩ.

The intracellular solution contained [mM] 130 K-methylsulfate, 10 HEPES, 4 MgCl$_2$, 4 Na$_2$ATP, 0.4 NaGTP, 10 Na phosphocreatine, and 2 ascorbate, at pH 7.2. The extracellular artificial cerebrospinal fluid was gassed with carbogen and contained [mM] 125 NaCl, 26 NaHCO$_3$, 1.25 NaH$_2$PO$_4$, 20 glucose, 2.5 KCl, 1 MgCl$_2$, and 2 CaCl$_2$. Due to the fragility of long-term granule cell recordings, experiments were performed at room temperature (~21°C). GCs were identified by their morphological appearance and the shape of current-evoked APs and firing [25]. The average input resistance of the investigated GCs was on the order of 1 GΩ and their resting potential was ranging from −80 to −70 mV, similar to our previous data [25, 26]. Leaky GCs with a holding current above ~−30 pA were rejected. A stable resting potential V_m (within a narrow range of a few mV) was found to be paramount for stable EPSP amplitude recordings; experiments that showed a substantial drift in V_m were rejected.

2.2. Extracellular Activation of MTCs. Glomerular stimulation was performed with a custom-built four-channel-electrode (Figure 5(b)). The four electrodes consisted of Teflon-coated silver wires (diameter uncoated 75 μm, coated 140 μm, item AG-3T, Science Products GmbH, Hofheim, Germany) and were aligned in parallel at a distance of 200 μm across two screws with the according pitch and embedded in epoxy glue. The electrode was connected to a 4-channel stimulator (STG 1004, Multi Channel Systems, Reutlingen, Germany), which is controlled from a PC via an USB connection. In current mode, the maximal stimulation strength per channel is 800 μA. The grounds from the stimulator channels were connected to a common wire and then to the bath. Alternatively, the ground was connected to the fourth stimulator wire; however, the first configuration was generally preferred due to its larger choice of stimulation options. The 4-channel electrode was lowered on top of the acute brain slice under visual control using a manual manipulator (Scientifica, East Sussex, UK). The stimulation strength was adjusted via the stimulator's software on the PC; the output of the stimulator was triggered from the electrophysiology software (Pulse, HEKA, Lambrecht, Germany). Stimulation strengths sufficient to elicit GC EPSPs were mostly in the range of 100–400 μA.

The 4-channel electrode was positioned on an olfactory bulb slice such that at least two electrode wires were located within individual glomeruli, usually with one nonstimulated glomerulus in between, since the diameter of a glomerulus is on the order of 100 μm (Figure 5(a)). This arrangement served two purposes, first to increase the success rate for finding connected granule cells and second to test for homosynaptic plasticity via intermittent stimulation of two separate glomerular inputs. Each of the two wires was found

to activate independent sets of synaptic inputs onto granule cells, as shown in Figure 5(c).

Previously we have shown that direct glomerular stimulation results in single MC spikes [25], with a latency between stimulation onset and MC AP peak of 4.9±4.4 ms ($n = 6$). The latencies between stimulation onset and the first granule cell EPSP of the responses observed here were thus in accordance with monosynaptic excitation of GCs via MTCs (5.6 ± 2.4 ms, $n = 28$).

2.3. Plasticity Measurement Including Induction Protocols. Synaptic plasticity experiments involved

(i) control: recording of a stable EPSP control at 0.1 Hz for 10 minutes,

(ii) induction: repetition of individual induction protocol at 0.1 Hz, 10 times,

(iii) long-term: recording of EPSPs at 0.1 Hz for at least 30 minutes.

The induction protocols used the same stimulation strength as the control recordings. All phases of the experiments used the same stimulation channel, except for the experiments on homoglomerular plasticity where a second channel was stimulated intermittently and no induction was applied to this second channel. Theta burst stimulation (TBS) involved five bursts at 40 Hz with 4 APs each, spaced at 4 Hz. "Θ-only" stimulation consisted of five APs at 4 Hz and "γ-only" stimulation of 20 APs at 40 Hz (same number of spikes as in TBS). Single burst stimulation (SBS) used just one burst at 40 Hz with 4 APs. All induction protocol sequences are shown in Figure 4(a).

2.4. Data Analysis and Selection. Analysis of EPSPs was performed using custom-written software based on Igor Pro (Wavemetrics, Lake Oswego, Oregon), as previously described [26]. Percentage values indicate the change in EPSP amplitude relative to the mean control amplitude. Each data point represents an average of 3.33 min of recording (22 sweeps maximum per point). The average long-term mean EPSP amplitude of an experiment was calculated across the interval of 10–30 min after induction or longer if the recording persisted (see Figure 1(d)). Before averaging across experiments, the EPSP amplitudes of each experiment were normalized to the mean control EPSP amplitude. Failures were very rarely observed and thus not accounted for in the analysis. The coefficient of variation (CV) was calculated as the standard deviation across EPSP amplitudes divided by their mean. It was analyzed only for TBS or SBS experiments; experiments with a high spontaneous activity or multiple response peaks where a precise determination of the first response amplitude was often compromised were excluded from CV analysis.

The criterion for successful induction of long-term plasticity was a stable change in the long-term mean EPSP amplitude of at least ±10% relative to the control average.

Cumulative data of whole sets of experiments are represented as mean ± standard deviation of the mean (SD).

Experimental data points and averages of data sets were compared statistically using nonparametric tests (Wilcoxon test for paired data sets and Mann-Whitney test for unpaired data). All averages are given ± SD unless indicated otherwise.

Short-term plasticity was measured in terms of relative fractions (later EPSP amplitudes divided by first EPSP amplitude). Later amplitudes were measured from the membrane potential right before the respective stimulus artifact, since fitting of the decay of V_m was not possible at 40 Hz. Thus later amplitudes are slightly underestimated, depending on the rise time of the EPSP.

2.5. Quantal Analysis of the SBS Experiments. The quantal properties of the synapses measured at the SBS experiments were estimated by fitting the mean and CV of their responses to the relevant measures of the quantal model of synaptic transmission [27]. In particular, a synaptic connection is considered to be composed of N independent release sites, from which a maximum of a single vesicle per site is released with probability p upon the arrival of a presynaptic action potential. Subsequently, the vesicle contributes a quantum q to the postsynaptic response. In the simplest case, in which the synaptic response variability is only governed by the vesicle release events (and not by other noise sources [28]), the expected mean and variance of the responses are

$$\text{Mean} = N \cdot p \cdot q, \tag{1}$$

$$\text{Variance} = q^2 \cdot N \cdot p \cdot (1 - p). \tag{2}$$

Subsequently, CV is

$$\text{CV} = \frac{\sqrt{\text{Variance}}}{\text{Mean}} = \frac{\sqrt{q^2 \cdot N \cdot p \cdot (1 - p)}}{N \cdot p \cdot q}$$
$$= \frac{1}{\sqrt{N}} \cdot \sqrt{\frac{1 - p}{p}}. \tag{3}$$

We used the following approach in order to fit the quantal parameters N, p, and q to the synaptic connections of the SBS experiments: an average release probability was assumed for the release sites at the control and long-term phases of the experiments, p_{control} and $p_{\text{long-term}}$. For each value of these probabilities (range 0.05–0.95), the number of release sites, $N_{i,\text{control}}$ (or for the long-term phase $N_{i,\text{long-term}}$) that explain best the experimental CV was calculated for each synaptic connection i (index i, running from 1 to the total number of SBS experiments within the CV analysis). Subsequently, the value of p_{control} ($p_{\text{long-term}}$) and the related set of $N_{i,\text{control}}$ ($N_{i,\text{long-term}}$) that minimized the overall mean-square distance of the fitted CVs from the measured CVs were the values that we assigned to the synaptic connection. Finally, $q_{i,\text{control}}$ ($q_{i,\text{long-term}}$) value of the release sites of a given synaptic connection was calculated from (1), by considering its measured mean response amplitude and the fitted p_{control} ($p_{\text{long-term}}$) and $N_{i,\text{control}}$ ($N_{i,\text{long-term}}$).
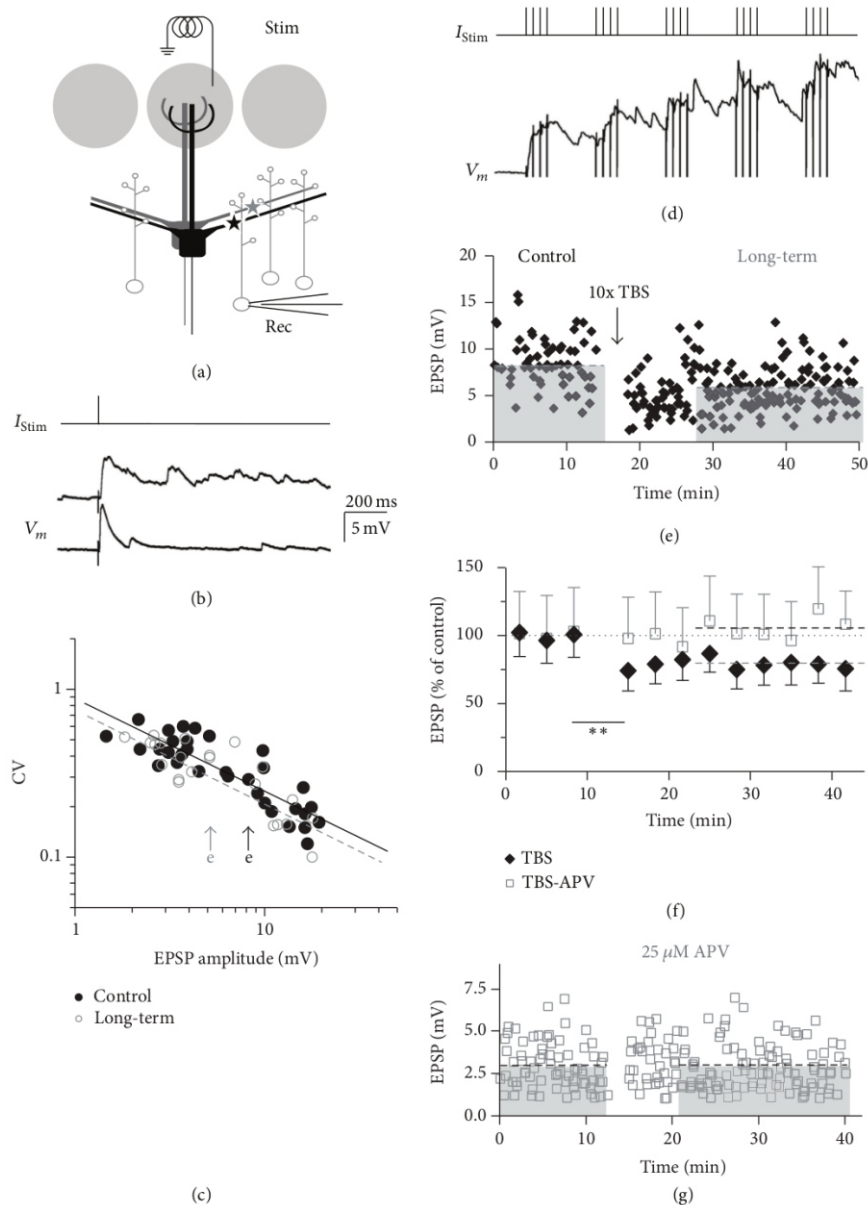
FIGURE 1: TBS induces LTD at the MTC-GC synapse. (a) Experimental design [25]. Glomerular stimulation (Stim) will activate the glomerular ensemble of mitral cells to a varying extent (depending on stimulation strength); thus inputs from several mitral cells onto the recorded GC (Rec) will be activated. (b) Response of individual granule cell to single glomerular stimulation (two individual responses shown, note the barrage of activity in the second response). (c) Coefficients of variation of EPSP amplitude of synaptic connections versus their mean EPSP amplitude for control data (black dots) and long-term data (grey circles). For control, the fit has a slope of -0.55 ± 0.06 (mean $\pm$ SD) on the log scale (black line) and for long-term the slope was -0.56 ± 0.08. The confidence intervals were calculated from $n = 200$ bootstrap replicas of the data. The arrows mark the data points from the connection shown in (e). (d) Response of the cell from (b) to TBS (average of the total of 10 stimulations). (e) EPSP amplitudes from individual GC recordings from the cell in (b) and (d) over time. Control mean 8.1 mV; long-term mean 6.3 mV (dashed lines). (f) Cumulative data (normalized to control) of all experiments with substantial LTD (black diamonds, $n = 10$) and of all experiments in the presence of 25 μM APV (grey squares, $n = 6$). Respective long-term averages shown as dashed lines (grey for TBS and black for TBS in APV). All data points $\pm$ SD across experiments. (g) Representative individual experiment in the presence of 25 μM APV. Control mean 2.9 mV; long-term mean 2.7 mV (dashed black lines). [**]The degree of the statistical difference between the last data point before TBS and the first data point after TBS (black diamonds).

3. Results

3.1. Properties of Synaptic Transmission between Glomeruli and Granule Cells.
To elicit granule cell EPSPs we stimulated single glomeruli with a monopolar, four-channel electrode (Figure 1(a); see Section 2.2). Individual MTC to GC synaptic connections are thought to involve no more than one single synaptic contact because of their anatomical arrangement [29], with a median unitary EPSP size at the soma of 2 mV [30]. Since we did not apply minimal stimulation, the recorded EPSPs were mostly not unitary but involved activation of several presynaptic MTCs (average EPSP size across all experiments without presence of APV 8.9 ± 6.4 mV, median 8.3 mV, range 1.4–31.2 mV, $n = 52$; similar EPSP distributions within sets of experiments; see the following).

In roughly half of the experiments, we observed a barrage of network activity following the first EPSP (see Figure 1(b)), which is likely due to stimulation of the OSN axon bundle leading up to a glomerulus, depending on the placement of the four-channel stimulator [31]. For evaluation of plasticity we analyzed only the first EPSP after stimulation; the occurrence of barrages was not correlated with the amplitude of the first EPSP ($r = -0.05$, $n = 45$).

The average coefficient of variation (CV) for these parallel inputs to a single GC was 0.35 ± 0.15 ($n = 32$, excluding experiments where the first EPSP was frequently summated with network activity). Figure 1(c) shows that on the logarithmic scale the CV values were linearly dependent on the mean EPSP amplitude, with fitted slopes of $-0.55 ± 0.06$ for the control and $-0.56 ± 0.08$ for the long-term measurement phase (mean ± SD from bootstrapping).

To control for systematic rundown, we performed 5 experiments where we recorded EPSPs for 30 min without any intervention. With a normalized average amplitude in the first 10 minutes (control) of 100 ± 28% ($n = 177$ data points), the average amplitude in the last 10 minutes was 101 ± 29% ($n = 172$ data points). Also, none of the individual experiments showed any depression in EPSP amplitude in the last 10 minutes compared to the first 10 minutes according to our criterion (>10% change below control). Moreover, we did not observe a systematic rundown over the entire recording period (40 min) in experiments with no induction in the recorded glomerular channel (see, e.g., Figure 6(d)). Thus GC EPSPs were generally stable at the basal stimulation frequency of 0.1 Hz.

At both of the higher stimulation frequencies used in the induction protocols (4 Hz and 40 Hz), the MTC-GC synapses underwent short-term depression after more than two pulses, while paired pulses showed either facilitation or depression, with a prevalence of depression (Figures 2(a)–2(d)). At 4 Hz ($n = 10$ GCs), the mean ratio of the second EPSP amplitude to the first (the paired pulse ratio) was 0.99 ± 0.12 ($P = 0.15$) and from the fifth to the first 0.69 ± 0.15 ($P < 0.01$, cf. Figure 2(a) for an individual example). At 40 Hz ($n = 10$ GCs), the mean ratio of the second EPSP amplitude to the first was 0.77 ± 0.51 ($P < 0.05$) and from the fifth to the first 0.28 ± 0.23 ($P < 0.01$, cf. Figures 2(b) and 1(d)).

3.2. Plasticity Induction by Θ-γ Coupling.
Our criterion for successful induction of long-term plasticity was a stable change in EPSP amplitude of at least 10% away from the control average that persisted from 10 to 30 min after induction. The TBS protocol reliably induced long-term depression (LTD) of EPSP amplitudes in most GCs tested (to 73 ± 13% of control, $n = 10$ of 14 experiments, $P < 0.005$, Figure 1(d)). If the remaining 4 cells were included, the average depression reached 82 ± 19% of control and was still highly significant ($P < 0.005$, distribution of all TBS-data shown in Figure 4(a)). There was no correlation between the mean control EPSP amplitude and the mean long-term EPSP amplitude ($P = 0.94$).

Onset of TBS-induced LTD was rapid (Figures 1(e) and 1(f)), as also evident from comparing the first data point after induction with control and the later data points: the mean EPSP amplitudes from the first averaged bin after induction were significantly below those from the last bin before induction (comparison of data means across experiments, Wilcoxon test, $P < 0.01$, $n = 10$) and at the same time statistically not different from for example the 5th bins after induction ($P = 0.45$). This observation also argues against systematic rundown.

In $n = 3$ experiments, the stability of GC recordings allowed for more than one induction with TBS. In 2 of these further LTD could be induced at 30 min after the first induction (to 75 ± 9% of the already depressed EPSP). Thus, this form of plasticity is most likely not saturated by a single induction.

Interestingly, postsynaptic spiking during TBS was no prerequisite for LTD induction since EPSP summation sufficient for spike generation occurred in only 7 out of the 14 experiments during induction, including 2 of the 4 experiments with no LTD. The mean long-term values relative to control between the two groups were not significantly different ($n = 7$ each, 87 ± 10% with spikes versus 76 ± 24% without, $P = 0.18$).

Next we tested whether the occurrence of barrages of network activity was related to the degree of plasticity induction. There was no correlation between the half duration $\tau\_1/2$ of the averaged control compound EPSP and the amount of LTD ($r = -0.31$, $P = 0.32$); changes in network activity after plasticity induction as measured by the ratio of the half duration value of the long-term phase to the control phase were also uncorrelated ($r = -0.25$, $P = 0.44$, each $n = 12$).

NMDA receptors play a major role at the MTC-GC synapse [25, 32]. Therefore, we blocked NMDA receptors by adding 25 μM APV to the bath from the beginning of the experiment. In the presence of APV, TBS no longer resulted in LTD (104 ± 17% of control, $n = 6$, $P < 0.05$ versus TBS without APV, Figures 1(f) and 1(g)).

Next, we were interested to see whether variations of the theta burst pattern might be also effective in plasticity induction. Theta stimulation alone ("Θ-only"; 87 ± 21%, $n = 8$, $P = 0.11$ versus no change, i.e., 100%, including 2 experiments without plasticity induction) or a train of 20 stimulations at gamma frequency ("γ-only"; 88 ± 10%, $n = 9$, $P = 0.07$ versus no change, i.e., 100%, including 3 experiments without plasticity induction; equal total number
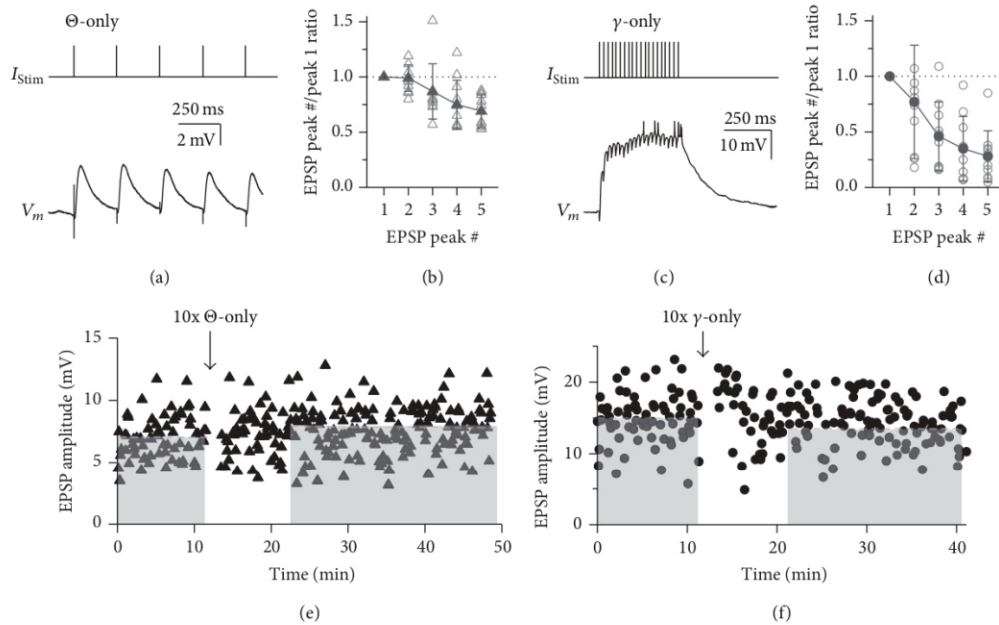
FIGURE 2: Short- and long-term plasticity in response to Θ-only and γ-only stimulation. (a) Representative example of response to Θ-only protocol averaged over the total of 10 stimulations. (b) Cumulative data of EPSP amplitude ratios relative to first peak in train ($n = 10$ cells). Open symbols: individual experiments. Solid symbols: averaged data. (c) Same as in (a) but for γ-only protocol. (d) Same as in (b) but for γ-only protocol. Cumulative data of EPSP amplitude ratios relative to first peak in train ($n = 10$ cells). (e, f) EPSP amplitudes of individual long-term experiments with induction responses shown in (a) and (c), respectively. Cumulative data for both Θ-only and γ-only data sets are shown in Figure 4(a). (e) Θ-only. Control mean 7.5 mV; long-term mean 8.1 mV (dashed lines). (f) γ-only. Control mean 15.1 mV; long-term mean 13.0 mV (dashed lines).

of stimulations in γ-only and TBS) were apparently less effective in inducing substantial plastic changes (see Figures 2(a) and 2(d) for individual experiments and Figure 4(a) for cumulative data). However, a more efficient induction of LTD by TBS compared to the two variants of the TBS paradigm could not be proven by statistical analysis due to the large variance across experiments within data sets. The distributions of control EPSP amplitudes for these sets of experiments were statistically indistinguishable from the respective distribution for the TBS experiments (Θ-only versus TBS: $P = 1$ and γ-only versus TBS: $P = 0.49$).

3.3. Plasticity Induction by "Single Sniff" Stimulation. Since it was observed by several groups that rats and other mammals, including humans, can detect and discriminate odors within single sniffs [33], we have also applied a "single sniff paradigm" using just a single 40 Hz burst for ten times at 0.1 Hz (single burst stimulation, SBS). Subsequently, either LTD or LTP or no plasticity was observed (total experiments $n = 32$; LTD: $76 \pm 10\%$ of control, $n = 13$, Figure 3(a); LTP: $145 \pm 40\%$, $n = 10$, Figure 3(b); no effect: $n = 9$). The average long-term mean of all SBS experiments was $104 \pm 37\%$, indicating a possible homeostatic mechanism of plasticity induction (see the following). The distribution of control mean EPSP amplitudes was not significantly different

from the respective distribution for TBS experiments ($P = 0.81$).

Again, onset of plasticity was often rapid for both LTP and LTD, as seen in the example experiments in Figure 3. Although overall this change was not yet significant between the last data bin before and the first bin after induction (in contrast to the TBS experiments), it became substantial across experiments for the last bin before and the second bin after induction (3.3–6.7 min after induction) for both LTP ($n = 10$, $P < 0.01$) and LTD ($n = 12$, $P < 0.005$, Figure 3(c)).

Similar to the LTD induced by TBS, bidirectional plasticity was independent of the occurrence of GC sodium spikes (Figure 3(d)) or the maximal depolarization during the induction in experiments without spikes (correlation coefficient $r = -0.29$, $P = 0.41$, and $n = 18$). Larger EPSPs involving more MTC-GC synapses showed less plasticity than small EPSPs (Figure 3(d)); see the following.

To better compare the effectiveness of the various paradigms for induction of plasticity, we define the parameter "long-term efficiency" or ΔLT as the absolute value of the difference between the average long-term mean relative to control and 100%, that is, control itself, which allows measuring the degree of bidirectional plasticity independently of its sign (ΔLT = |(long term mean normalized to control − 100%)|). The values for ΔLT for all induction paradigms
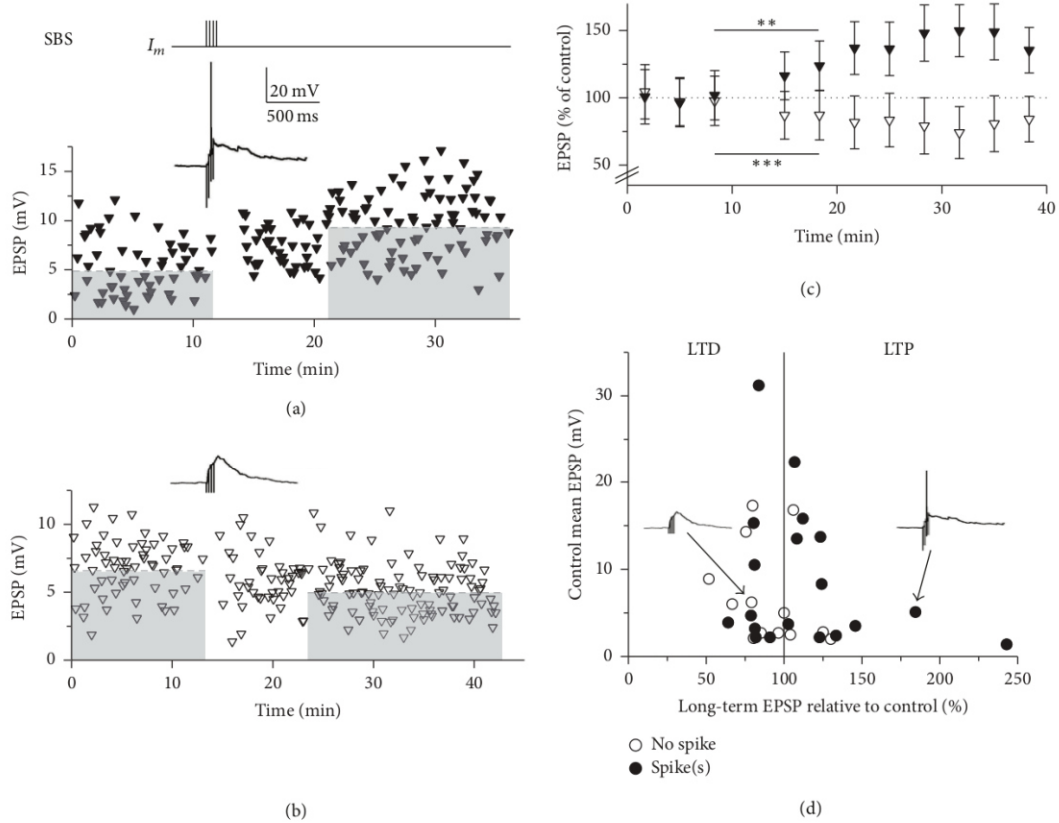
FIGURE 3: Single burst stimulation (SBS) results in bidirectional plasticity. Top: SBS induction protocol. (a) Individual experiment resulting in LTP. Control mean 5.1 mV; long-term mean 9.4 mV (dashed lines). Inset shows averaged response to SBS stimulation. (b) Individual experiment resulting in LTD. Control mean 6.2 mV; long-term mean 4.9 mV (dashed lines). Inset shows averaged response to SBS stimulation (same scale as in (a)). (c) Cumulative data (normalized to control) of SBS experiments with substantial LTP (solid triangles, $n = 10$) and substantial LTD (open triangles, $n = 10$). All data points $\pm$ SD across experiments. From the second data bins after induction onwards, bins were significantly different from the respective last data bins before induction. $**$ and $***$ refer to the statistical comparison between the last data point before induction and the second data point after induction for LTP (black triangles) and LTD (open triangles), respectively. (d) Cumulative display of control mean EPSP amplitudes versus the long-term change of individual experiments normalized to control of individual experiments. Open circles: experiments without action potentials (APs) during SBS; filled circles: experiments with APs during SBS. The two experiments shown in (a, b) are indicated by their SBS averages and arrows.

are given in Figure 4(a). Upon statistical comparison of ΔLT across paradigms, only γ-only was found to be significantly different from SBS ($P < 0.05$). All paradigms were more efficient than the control experiments without induction (Figure 4(c); versus SBS, TBS: $P < 0.005$; versus Θ-only, γ-only: $P < 0.05$).

Since paired pulse ratios (PPR) at an interstimulus interval of 25 ms (40 Hz) were highly variable across experiments (cf. Figure 2(d)), we tested whether PPRs could predict the direction and/or the efficiency of plasticity induction ΔLT. No significant correlation was found for either direction or efficiency ($n = 24, r = 0.28, P = 0.18$, and $r = 0.31, P = 0.17$).

Next we tested whether the occurrence of barrages of network activity was related to the degree and the sign of bidirectional plasticity induction. There was no correlation

between the half duration of the control compound EPSP and the observed plasticity ($r = 0.20, P = 0.29$, and $n = 31$). Changes in network activity after plasticity induction as estimated by the ratio of the half duration value of the long-term phase to the control phase were also frequently observed (>20% away from control in 16 out of 31 experiments) but had no net effect across experiments (average $104 \pm 28\%$, $n = 31$) and were also uncorrelated to plasticity ($r = -0.04$, $P = 0.80$, and each $n = 31$). This finding also held, when the analysis was restricted to the subset of experiments with substantial network activity ($\tau\_1/2_{EPSP} > 100$ ms, $n = 16$). Thus the presence of barrages and changes in their duration were not predictive of bidirectional plasticity and vice versa.

In 4 GCs the recordings were stable enough to allow for a second plasticity induction in a glomerular channel different
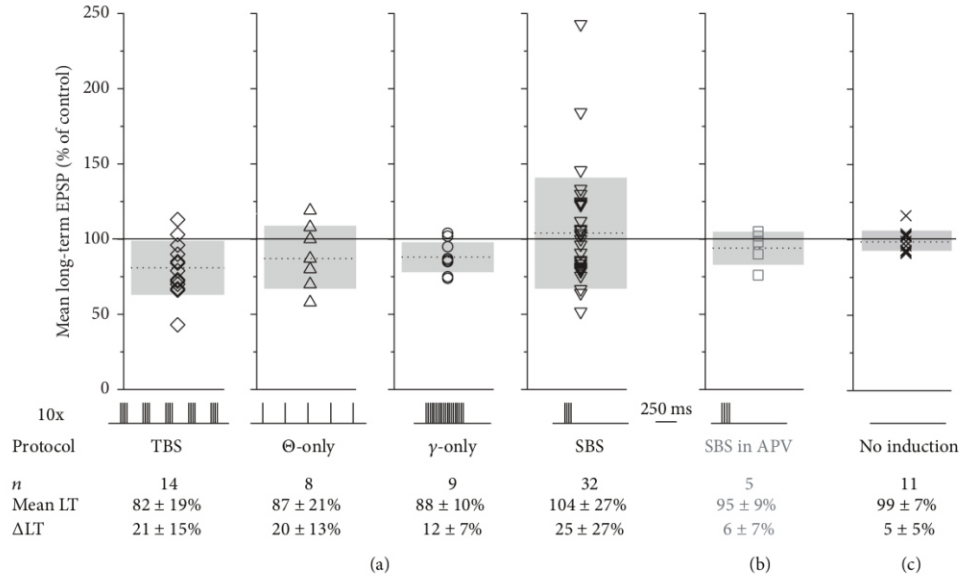
FIGURE 4: Synopsis of plasticity experiments. SBS plasticity is NMDAR-dependent. Bottom: temporal sequence of induction protocol, number of experiments, average long-term plasticity (mean LT), and average efficiency of long-term plasticity induction (ΔLT, absolute value of plastic changes). All data ± SD. (a) Cumulative display of mean long-term change for all induction protocols with individual data sets, means (dotted lines), and SD (extent of grey bars). (b) Mean long-term change of SBS experiments in the presence of 25 μM APV. Note the substantially reduced variance. (c) Mean long-term change of experiments without induction ($n = 11$: 5 without induction and 6 recorded from heteroglomerular control channel that was not induced with SBS; see Figure 5).

from the first. In two of the cells, one induction resulted in LTD and the other in LTP; in the two others, one induction did not result in plasticity whereas the other resulted in LTD or LTP. Therefore the occurrence of bidirectional plasticity *per se* is most likely not cell-specific (at least at this age of animals) but rather depends on the summated plastic changes across the activated set of synapses (see also Section 3.5.).

In the presence of 25 μM APV, SBS no longer induced plasticity in any out of 5 experiments ($n = 5$, $95 \pm 9\%$, ΔLT = $6 \pm 7\%$, Figure 4(b); note the strongly reduced variance and ΔLT compared to control SBS, $P < 0.02$). Thus, NMDA receptor mediated signalling is crucial for both TBS- and SBS-induced plastic changes.

3.4. Homosynaptic Plasticity. To establish synaptic specificity of SBS-induced plasticity we used the four-channel stimulation electrode for the independent activation of two glomerular inputs on a given GC. To prevent coactivation by extracellular currents, stimulated glomeruli were separated by at least one nonstimulated glomerulus (see Section 2; Figures 5(a) and 5(b)). EPSP amplitudes from two distinct glomerular pathways did sum linearly or supralinearly upon combined stimulation of both pathways, indicating nonoverlapping sets of activated synapses ($n = 13$ GCs, ratio sum individual stimulations to combination 1.35 ± 0.53, $P < 0.05$ compared to strictly linear summation, Figure 5(c)). The supralinearity occurred mostly for larger input amplitudes >10 mV (sum of both EPSPs) and might be due to activation

of GC T-type Ca^{2+} channels [30] or other dendritic voltage-dependent mechanisms such as NMDA receptors (see, e.g., [34]).

For plasticity induction, only one glomerulus was stimulated with the SBS protocol while the other served as control input pathway. Figures 5(d)–5(f) show that the observed plasticity was specific to the input pathway which received the plasticity induction protocol, since it was not registered in the neighboring glomerular control input pathways ($n = 6$, total induced plasticity in stimulated input pathway ΔLT = $24 \pm 14\%$, total change in control pathways ΔLT = $3 \pm 3\%$, $P < 0.025$; independence of inputs tested for all these experiments as described above). Thus, this type of plasticity is clearly "homoglomerular," a finding that most likely also holds for TBS-induced LTD (not tested).

3.5. Mechanism of the SBS-Induced Plasticity: Changes in the Number of Release Sites. The observed slopes of -0.5 of the linear relations between the CV and the mean of the synaptic responses (in the logarithmic space, Figure 1(c)) indicate a specific mechanistic explanation for the bidirectional plasticity. That is, when a synapse becomes stronger (or weaker), it is mainly due to an increase (decrease) in its number of release sites and not due to changes in the release probability or quantal size [35, 36]. To examine the extent to which this mechanism can explain the plasticity at the MTC to GC synaptic connections, we performed a simple quantal analysis of the synaptic connections for which the CV could

(a)

(b)

(c)

(d)

(e)

(f)
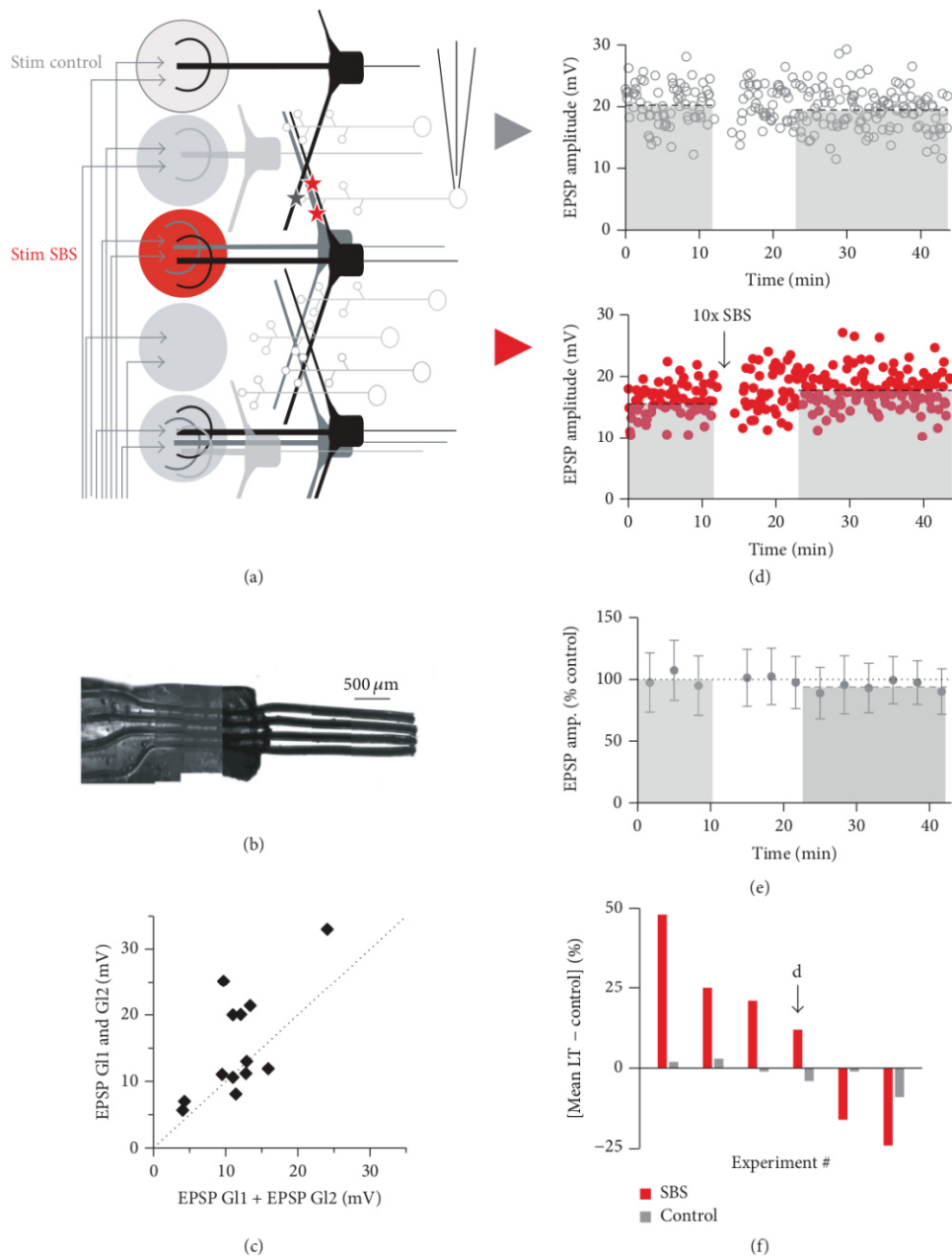
FIGURE 5: SBS results in homoglomerular plasticity. (a) Scheme of experimental configuration for intermittent stimulation of glomeruli. Two stimulated glomeruli were separated by at least one nonstimulated glomerulus. (b) Photograph of custom-built stimulation electrode (see Section 2). The wires appear wider than their actual size of 75 μm due to their Teflon coating. (c) Test for independence of sets of synapses ($n = 14$ experiments). Scatterplot of EPSP amplitudes of combined activation of two neighboring electrodes versus added EPSP amplitudes in response to individual stimulation of these glomeruli. (d) Individual experiment with intermittent stimulation. Top: control glomerular pathway without induction. Control mean 20.2 mV; long-term mean 19.3 mV (dashed black lines). Bottom: glomerular pathway with SBS induction. Control mean 15.8 mV; long-term mean 17.7 mV (dashed black lines). (e) Cumulative data from control glomerular pathway normalized to baseline ($n = 6$, long-term mean 98 ± 5% of control, dashed grey line). (f) Cumulative display of experiments. Red bars: long-term change (LT mean − control mean) in SBSed glomerular pathway; grey bars: long-term change in control glomerular pathway. The black arrow indicates the experiment shown in (d).

FIGURE 6: Plasticity induction relies on changes in N. Population quantal analysis of the synaptic connections from the SBS experiments. (a) The numbers of release sites N were strongly correlated with the synaptic efficacy at both the control ($r = 0.91$, $P < 0.01$) and long-term ($r = 0.82$, $P <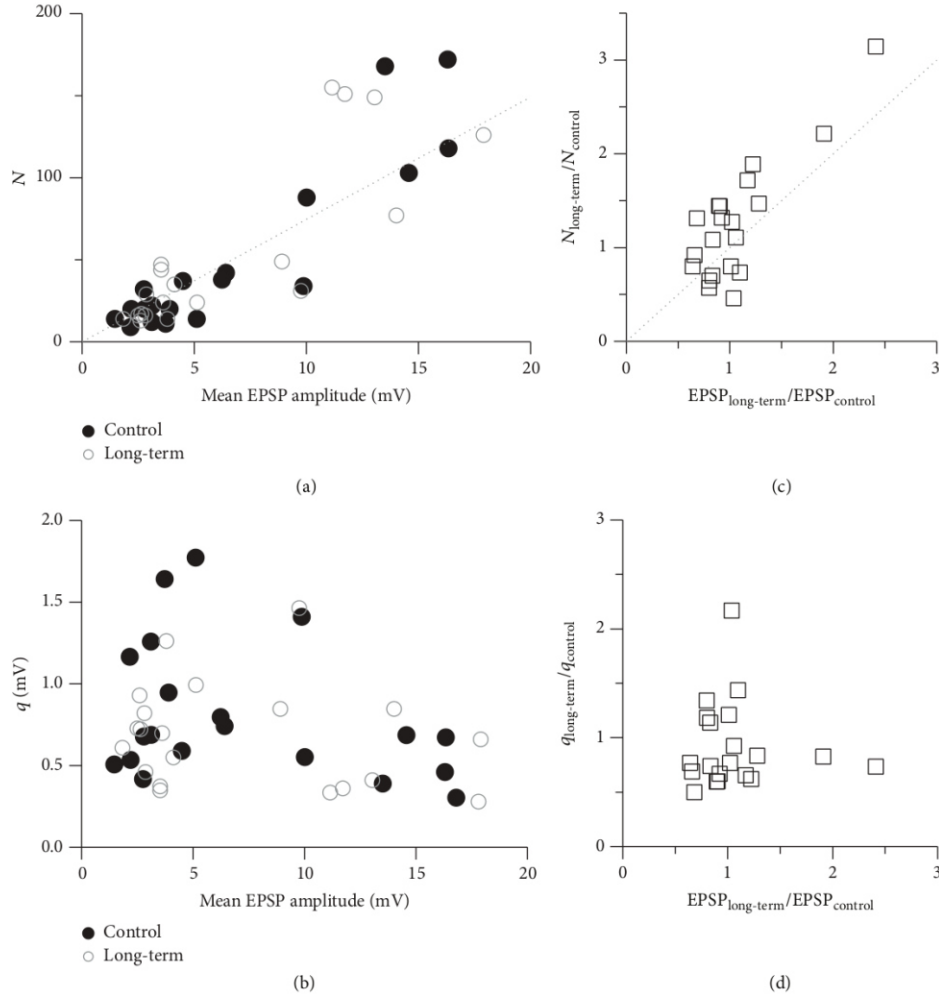 0.01$) measurement phases. The dotted line represents the linear relation between N and EPSP amplitude (see (1) in Section 2) for the averaged quantal size $\langle q \rangle = (q_{control} + q_{long\text{-}term})/2 = 0.80$ mV and the averaged release probability $\langle p \rangle = (p_{control} + p_{long\text{-}term})/2 = 0.265$ resulting from the quantal analysis: $N = (\text{Mean EPSP})/(\langle p \rangle \langle q \rangle)$. (c) Scatterplot of the relative change in the number of release sites N versus the observed relative plasticity. There is a strong correlation ($r = 0.83$, $P < 0.01$). (b, d) In contrast, the quantal sizes q and the relative change in their sizes were not correlated with the synaptic efficacies and the observed relative plasticity.

be determined at both the control and long-term phases of the SBS experiments ($n = 20$). We have found that the number of release sites at the different synaptic connections was indeed strongly correlated with their efficacy in both experimental phases (control: $r = 0.91$, $P < 0.001$; long-term: $r = 0.82$, $P < 0.001$; Figure 6(a)). In particular, the changes in the number of release sites were strongly correlated with the plasticity in the synaptic efficacies, that is, the mean EPSP amplitude ($r = 0.83$, $P < 0.001$; Figure 6(c)). The average release probability of the connections, on the other hand, was similar before and after plasticity was induced, with $p_{control} = 0.25 \pm 0.05$ and $p_{long\text{-}term} = 0.28 \pm 0.07$ (mean $\pm$ SD; calculated

from 200 bootstrap replicas of the data). The calculated quantal sizes, with a mean and standard deviation of $q_{control} = 0.82 \pm 0.41$ mV and $q_{long\text{-}term} = 0.78 \pm 0.35$ mV, were not correlated with the synaptic efficacy (Figure 6(b)). That is, the release sites of both weaker and stronger synaptic connections had comparable quantal sizes, and the quantal size and release probability of new release sites, which were added at potentiated connections, were of the same magnitude as for the existing release sites. Similarly, the release sites that disappeared at depressed synaptic connections had the same average size and release probability as the remaining sites (Figure 6(d)).

4. Discussion

4.1. Functional Role of Long-Term Plasticity Induced by Bursting Activity in the Sensory Input to GCs.

We have shown that physiologically motivated induction protocols are capable of inducing long-term plasticity at the MTC-GC synapse. In line with the experiments by Ma et al. [16] who used extracellular stimulation in the external plexiform layer, we find that TBS of MTC inputs via glomerular stimulation results in LTD to about 80% of control. Both Ma et al. [16] and Gao and Strowbridge [37] observed LTP following TBS or spike-timing dependent plasticity (STDP) protocols of cortical inputs onto GCs but did not show LTP at the MTC-GC inputs. We now provide a proof of principle for LTP at this synapse, using a "single-sniff" paradigm. These findings—of both LTD and LTP—are conceptually relevant to prove that these synapses could actually participate in olfactory memory formation (e.g., [38]). In particular, we show that LTP requires short bursts of activity, since longer trains at 40 Hz (γ-only) were not effective for inducing LTP.

In olfaction, short bursts should correspond to physiologically relevant sensory inputs, because of both respiratory patterning and the properties of olfactory stimuli in the wild (see Section 1). In a sense, there appears to be a plastic resonance at short bursts compared to longer input at the MTC-GC synapse. Taking into account also the rapid induction of both TBS-LTD and SBS plasticity, it is tempting to speculate that these forms of plasticity might facilitate the search for distant odor sources.

4.2. Mechanism and Function of Bidirectional Plasticity.

Bidirectional plasticity as observed here for the "single-sniff" paradigm is also known from a few other synapses. In the olfactory bulb, Pimentel and Margrie [39] observed local excitatory glomerular interactions between mitral cell apical dendritic tufts that were mediated by AMPA receptors and that underwent bidirectional plastic changes in response to TBS. Since we did not observe bidirectional plasticity for TBS, it is unlikely that our glomerular stimulation technique also acted at the same site, rather than at the MTC-GC synapse. Thus, the olfactory pathway seems to dispose of several loci for bidirectional tuning. Other examples for bidirectional plasticity were observed in the lateral amygdala [40], following pairing of synaptic stimulation and dendritic Ca^{2+} spikes. Since in our experiments bidirectional plasticity occurred preferentially for smaller inputs, an involvement of Ca^{2+} spikes is unlikely even though these spikes exist also in GCs [25, 41]. Similarly, we found that global GC Na^+ spikes also had no apparent influence on bidirectional plasticity induction in GCs (see also Section 4.4). Therefore, STDP is unlikely to play a role at GC reciprocal spines. Although bidirectional modifications based on STDP have been reported at a huge diversity of synapses [42], including the olfactory nerve to mitral cell synapse where short bursts were paired with EPSPs [16], STDP is fundamentally different from the plasticity described here since in STDP the direction of plastic change depends on the relative timing between the post- and presynaptic activity and thus can be tuned experimentally.

As to the mechanism of bidirectional plasticity, we have found that both before and after plasticity induction the relation between the CV of the synaptic responses and their mean amplitude is linear with a slope of −0.5 (on the logarithmic scale). Together with the results of our basic quantal analysis this observation implies that the bidirectional changes in synaptic strength due to the SBS stimulation protocol can be explained by the addition or removal of release sites (rather than changes in quantal size or release probability), similar to previous findings for cortical L5 glutamatergic connections [35, 36]. The release probability that we found was lower than at the cortical connections (~0.2 versus ~0.45). Since optical quantal analysis yielded an average release probability of 0.5 at a given reciprocal spine [25] and there are certainly less dendrodendritic synaptic contacts between a glomerulus and GC than the number of release sites obtained from the quantal analysis (Figure 6(a); [43]), a synaptic contact is predicted to contain on average 3 release sites ($(1 - (1 - p_r)^3) = 0.49$, neglecting potential axodendritic inputs). This prediction is further supported by the quantal size obtained here (~0.75 mV), because the median unitary EPSP amplitude at this connection was found to be ~2 mV [unpublished observations, [30]]. The rather large value of q in comparison to the cortical connections (~0.1 mV) could be explained by the compactness of the GC dendritic tree and the hybrid nature of this axodendrite that involves local postsynaptic amplification of EPSPs via various mechanisms [44].

Notably, at cortical synapses LTP is thought to be initially governed by modifications to the release probability, while the structural changes follow on a longer time scale [45, 46]. At the MTC-GC synapse, on the other hand, it appears as if the structural changes are rapid, suggesting an adapted mechanism for fast and stable structural modifications even for short stimuli such as the SBS.

Bidirectional plasticity as observed here is homeostatic, thus the total GC excitability would not be changed via individual short odor samplings. While larger data sets are required to fully establish this important observation, the SBS stimulation type might lead to an exploration within the neural circuit, in search for synaptic pathways that would react with a meaningful response. In reinforcement learning theory such a characteristic follows from the lack of a correlation between stimuli and the reward to the system (i.e., constant reward) [47, 48] and the observed changes may therefore depend on a random state of a yet unknown component of the synapse. Since the experiments were done in acute slices, the observed plasticity is independent of external reward top-down signals. However, in an intact brain this plasticity might be directed via centrifugal inputs on GCs [49].

Although SBS on the whole was found to act homeostatically, recurrent inhibition and lateral inhibition will be tuned at individual contacts between MTCs and GCs, such that different MTCs will be differentially modulated. Thus, bidirectional plasticity might be relevant for the establishment and refinement of the highly complex receptive fields GCs have been suggested to dispose of. The precise nature of these receptive fields is as of yet not fully known but might

be related for example to discontinuous representations of the stimulus within the bulb [50], to an incomplete inhibitory mirror image of odorants provided by GCs and governed by centrifugal inputs [51], to the formation of GC columns corresponding to glomerular functional units [52], or to dynamic connectivity as invoked by activity-dependent lateral inhibition [53]. Bidirectional plasticity might also subserve the optimization of the complex and sensitive temporal coding in the bulb, such as fast correlation and slow decorrelation in heteroglomerular simultaneous MC spike trains [54] or the latency coding powered specifically by mitral cells [1, 3]. Finally, MCs were recently reported to undergo a decrease in activity in relation to olfactory memory formation *in vivo* [55], which might require the form of LTP at the MC-GC synapses described here.

While at the network level bidirectional plasticity would affect mainly local processing at individual GC spines, TBS-induced LTD will reduce GC overall excitability within a rather short time span and thus reduce the amount of global lateral inhibition provided by the GCs associated with the active glomerulus. Thus its influence will be downregulated, with further interesting implications for bulbar network processing. Whether local recurrent inhibition is also reduced depends on the precise mechanism of TBS-LTD; if LTD was ultimately related to an increase in spine neck resistance (as suggested above for SBS-mediated plasticity), local recurrent inhibition could be even increased. A stimulation paradigm capable of inducing mainly LTP still remains to be discovered, since LTP would be required to implement, for example, a sparsification of mitral cell responses to known odors [56] or other aspects of olfactory memory. Since reliable correlations between glomerular network activity and the plasticity of input to GCs could not be observed within the scope of our study, interactions between MC-GC plasticity and glomerular processing remain to be elucidated.

4.3. Sources of Variability That Might Also Contribute to Bidirectional Plasticity.

Several other factors might also play a role in the phenomenon of bidirectional plasticity. First, the short-term plasticity of the MTC-GC synapse described here is in line with previous voltage clamp experiments [54, 57, 58] where both depression and facilitation were observed for paired pulse inputs onto GCs. Interestingly, facilitation was found to be a property of proximal inputs on the GC apical dendrite (which are thought to consist of both cortical inputs and mitral cell axon collaterals), whereas inputs from reciprocal spines rather underwent depression [41, 59]. Since the cortical feedback loop was most likely not conserved in our slice preparation, the facilitating cases might correspond to sets of synapses that consisted predominantly of proximal inputs established by MC axon collaterals, whose influence on GC processing is not well known. This diversity of inputs could also contribute to bidirectional plasticity; however, we did not observe any correlation between short-term and long-term plasticity.

Another source of variability might originate from glomerular activation of disynaptic pathways onto GCs, in particular via inhibitory deep short-axon cells [31, 60], which might also undergo plastic changes.

Similarly, even though we found that bidirectional plasticity was most likely not specific to a given cell, bidirectional plasticity might be due to differing maturational stages of GCs and their synapses, since the early development of the olfactory bulb network is not yet terminated in two-week old animals (e.g., [61]). While the GCs in our sample appeared mature with respect to their anatomy and action potential firing [62], more subtle gradations of maturation could affect plasticity. Also, at this age rodents just begin to actively explore their environment and sniffing behavior is about fully established around PND 11 [63, 64]. Moreover, adult-born GCs differ in their plasticity from early-born GCs, as documented for an NMDAR-independent form of TBS-LTP in new, adult-born GCs [42]. A recent *in vivo* study by Alonso et al. [65] showed that optogenetic stimulation of specifically adult-born GCs (versus early-born GCs) during an olfactory memory task could facilitate learning when applied at 40 Hz (with exactly the same duration as in our "γ-only" experiments) rather than at 10 Hz. Since our GC population consists entirely of early-born GCs, it remains to be tested whether the observed weak "γ-only" plasticity would be enhanced in adult-born GCs in acute slices.

Finally there are several subtypes of both MTCs and GCs [66] which also might differ with respect to their synaptic plasticity.

4.4. Mechanisms of Long-Term Plasticity: Role of the NMDA Receptor in GCs.

Blockade of NMDA receptors abolished both TBS-induced LTD and bidirectional plasticity. So, as in many other established forms of long-term plasticity, the NMDA receptor appears to be the key element mediating plastic effects. In contrast to one of the main dogmas held with respect to NMDA receptor mediated long-term plasticity, the occurrence of spikes and the total maximal depolarization during induction as measured at the GC soma were not correlated to the outcome of plasticity induction for both paradigms.

At the MTC-GC synapse, NMDA receptors are already involved in normal synaptic transmission and postsynaptic Ca^{2+} signalling [25, 67], even though the resting potential of GCs is rather hyperpolarized. This observation can now be explained by the strong local postsynaptic depolarization within GC reciprocal spines that is powered mostly by AMPA receptors; NMDA receptor activation appears to occur independently of additional local Na_v-channel mediated boosting [44]. Thus, plasticity induction is probably based on purely local signalling at the GC spines (although a coupling to regional dendritic events or additional contributions by non-GC NMDA receptors located, e.g., within the stimulated glomerulus cannot be excluded from our data).

Therefore the contribution of the NMDA receptor to plasticity induction must rely on a cooperative effect that occurs during burst stimulation, for example, a summation of postsynaptic Ca^{2+} levels past a certain threshold, while independent of backpropagation of action potentials or dendritic spikes. Such a scenario might also explain bidirectional

plasticity by involving two site-specific thresholds that feed into opposing plasticity mechanisms (e.g., [68]).

If cooperative entry of Ca^{2+} is indeed required for plasticity induction, a remaining conundrum is why high frequency stimulation with 20 spikes at 40 Hz ("γ-only") was not effective. Why and how is Ca^{2+} rise cancelled in this case? Larson and Munkácsy [15] similarly found that TBS was more efficient in plasticity induction in the hippocampus than high frequency stimulation (HFS) with the same number of spikes; they propose an underlying depletion of glutamate during HFS. However, this scenario still does not explain the higher induction efficiency of SBS compared to "γ-only." Rather, there might be a negative feedback signal triggered by an "overstimulation" with glutamate and/or postsynaptic Ca^{2+}, for example, via MTC or GC mGluRs or the TRPC channels in GC spines that require strong, NMDA receptor dependent stimulation to become activated [69, 70]. Finally, "γ-only" might also trigger local plastic changes that are not seen at the GC soma because of filtering by the reciprocal spine neck resistance R_{neck} [44], changes that nevertheless could affect GABA release from the spine, for example, via modulation of high-voltage-activated Ca^{2+} currents. Moreover, changes in R_{neck} might provide a general explanation for the fast plasticity induction at the MTC-GC synapse, similar to the rapid R_{neck} decrease associated with LTP that has been observed for hippocampal spines [59].

4.5. Sniffing and Olfactory Coding; Theta-Gamma Coupling in the Olfactory Bulb and in the Hippocampus. Ongoing theta in the hippocampus is reported mostly from rats and mice (but not bats and humans [71]) and is most likely driven from extrahippocampal structures such as the medial septum [72]. Ongoing theta in the olfactory bulb on the other hand appears to be a universal phenomenon in breathing vertebrates, with both MTC and GC membrane potentials being modulated by it (see Section 1 and [73–75]). Both theta and fast oscillations are most likely originating within the bulb itself [76, 77], with the fast oscillations being generated at the MTC-GC reciprocal synapse [6, 7]. Hippocampal and bulbar theta rhythms are reciprocally transmitted to the bulb and hippocampus, respectively [72, 78–80].

While gamma oscillations coordinate activity of neurons on the time scale of EPSPs and thus would be well suited to provide patterns of activity that are optimal for the induction of STDP, we did not observe a prominent role of spikes in GC plasticity. In analogy to observations in the hippocampal system, the observed plasticity at the MTC-GC synapse might not just be induced by TBS but might also be acting as a driver for gamma bursting via recurrent inhibition, since nested gamma bursts in the entorhinal cortex were shown to be driven by TBS via feedback inhibition [81]. Also, gamma oscillations could serve to feed into theta via dendritic integration in both mitral and granule cells involving slow conductances such as HCN and TRP channels, as proposed for hippocampal CA1 neurons [82]. Finally, the higher frequency sniffing of rodents during active exploration enhances gamma power [83], which might also contribute to a higher degree of plasticity. Interestingly, active sampling of odor plumes in insects was also found to synchronize oscillations in antennal lobe networks, in line with other plastic changes on a short time scale [20].

5. Conclusions

In summary, we have demonstrated burst-induced forms of plasticity of the MTC-GC reciprocal synapse with a fast onset that might endow the olfactory system with the sensitivity required for fast learning of new, weak stimuli, for example during exploration. This property might be particularly relevant for olfaction because of the huge space of potential stimuli most of which is unknown to the organism at any point in its life. The finding of both LTD and LTP at this synapse is relevant for its versatility within bulbar processing.

Abbreviations

AP: Action potential
GC: Granule cell
MTC: Mitral and/or tufted cell
TBS: Theta burst stimulation
SBS: Single burst stimulation
PND: Postnatal day
LTP: Long-term potentiation
LTD: Long-term depression
CV: Coefficient of variance.

Competing Interests

The authors declare no competing interests.

Authors' Contributions

Veronica Egger designed experiments; Mahua Chatterjee, Fernando Perez de los Cobos Pallares, Michael Lukas, and Veronica Egger performed experiments; Mahua Chatterjee, Fernando Perez de los Cobos Pallares, and Veronica Egger analyzed data; Alex Loebel contributed the quantal modeling and the respective parts of the paper; Veronica Egger wrote the paper.

Acknowledgments

References

[1] T. W. Margrie and A. T. Schaefer, "Theta oscillation coupled spike latencies yield computational vigour in a mammalian sensory system," *The Journal of Physiology*, vol. 546, no. 2, pp. 363–374, 2003.

[2] R. M. Carey and M. Wachowiak, "Effect of sniffing on the temporal structure of mitral/tufted cell output from the olfactory bulb," *The Journal of Neuroscience*, vol. 31, no. 29, pp. 10615–10626, 2011.

[3] I. Fukunaga, M. Berning, M. Kollo, A. Schmaltz, and A. T. Schaefer, "Two distinct channels of olfactory bulb output," *Neuron*, vol. 75, no. 2, pp. 320–329, 2012.

[4] R. Shusterman, M. C. Smear, A. A. Koulakov, and D. Rinberg, "Precise olfactory responses tile the sniff cycle," *Nature Neuroscience*, vol. 14, no. 8, pp. 1039–1044, 2011.

[5] J. E. Lisman and O. Jensen, "The theta-gamma neural code," *Neuron*, vol. 77, no. 6, pp. 1002–1016, 2013.

[6] H. Manabe and K. Mori, "Sniff rhythm-paced fast and slow gamma-oscillations in the olfactory bulb: relation to tufted and mitral cells and behavioral states," *Journal of Neurophysiology*, vol. 110, no. 7, pp. 1593–1599, 2013.

[7] N. Fourcaud-Trocmé, E. Courtiol, and N. Buonviso, "Two distinct olfactory bulb sublaminar networks involved in gamma and beta oscillation generation: a CSD study in the anesthetized rat," *Frontiers in Neural Circuits*, vol. 8, article 88, 2014.

[8] K. M. Igarashi, N. Ieki, M. An et al., "Parallel mitral and tufted cell pathways route distinct odor information to different targets in the olfactory cortex," *The Journal of Neuroscience*, vol. 32, no. 23, pp. 7970–7985, 2012.

[9] G. H. Otazu, H. Chae, M. B. Davis, and D. F. Albeanu, "Cortical feedback decorrelates olfactory bulb output in awake mice," *Neuron*, vol. 86, no. 6, pp. 1461–1477, 2015.

[10] J. A. Gottfried, "Central mechanisms of odour object perception," *Nature Reviews Neuroscience*, vol. 11, no. 9, pp. 628–641, 2010.

[11] N. M. Abraham, H. Spors, A. Carleton, T. W. Margrie, T. Kuner, and A. T. Schaefer, "Maintaining accuracy at the expense of speed: stimulus similarity defines odor discrimination time in mice," *Neuron*, vol. 44, no. 5, pp. 865–876, 2004.

[12] N. M. Abraham, V. Egger, D. R. Shimshek et al., "Synaptic inhibition in the olfactory bulb accelerates odor discrimination in mice," *Neuron*, vol. 65, no. 3, pp. 399–411, 2010.

[13] D. Nunes and T. Kuner, "Disinhibition of olfactory bulb granule cells accelerates odour discrimination in mice," *Nature Communications*, vol. 6, article 8950, 2015.

[14] M. Alonso, C. Viollet, M.-M. Gabellec, V. Meas-Yedid, J.-C. Olivo-Marin, and P.-M. Lledo, "Olfactory discrimination learning increases the survival of adult-born neurons in the olfactory bulb," *The Journal of Neuroscience*, vol. 26, no. 41, pp. 10508–10513, 2006.

[15] J. Larson and E. Munkácsy, "Theta-burst LTP," *Brain Research*, vol. 1621, pp. 38–50, 2015.

[16] T.-F. Ma, X.-L. Zhao, L. Cai et al., "Regulation of spike timing-dependent plasticity of olfactory inputs in mitral cells in the rat olfactory bulb," *PLoS ONE*, vol. 7, no. 4, Article ID e35001, 2012.

[17] E. Balkovsky and B. I. Shraiman, "Olfactory search at high Reynolds number," *Proceedings of the National Academy of Sciences of the United States of America*, vol. 99, no. 20, pp. 12589–12593, 2002.

[18] K. C. Daly, F. Kalwar, M. Hatfield, E. Staudacher, and S. P. Bradley, "Odor detection in *Manduca sexta* is optimized when odor stimuli are pulsed at a frequency matching the wing beat during flight," *PLoS ONE*, vol. 8, no. 11, Article ID e81863, 2013.

[19] P. Szyszka, R. C. Gerkin, C. G. Galizia, and B. H. Smith, "High-speed odor transduction and pulse tracking by insect olfactory receptor neurons," *Proceedings of the National Academy of Sciences of the United States of America*, vol. 111, no. 47, pp. 16925–16930, 2014.

[20] S. J. Huston, M. Stopfer, S. Cassenaer, Z. N. Aldworth, and G. Laurent, "Neural encoding of odors during active sampling and in turbulent plumes," *Neuron*, vol. 88, no. 2, pp. 403–418, 2015.

[21] J. A. Riffell, E. Shlizerman, E. Sanders et al., "Flower discrimination by pollinators in a dynamic chemical environment," *Science*, vol. 344, no. 6191, pp. 1515–1518, 2014.

[22] N. Uchida, A. Kepecs, and Z. F. Mainen, "Seeing at a glance, smelling in a whiff: rapid forms of perceptual decision making," *Nature Reviews Neuroscience*, vol. 7, no. 6, pp. 485–491, 2006.

[23] D. Rinberg, A. Koulakov, and A. Gelperin, "Speed-accuracy tradeoff in olfaction," *Neuron*, vol. 51, no. 3, pp. 351–358, 2006.

[24] A. G. Khan, M. Sarangi, and U. S. Bhalla, "Rats track odour trails accurately using a multi-layered strategy with near-optimal sampling," *Nature Communications*, vol. 3, article 703, 2012.

[25] V. Egger, K. Svoboda, and Z. F. Mainen, "Dendrodendritic synaptic signals in olfactory bulb granule cells: local spine boost and global low-threshold spike," *The Journal of Neuroscience*, vol. 25, no. 14, pp. 3521–3530, 2005.

[26] V. Egger, D. Feldmeyer, and B. Sakmann, "Coincidence detection and changes of synaptic efficacy in spiny stellate neurons in rat barrel cortex," *Nature Neuroscience*, vol. 2, no. 12, pp. 1098–1105, 1999.

[27] J. Del Castillo and B. Katz, "Quantal components of the end-plate potential," *The Journal of Physiology*, vol. 124, no. 3, pp. 560–573, 1954.

[28] C. Saviane and R. A. Silver, "Errors in the estimation of the variance: implications for multiple-probability fluctuation analysis," *Journal of Neuroscience Methods*, vol. 153, no. 2, pp. 250–260, 2006.

[29] T. B. Woolf, G. M. Shepherd, and C. A. Greer, "Serial reconstructions of granule cell spines in the mammalian olfactory bulb," *Synapse*, vol. 7, no. 3, pp. 181–192, 1991.

[30] V. Egger, K. Svoboda, and Z. F. Mainen, "Mechanisms of lateral inhibition in the olfactory bulb: efficiency and modulation of spike-evoked calcium influx into granule cells," *The Journal of Neuroscience*, vol. 23, no. 20, pp. 7551–7558, 2003.

[31] S. D. Burton and N. N. Urban, "Rapid feedforward inhibition and asynchronous excitation regulate granule cell activity in the mammalian main olfactory bulb," *The Journal of Neuroscience*, vol. 35, no. 42, pp. 14103–14122, 2015.

[32] J. S. Isaacson and B. W. Strowbridge, "Olfactory reciprocal synapses: dendritic signaling in the CNS," *Neuron*, vol. 20, no. 4, pp. 749–761, 1998.

[33] A. Kepecs, N. Uchida, and Z. F. Mainen, "The sniff as a unit of olfactory processing," *Chemical Senses*, vol. 31, no. 2, pp. 167–179, 2006.

[34] J. K. Makara and J. C. Magee, "Variable dendritic integration in hippocampal CA3 pyramidal neurons," *Neuron*, vol. 80, no. 6, pp. 1438–1450, 2013.

[35] A. Loebel, G. Silberberg, D. Helbig, H. Markram, M. Tsodyks, and M. J. E. Richardson, "Multiquantal release underlies the distribution of synaptic efficacies in the neocortex," *Frontiers in Computational Neuroscience*, vol. 3, article 27, 2009.

[36] A. Loebel, L. B. Jean-Vincent, M. J. E. Richardson, H. Markram, and A. V. M. Herz, "Matched pre- and post-synaptic changes underlie synaptic plasticity over long time scales," *The Journal of Neuroscience*, vol. 33, no. 15, pp. 6257–6266, 2013.

[37] Y. Gao and B. W. Strowbridge, "Long-term plasticity of excitatory inputs to granule cells in the rat olfactory bulb," *Nature Neuroscience*, vol. 12, no. 6, pp. 731–733, 2009.

[38] S. Nabavi, R. Fox, C. D. Proulx, J. Y. Lin, R. Y. Tsien, and R. Malinow, "Engineering a memory with LTD and LTP," *Nature*, vol. 511, no. 7509, pp. 348–352, 2014.

[39] D. O. Pimentel and T. W. Margrie, "Glutamatergic transmission and plasticity between olfactory bulb mitral cells," *Journal of Physiology*, vol. 586, no. 8, pp. 2107–2119, 2008.

[40] Y. Humeau and A. Lüthi, "Dendritic calcium spikes induce bidirectional synaptic plasticity in the lateral amygdala," *Neuropharmacology*, vol. 52, no. 1, pp. 234–243, 2007.

[41] G. Pinato and J. Midtgaard, "Regulation of granule cell excitability by a low-threshold calcium spike in turtle olfactory bulb," *Journal of Neurophysiology*, vol. 90, no. 5, pp. 3341–3351, 2003.

[42] H. Markram, W. Gerstner, and P. J. Sjöström, "Spike-timing-dependent plasticity: a comprehensive overview," *Frontiers in Synaptic Neuroscience*, vol. 4, article 2, 2012.

[43] V. Egger and N. N. Urban, "Dynamic connectivity in the mitral cell-granule cell microcircuit," *Seminars in Cell and Developmental Biology*, vol. 17, no. 4, pp. 424–432, 2006.

[44] W. G. Bywalez, D. Patirniche, V. Rupprecht et al., "Local post-synaptic voltage-gated sodium channel activation in dendritic spines of olfactory bulb granule cells," *Neuron*, vol. 85, no. 3, pp. 590–601, 2015.

[45] J. Lisman and S. Raghavachari, "A unified model of the presynaptic and postsynaptic changes during LTP at CA1 synapses," *Science's STKE: Signal Transduction Knowledge Environment*, vol. 2006, no. 356, article re11, 2006.

[46] R. L. Redondo and R. G. M. Morris, "Making memories last: the synaptic tagging and capture hypothesis," *Nature Reviews Neuroscience*, vol. 12, no. 1, pp. 17–30, 2011.

[47] H. S. Seung, "Learning in spiking neural networks by reinforcement of stochastic synaptic transmission," *Neuron*, vol. 40, no. 6, pp. 1063–1073, 2003.

[48] X. Xie and H. S. Seung, "Learning in neural networks by reinforcement of irregular spiking," *Physical Review E: Statistical, Nonlinear, and Soft Matter Physics*, vol. 69, no. 4, part 1, Article ID 041909, 10 pages, 2004.

[49] C. L. Kiselycznyk, S. Zhang, and C. Linster, "Role of centrifugal projections to the olfactory bulb in olfactory processing," *Learning & Memory*, vol. 13, no. 5, pp. 575–579, 2006.

[50] A. L. Fantana, E. R. Soucy, and M. Meister, "Rat olfactory bulb mitral cells receive sparse glomerular inputs," *Neuron*, vol. 59, no. 5, pp. 802–814, 2008.

[51] A. A. Koulakov and D. Rinberg, "Sparse incomplete representations: a potential role of olfactory granule cells," *Neuron*, vol. 72, no. 1, pp. 124–136, 2011.

[52] M. Migliore, F. Cavarretta, A. Marasco et al., "Synaptic clusters function as odor operators in the olfactory bulb," *Proceedings of the National Academy of Sciences of the United States of America*, vol. 112, no. 27, pp. 8499–8504, 2015.

[53] N. N. Urban and A. C. Arevian, "Computing with dendroden-dritic synapses in the olfactory bulb," *Annals of the New York Academy of Sciences*, vol. 1170, pp. 264–269, 2009.

[54] A. Nissant, C. Bardy, H. Katagiri, K. Murray, and P.-M. Lledo, "Adult neurogenesis promotes synaptic plasticity in the olfactory bulb," *Nature Neuroscience*, vol. 12, no. 6, pp. 728–730, 2009.

[55] H. K. Kato, M. W. Chu, J. S. Isaacson, and T. Komiyama, "Dynamic sensory representations in the olfactory bulb: modulation by wakefulness and experience," *Neuron*, vol. 76, no. 5, pp. 962–975, 2012.

[56] S. Zhou, M. Migliore, and Y. Yu, "Odor experience facilitates sparse representations of new odors in a large-scale olfactory bulb model," *Frontiers in Neuroanatomy*, vol. 10, article 10, 2016.

[57] S. B. Dietz and V. N. Murthy, "Contrasting short-term plasticity at two sides of the mitral-granule reciprocal synapse in the mammalian olfactory bulb," *Journal of Physiology*, vol. 569, no. 2, pp. 475–488, 2005.

[58] R. Balu, R. T. Pressler, and B. W. Strowbridge, "Multiple modes of synaptic excitation of olfactory bulb granule cells," *The Journal of Neuroscience*, vol. 27, no. 21, pp. 5621–5632, 2007.

[59] J. Tønnesen, G. Katona, B. Rózsa, and U. V. Nägerl, "Spine neck plasticity regulates compartmentalization of synapses," *Nature Neuroscience*, vol. 17, no. 5, pp. 678–685, 2014.

[60] C. Labarrera, M. London, and K. Angelo, "Tonic inhibition sets the state of excitability in olfactory bulb granule cells," *The Journal of Physiology*, vol. 591, no. 7, pp. 1841–1850, 2013.

[61] S. B. Dietz, F. Markopoulos, and V. N. Murthy, "Postnatal development of dendrodendritic inhibition in the mammalian olfactory bulb," *Frontiers in Cellular Neuroscience*, vol. 5, article 10, 2011.

[62] A. Carleton, C. Rochefort, J. Morante-Oria et al., "Making scents of olfactory neurogenesis," *Journal of Physiology Paris*, vol. 96, no. 1-2, pp. 115–122, 2002.

[63] J. R. Alberts and B. May, "Ontogeny of olfaction: development of the rats' sensitivity to urine and amyl acetate," *Physiology & Behavior*, vol. 24, no. 5, pp. 965–970, 1980.

[64] P. E. Sharp, M. C. La Regina, and M. A. Suckow, *The Laboratory Rat*, The Laboratory Animal Pocket Reference Series, CRC Press, Boca Raton, Fla, USA, 1998.

[65] M. Alonso, G. Lepousez, S. Wagner et al., "Activation of adult-born neurons facilitates learning and memory," *Nature Neuroscience*, vol. 15, no. 6, pp. 897–904, 2012.

[66] S. Nagayama, R. Homma, and F. Imamura, "Neuronal organization of olfactory bulb circuits," *Frontiers in Neural Circuits*, vol. 8, article 98, 2014.

[67] N. E. Schoppa, J. M. Kinzie, Y. Sahara, T. P. Segerson, and G. L. Westbrook, "Dendrodendritic inhibition in the olfactory bulb is driven by NMDA receptors," *The Journal of Neuroscience*, vol. 18, no. 17, pp. 6790–6802, 1998.

[68] O. Camiré and L. Topolnik, "Dendritic calcium nonlinearities switch the direction of synaptic plasticity in fast-spiking interneurons," *The Journal of Neuroscience*, vol. 34, no. 11, pp. 3864–3877, 2014.

[69] H.-W. Dong, T. Heinbockel, K. A. Hamilton, A. Hayar, and M. Ennis, "Metabotropic glutamate receptors and dendrodendritic synapses in the main olfactory bulb," *Annals of the New York Academy of Sciences*, vol. 1170, pp. 224–238, 2009.

[70] O. Stroh, M. Freichel, O. Kretz, L. Birnbaumer, J. Hartmann, and V. Egger, "NMDA receptor-dependent synaptic activation of TRPC channels in olfactory bulb granule cells," *Journal of Neuroscience*, vol. 32, no. 17, pp. 5737–5746, 2012.

[71] M. M. Yartsev, M. P. Witter, and N. Ulanovsky, "Grid cells without theta oscillations in the entorhinal cortex of bats," *Nature*, vol. 479, no. 7371, pp. 103–107, 2011.

[72] L. L. Colgin, "Mechanisms and functions of theta rhythms," *Annual Review of Neuroscience*, vol. 36, pp. 295–312, 2013.

[73] M. E. Phillips, R. N. S. Sachdev, D. C. Willhite, and G. M. Shepherd, "Respiration drives network activity and modulates synaptic and circuit processing of lateral inhibition in the olfactory bulb," *The Journal of Neuroscience*, vol. 32, no. 1, pp. 85–98, 2012.

[74] I. A. Youngstrom and B. W. Strowbridge, "Respiratory modulation of spontaneous subthreshold synaptic activity in olfactory bulb granule cells recorded in awake, head-fixed mice," *Journal of Neuroscience*, vol. 35, no. 23, pp. 8758–8767, 2015.

[75] V. Briffaud, N. Fourcaud-Trocmé, B. Messaoudi, N. Buonviso, and C. Amat, "The relationship between respiration-related membrane potential slow oscillations and discharge patterns in mitral/tufted cells: what are the rules?" *PLoS ONE*, vol. 7, no. 8, Article ID e43964, 2012.

[76] F. P. de los Cobos Pallarés, D. Stanić, D. Farmer, M. Dutschmann, and V. Egger, "An arterially perfused nose-olfactory bulb preparation of the rat," *Journal of Neurophysiology*, vol. 114, no. 3, pp. 2033–2042, 2015.

[77] E. C. Sobel and D. W. Tank, "Timing of odor stimulation does not alter patterning of olfactory bulb unit activity in freely breathing rats," *Journal of Neurophysiology*, vol. 69, no. 4, pp. 1331–1337, 1993.

[78] L. M. Kay, "Theta oscillations and sensorimotor performance," *Proceedings of the National Academy of Sciences of the United States of America*, vol. 102, no. 10, pp. 3863–3868, 2005.

[79] C. Martin, J. Beshel, and L. M. Kay, "An olfacto-hippocampal network is dynamically involved in odor-discrimination learning," *Journal of Neurophysiology*, vol. 98, no. 4, pp. 2196–2205, 2007.

[80] V. N. Chi, C. Müller, T. Wolfenstetter et al., "Hippocampal respiration-driven rhythm distinct from theta oscillations in awake mice," *The Journal of Neuroscience*, vol. 36, no. 1, pp. 162–177, 2016.

[81] H. Pastoll, L. Solanka, M. C. W. van Rossum, and M. F. Nolan, "Feedback inhibition enables theta-nested gamma oscillations and grid firing fields," *Neuron*, vol. 77, no. 1, pp. 141–154, 2013.

[82] S. P. Vaidya and D. Johnston, "Temporal synchrony and gamma-to-theta power conversion in the dendrites of CA1 pyramidal neurons," *Nature Neuroscience*, vol. 16, no. 12, pp. 1812–1820, 2013.

[83] M. A. Rosero and M. L. Aylwin, "Sniffing shapes the dynamics of olfactory bulb gamma oscillations in awake behaving rats," *European Journal of Neuroscience*, vol. 34, no. 5, pp. 787–799, 2011.

4.   **DISCUSSION**

4.1.   Clinical importance of the olfactory system

The olfactory bulb is a highly plastic neural network that changes continuously. Its volume varies across an animal's life followed by changes in the olfactory function (Buschuter, Smitka et al. 2008). So far, aging has been reported to be the major cause of olfactory dysfunction which relates to olfactory bulb volume and functionality and might have a direct impact on well-being and quality of life (Landis, Konnerth et al. 2004; Doty and Kamath 2014). Dysfunction of the olfactory system has been related to different neurodegenerative diseases such as Alzheimer (AD) (Wilson, Arnold et al. 2009; Wesson, Levy et al. 2010; Wesson, Wilson et al. 2010; Stamps, Bartoshuk et al. 2013; Alves, Petrosyan et al. 2014), Parkinson (PD) (Doty 2007; Haehner, Hummel et al. 2009; Haehner, Hummel et al. 2011; Doty 2012; Casjens, Eckert et al. 2013), multiple sclerosis (MS) (Caminiti, De Salvo et al. 2014; Li, Yang et al. 2016; Lucassen, Turel et al. 2016; Yaldizli, Penner et al. 2016) and Huntington disease (HD) (Hamilton, Murphy et al. 1999; Barrios, Gonzalez et al. 2007; Lazic, Goodman et al. 2007; Barresi, Ciurleo et al. 2012; Delmaire, Dumas et al. 2013) and has been proposed as a biomarker for these diseases (Barresi, Ciurleo et al. 2012). Different factors might account for age-related olfactory dysfunction like damage of the olfactory epithelium, ossification of the cribriform plate and loss of selectivity of receptor cells to odor molecules. Moreover, synaptic failure and/or degeneration of different neuromodulatory systems targeting dendrodendritic synapses in the OB might account for alterations in OB activity leading to loss of olfaction. In other brain areas this is reflected at the population level where oscillatory activity and its synchronization has been shown to be altered at different frequency bands in patients with some disorders or diseases including depression, schizophrenia, epilepsy, autism or previously mentioned neurodegenerative diseases when compared to healthy subjects (Uhlhaas and Singer 2006). Since neural oscillations are involved in the maturation and synaptic plasticity of neural networks, desynchronization of neural activity might be critical at different stages of development as well as for age-related neurodegeneration (Uhlhaas and Singer 2006; Barresi, Ciurleo et al. 2012).

4.2. Characteristics of the nose - olfactory bulb - brainstem preparation (NOBBP)

In the early stages of the method´s development, semi intact preparations did not become popular due to experimental limitations, such as tissue hypoxia. The nose-olfactory bulb preparation is a good alternative to more popular *in vivo* and *in vitro* approaches. It has obvious advantages like the lack of anesthesia, an intact olfactory pathway and a preserved *in-vivo* like olfactory network. The coupling to respiratory networks makes the preparation suitable to study local networks in the olfactory bulb and its interaction with respiration. In this preparation, adjacent fragments of the piriform cortex are preserved not to compromise the anatomical integrity of the OB. These fragments are thought to suffer hypoxia since branches of the corticostriate artery supplying part of the piriform cortex are completely removed during surgery. Therefore, this preparation is suitable to study odor processing at the level of the olfactory bulb lacking centrifugal inputs. The viability of this preparation is based on proper oxygenation of the remaining bulbar and respiratory networks and proper oxygenation of the latter triggering physiological phrenic bursts is a good indicator of the preparation's viability.

Characterization of eupneic phrenic bursts in a semi intact preparation compared to *in vivo* was adressed in detail in several papers (see Richter and Spyer 2001). Thus, inspiratory events observed using the perfused nose-brain preparation are not gasping events. This implies that the perfusion pressure and flow rate are sufficient to oxygenate the BS and consequently the OB properly. Unfortunately there is no defined protocol that could be applied to reactivate the respiratory network since these aspects are complex and variable across experiments. Even so, proper oxygenation of the OB does not guarantee an active olfactory network. I observed that the OB needed to be "reactivated" via prolonged odor stimulation. A possible explanation for this "rebooting" process could be a potential collapse of the olfactory network during early stages of the preparation since it lacked constant rhythmic airflow or other sensory stimuli. Nevertheless, proper "tuning" of the preparation elicits spontaneous respiratory activity which can last up to four hours while recording odor-evoked responses.

4.3. Odor - evoked responses in the NOBBP

Proof of the success of this preparation is to give evidence of its functionality. Nasal stimulation with a computer controlled olfactometer elicited odor-evoked activity. "Rebooting" of the olfactory network implies an initial reactivation of OSNs detecting odor molecules and changes in mechanosensation. Continuous stimulation succeeded to reactivate the olfactory network. In line with what is observed in *in vivo* studies, observation of excitatory and inhibitory responses to stimulation with oil-diluted odorants confirms the proper preservation of the olfactory network and its functionality (Davison and Katz 2007). The generation of spontaneous and odor-evoked oscillations confirms that the neuronal networks distributed in the different layers are properly preserved and oxygenated. Most of the responses observed were locked to stimulation. In some cases, some neurons became tonically active after odor presentation, which can be explained as an OFF response. Maritan et al. showed the presence of odorant receptors at the axon terminals of the OSNs. Lacking a proper odorant suction system, the remaining volatile molecules after stimulation, which potentially bind receptors on the growth cone, could partly explain these delayed responses (Maritan, Monaco et al. 2009). As explained in the introduction, many centrifugal projections and different neuromodulators project to the OB, shaping bulbar activity. Due to ethical issues, removal of the midbrain was needed. Thus, all responses were localized in the OB in the absence of centrifugal or neuromodulatory modulation.

This preparation might be suitable to study how odors are represented in the OB. Stimulation with odorants sharing similar molecular features tends to activate similar areas in the OB. However similar odors do not necessarily activate nearby glomeruli (Ma, Qiu et al. 2012; Imai 2014). Still, the olfactory map representation is state-dependent where a well preserved and intact olfactory network is vital, as it occurs in the *in vivo* awake approach. Awake animals show more sparse responses to odors due to a stronger activation of the GCL. That implies that odor representations in the OB might depend on spatio-temporal patterns (Uchida, Poo et al. 2014), known to be dependent on the response latency of glomeruli, odor identity and to be concentration-specific (Spors and Grinvald 2002; Kepecs, Uchida et al. 2006; Shusterman, Smear et al. 2011; Fukunaga, Berning et al. 2012).

Moreover, exposure of the lateral sides of the olfactory bulb migh allow mapping of hitherto inaccessible OB glomeruli contributing to understand how odors are represented in the OB.

4.4. Oscillatory activity

Oscillatory activity in the bulb has been widely studied since the pioneer work of E.D. Adrian in which he observed oscillatory activity in the hedgehog olfactory bulb (Adrian 1942; Adrian 1952). Since then, much research on that field has been performed studying electroencephalograms (EEG) and local field potentials (LFP) in the OB in both *in vitro* and *in vivo* (anesthetized and awake head-fixed) (Freeman 1978; Freeman and Schneider 1982; Chabaud, Ravel et al. 1999; Buonviso, Amat et al. 2003; Martin, Gervais et al. 2004; Kay 2005; Litaudon, Garcia et al. 2008; Cenier, David et al. 2009; Fourcaud-Trocme, Courtiol et al. 2014; Martin and Ravel 2014; David, Courtiol et al. 2015). Oscillatory activity has been also studied in different semi intact preparations with natural odor stimulation (in the frog, Delaney and Hall 1996; in guinea-pig, Ishikawa 2007). So far, it has never been tested in rodents keeping an intact olfactory pathway combined with a preserved respiratory network. In the nose olfactory bulb preparation I show evidence for a well preserved and oxygenated olfactory network. Reactivation of the olfactory function leads to the generation of spontaneous and odor-evoked oscillations. Activity at a low frequency is known from many *in vivo* studies to be coupled to the respiratory rhythm (Margrie and Schaefer 2003; Buonviso, Amat et al. 2006). Nevertheless, since this preparation lacks a respiration-like rhythm, the observation of slow oscillations suggests that the olfactory network might have sufficient intrinsic machinery to generate activity at this frequency. This is reminiscent of what is observed in other brain areas such as the HPC, where generation of activity at a theta frequency occurred spontaneously in *in vitro* acute slices (Colgin and Moser 2009; Goutagny, Jackson et al. 2009; Colgin 2013). Bulbar networks generating theta activity might couple to external inputs, like respiratory networks or the HPC, and since this preparation lacks bottom-up inputs, it might help to decipher bulbar contributions to odor-induced plasticity in the absence of higher cortical areas. Coherence between olfactory bulb and hippocampal theta activity has been reported in several studies and it has been associated with different cognitive processes (Kay 2005; Colgin 2013). Importantly, a recent study has shown

that bulbar theta locked to respiration causes theta activity in the HPC at exactly the same frequency. Nevertheless, activity in another theta frequency band is also observed in the HPC which directly modulates bulbar networks at the same frequency (Nguyen Chi, Muller et al. 2016). Odor-evoked responses display activity at high frequencies, which was observed in many in vivo awake or anesthetized studies (Davison and Katz 2007; Kato, Chu et al. 2012). The generation of beta oscillations is known to be dependent on distal cortico-bulbar networks while gamma oscillations are thought to be generated by local networks (Neville and Haberly 2003; Galan, Fourcaud-Trocme et al. 2006). Notably, this preparation allows the study of local networks just within the OB responsible for gamma oscillations while is more unlikely for beta oscillations since it lacks cortical centrifugal input. Cortical feedback to the OB is known to modulate bulbar oscillations (Boyd, Sturgill et al. 2012) and their contribution as well as the role of different neuromodulators to oscillatory activity is well known since isolation of the OB from the rest of the brain abolishes beta waves while gamma activity increases (Neville and Haberly 2003). Noradrenergic modulation is known to contribute to network excitability (Devore and Linster 2012). Supporting this, there are studies that have shown an increment of gamma activity in bulbar acute slices in the presence of noradrenaline (Gire and Schoppa 2008). Reminiscent of other cortical areas, different bulbar subpopulations might generate activity at different frequencies based on synapses between excitatory-inhibitory neurons or inhibitory-inhibitory neurons. Still, more research is needed to clarify the contribution of these interactions. This raises the question how these different oscillations might interact. For cortical areas it is hypothesized that these oscillations might cooperate or compete, in which the oscillatory event with a higher frequency might "win" and thereby synchronizes with the other population (Viriyopase, Memmesheimer et al. 2016). Still, these mechanisms are not fully understood despite the advances made in the electrophysiological and computational field to understand how these populations communicate.

Importantly, maintenance of the preparation at a non physiological temperature (31°C) might influence the oscillatory activity observed. Nevertheless, in a set of experiments, controls for temperature were performed setting the perfusion temperature at 36°C or 26°C observing increases or decreases in frequency activity, respectively. In any case, there was no abolishment of oscillatory activity.

4.5. <u>Plasticity of the OB network</u>

To cope with the environment, different brain areas have the ability to modify their internal functionality in response to different stimuli. The mechanisms underlying plasticity are represented as structural changes, formation of new synapses, modifications in membrane excitability or changes in synaptic efficiency, e.g. via an altered number of neurotransmitter receptors located on a synapse. These changes could lead to long-term plasticity and they are thought to be essential for different cognitive processes like learning and memory, which was first discovered in the hippocampus (Bliss and Lomo 1973). However, there is evidence that the OB circuitry might be involved in these processes, which imply a plastic circuitry. At the level of the OB, plasticity mechanisms occur at different levels, e.g. at the stage of odorant detection, where OSN axon terminals undergo changes which are likely to be behavior-dependent (Kass, Rosenthal et al. 2013) and to be modulated by centrifugal projections and interneurons in the glomerular layer. Within the OB, synaptic plasticity at the level of MCs is mediated via dendrodendritic synapses with GABAergic GCs (Dietz and Murthy 2005; Egger and Urban 2006; Gao and Strowbridge 2009) and has been proposed as a mechanism for olfactory memory (Wilson, Best et al. 2004; Fletcher and Chen 2010; Lepousez, Nissant et al. 2014), sensory adaptation (Li 1990) and olfactory discrimination (Wilson, Best et al. 2004). Specifically, NMDARs are known to play a key role in this synapses being crucial to mediate synaptic plasticity. Besides MC-GC interactions, lateral excitation between MCs exhibits also bidirectional plasticity (Pimentel and Margrie 2008). These mechanisms could serve to normalize sensory information and provide similar output patterns to downstream structures (Suzuki and Bekkers 2006). Still, it is hypothesized that the major form of plasticity at the level of the OB relies on neurogenesis where adult-born neurons are continuously integrated in the OB circuitry over time (Lledo, Alonso et al. 2006; Mizrahi 2007).

4.6. An olfactory nasal - trigeminal pathway modulates respiration

Rhythmogenesis of breathing has been studied in the last decades using *in vivo* (Alheid, Gray et al. 2002) and *in vitro* (Smith, Ellenberger et al. 1991; Ballanyi, Onimaru et al. 1999) preparations as well as semi intact perfused animals (Paton 1996; Dutschmann and Paton 2003). In the latter, resuscitation of the network via oxygenation of the brainstem elicits spontaneous respiratory movements. Eupneic inspiratory bursts have been shown to be comparable to the *in vivo* approach since there is no disruption of synaptic connections. They display similar rhythmic patterns and are distinct from different "normal" behavioral rhythms such as gasping, sighing or sneezing (Richter and Spyer 2001). Sniffing behavior, described as high frequency eupneic breathing is observed during specific behaviors. It has been studied by different workgroups and it is defined based on its short duration which has been measured with a thermocouple device or in diaphragm EMG bursts during olfactory tasks (Rojas-Libano and Kay 2012). So far, the specific neural networks responsible for these fast and short duration bursts are still unknown. Within this thesis, I give evidence of a potential involvement of a trigeminal pathway to modulate respiratory networks during odor presentation as well as to generate putative sniffs. Trigeminal afferents located in the nasal mucosa have been characterized in several studies for triggering protective breath holds like the diving reflex or sneeze to prevent the inhalation of potential noxious molecules (Wallois, Gros et al. 1995; Hummel, Mohammadian et al. 2003). Nasal-trigeminal pathways have been mostly investigated using behavioral paradigms involving cortical and limbic neural networks. Using the nose - brain preparation in the absence of midbrain structures allowed to prove the direct impact of trigeminal odor stimulation on the respiratory brainstem. So-called trigeminal odors triggered putative short sniffs and also respiratory modulation, suggesting a potential mechanism of subconscious odor detection which has been proposed a decade ago (Jacquot, Monnin et al. 2004). The localization of networks in the brainstem responsible for sniffing generation is still under debate. Nasal-trigeminal afferents from the ethmoidal nerve have terminal fields in the caudal nucleus of the sensory spinal trigeminal tract (Sp5C). Besides, there are terminal fields in the NTS and in the KF. Stimulation of the ethmoidal nerve activates these pathways triggering sneeze responses or the diving reflex (Dutschmann and Herbert 1997; Jakus, Halasova et al. 2004) as it has also been shown to be activated during odor presentation. Since the sniff motor pattern described in detail in this thesis (see

for details section 3.2) is different from eupneic respiratory activity it suggests the involvement of different central pattern generators. A possible candidate to gate sniffing generation is the KF since it receives direct naso-trigeminal input (Panneton 1991) and it is also involved in ethmoidal nerve-mediated responses like breath holds (Dutschmann and Dick 2012). Moreover, this is supported by the fact that similar brainstem pathways could be activated via cortico-limbic projections similar to what has been shown in a recent study (McCulloch, Warren et al. 2016). In that way, the same respiratory networks in the brainstem might be targeted by different pathways to provide a fast respiratory response to odor stimuli, on the one hand a naso-trigeminal pathway to evoke fast protective reflexes and on the other hand cortico-limbic networks gating behavioral inputs.

4.7. <u>Future perspectives</u>

This thesis is based on the description of a new promising technique to study bulbar network properties as well as a good method to study interactions between olfaction and respiration. Still, the spectrum of possibilities that this preparation offers are quite variable. This preparation has been performed in juvenile Wistar rats at the age between 12 and 17 post-natal days. Nevertheless, it could be possible to adapt this technique to neonate rats since they already have a functional olfactory system (Wilson and Sullivan 1994) as well as in older animals (Paton 1996). This could allow studies concerning neural development and oscillatory patterns at the level of the olfactory bulb. Moreover, the experimental setup allows pharmacological studies to investigate synaptic mechanisms and its effects in oscillatory activity.

Similar to conventional *in vivo* experiments, all the data presented in this thesis have been recorded from the dorsal side of the olfactory bulb. Nevertheless, one promising adaptation of this preparation is the exposure of the lateral sides of the olfactory bulb for the first time, which might allow different electrophysiological recordings. Moreover, it could be possible to study bulbar network properties both in dorsal and lateral sides of the bulb during odor presentation using two-photon calcium imaging applying the bolus loading technique (Stosiek, Garaschuk et al. 2003; Garaschuk, Milos et al. 2006). All the existing defined protocols using this technique have been established under *in vivo* or *in vitro* conditions. Application of these defined protocols are likely to not succeed in perfused semi intact animals because the perfusion condition of the preparation might wash out part of the dye, the maintenance of the preparation occurs at a non-physiological temperature and the preparation lacks internal mechanisms to counteract the toxicity effects of the dye´s solvent. These protocols are established taking into account different variables such as concentration, duration time and injection pressure of the dye. Unfortunately, there is still no effective bolus loading protocol defined for injections in the OB in semi intact preparations of rats and variations of these parameters might be crucial for its optimization. Another potential future pathway concerning imaging techniques related to this preparation, might be the loading of the nasal epithelium with dextran dyes (Wachowiak and Cohen 2001). Staining of OSNs might allow to visualize glomerular neuropil and to study intra and interglomerular networks during odor presentation which are thought to be crucial for generation of slow wave activity (Fourcaud-Trocme, Courtiol et al. 2014). Although

not shown in this thesis, I performed some proof of principle experiments for both imaging techniques which showed promising results for future experiments. Nevertheless, more experimental data is needed for both techniques to be further developed and to establish practicable imaging techniques for upcoming new semi intact preparations.

The odor set used for experiments within this thesis was restricted to a few oil-based odors using a computer controlled olfactometer. However, single odor molecule stimulation could be also a potential alternative to investigate odor map representations at the level of the olfactory bulb. Moreover, using an olfactometer with a higher temporal resolution might improve the precision of the odor presentation.

4.8. Final remarks

Conclusively, the olfactory bulb underlies many processes which are vital for the survival of many animals. This thesis presents a new valuable research technique as an alternative to different approaches. Its suitability is based on the recording of odor responses compared to already established techniques. The preservation of an intact olfactory pathway allows to study olfactory network properties at different levels. Furthermore, the possibility to link directly olfaction to respiration in the absence of cortical areas represents a good direction for research in both olfactory and respiratory fields as well as the study of their interaction.

5. <u>Bibliography</u>

Abraham, N. M., V. Egger, et al. (2010). "Synaptic inhibition in the olfactory bulb accelerates odor discrimination in mice." <u>Neuron</u> **65**(3): 399-411.

Ackels, T., B. von der Weid, et al. (2014). "Physiological characterization of formyl peptide receptor expressing cells in the mouse vomeronasal organ." <u>Frontiers in Neuroanatomy</u> **8**: 134.

Adrian, E. D. (1942). "Olfactory reactions in the brain of the hedgehog." <u>J Physiol</u> **100**(4): 459-473.

Adrian, E. D. (1952). "[The discrimination of odours by the nose]." <u>Schweizerische medizinische Wochenschrift</u> **82**(39): 973-974.

Ahrens, K. F. and W. J. Freeman (2001). "Response dynamics of entorhinal cortex in awake, anesthetized, and bulbotomized rats." <u>Brain Research</u> **911**(2): 193-202.

Alheid, G. F., P. A. Gray, et al. (2002). "Parvalbumin in respiratory neurons of the ventrolateral medulla of the adult rat." <u>Journal of neurocytology</u> **31**(8-9): 693-717.

Alimohammadi, H. and W. L. Silver (2000). "Evidence for nicotinic acetylcholine receptors on nasal trigeminal nerve endings of the rat." <u>Chem Senses</u> **25**(1): 61-66.

Alves, J., A. Petrosyan, et al. (2014). "Olfactory dysfunction in dementia." <u>World journal of clinical cases</u> **2**(11): 661-667.

Apicella, A., Q. Yuan, et al. (2010). "Pyramidal cells in piriform cortex receive convergent input from distinct olfactory bulb glomeruli." <u>The Journal of neuroscience : the official journal of the Society for Neuroscience</u> **30**(42): 14255-14260.

Baker, T. L., D. D. Fuller, et al. (2001). "Respiratory plasticity: differential actions of continuous and episodic hypoxia and hypercapnia." <u>Respiration physiology</u> **129**(1-2): 25-35.

Ballantyne, D. and P. Scheid (2001). "Central chemosensitivity of respiration: a brief overview." <u>Respiration physiology</u> **129**(1-2): 5-12.

Ballanyi, K., H. Onimaru, et al. (1999). "Respiratory network function in the isolated brainstem-spinal cord of newborn rats." <u>Progress in neurobiology</u> **59**(6): 583-634.

Barnes, D. C. and D. A. Wilson (2014). "Sleep and olfactory cortical plasticity." <u>Frontiers in behavioral neuroscience</u> **8**: 134.

Barresi, M., R. Ciurleo, et al. (2012). "Evaluation of olfactory dysfunction in neurodegenerative diseases." <u>Journal of the neurological sciences</u> **323**(1-2): 16-24.

Barrios, F. A., L. Gonzalez, et al. (2007). "Olfaction and neurodegeneration in HD." <u>Neuroreport</u> **18**(1): 73-76.

Bathellier, B., S. Lagier, et al. (2006). "Circuit properties generating gamma oscillations in a network model of the olfactory bulb (vol 95, pg 2678, 2006)." <u>Journal of Neurophysiology</u> **95**(6): 3961-3962.

Berghard, A. and L. B. Buck (1996). "Sensory transduction in vomeronasal neurons: Evidence for G alpha o, G alpha i2, and adenylyl cyclase II as major components of a pheromone signaling cascade." <u>Journal of Neuroscience</u> **16**(3): 909-918.

Bernard, D. G., A. Li, et al. (1996). "Evidence for central chemoreception in the midline raphe." <u>Journal of applied physiology</u> **80**(1): 108-115.

Bianchi, A. L. and C. Gestreau (2009). "The brainstem respiratory network: an overview of a half century of research." <u>Respiratory physiology & neurobiology</u> **168**(1-2): 4-12.

Bliss, T. V. and T. Lomo (1973). "Long-lasting potentiation of synaptic transmission in the dentate area of the anaesthetized rabbit following stimulation of the perforant path." <u>J Physiol</u> **232**(2): 331-356.

Borowsky, B., N. Adham, et al. (2001). "Trace amines: identification of a family of mammalian G protein-coupled receptors." <u>Proceedings of the National Academy of Sciences of the United States of America</u> **98**(16): 8966-8971.

Boudreau, J. C. (1962). "Electrical activity in the olfactory tract of the catfish." <u>The Japanese journal of physiology</u> **12**: 272-278.

Boyd, A. M., H. K. Kato, et al. (2015). "Broadcasting of cortical activity to the olfactory bulb." Cell reports **10**(7): 1032-1039.

Boyd, A. M., J. F. Sturgill, et al. (2012). "Cortical feedback control of olfactory bulb circuits." Neuron **76**(6): 1161-1174.

Brechbuhl, J., M. Klaey, et al. (2008). "Grueneberg ganglion cells mediate alarm pheromone detection in mice." Science **321**(5892): 1092-1095.

Brennan, P. A. (2010). Pheromones and Mammalian Behavior. The Neurobiology of Olfaction. A. Menini. Boca Raton (FL).

Bressler, S. L. (1988). "Changes in electrical activity of rabbit olfactory bulb and cortex to conditioned odor stimulation." Behavioral neuroscience **102**(5): 740-747.

Bressler, S. L. and W. J. Freeman (1980). "Frequency analysis of olfactory system EEG in cat, rabbit, and rat." Electroencephalography and clinical neurophysiology **50**(1-2): 19-24.

Brill, J., Z. Shao, et al. (2016). "Serotonin increases synaptic activity in olfactory bulb glomeruli." Journal of Neurophysiology **115**(3): 1208-1219.

Brinon, J. G., R. Arevalo, et al. (1998). "Neurocalcin immunoreactivity in the rat main olfactory bulb." Brain Research **795**(1-2): 204-214.

Brinon, J. G., F. J. Martinez-Guijarro, et al. (1999). "Coexpression of neurocalcin with other calcium-binding proteins in the rat main olfactory bulb." J Comp Neurol **407**(3): 404-414.

Brunert, D., Y. Tsuno, et al. (2016). "Cell-Type-Specific Modulation of Sensory Responses in Olfactory Bulb Circuits by Serotonergic Projections from the Raphe Nuclei." The Journal of neuroscience : the official journal of the Society for Neuroscience **36**(25): 6820-6835.

Brunjes, P. C., K. R. Illig, et al. (2005). "A field guide to the anterior olfactory nucleus (cortex)." Brain research. Brain research reviews **50**(2): 305-335.

Buonviso, N., C. Amat, et al. (2006). "Respiratory modulation of olfactory neurons in the rodent brain." Chem Senses **31**(2): 145-154.

Buonviso, N., C. Amat, et al. (2003). "Rhythm sequence through the olfactory bulb layers during the time window of a respiratory cycle." Eur J Neurosci **17**(9): 1811-1819.

Buschuter, D., M. Smitka, et al. (2008). "Correlation between olfactory bulb volume and olfactory function." NeuroImage **42**(2): 498-502.

Bushdid, C., M. O. Magnasco, et al. (2014). "Humans Can Discriminate More than 1 Trillion Olfactory Stimuli." Science **343**(6177): 1370-1372.

Buzsaki, G. and X. J. Wang (2012). "Mechanisms of gamma oscillations." Annual Review of Neuroscience **35**: 203-225.

Caminiti, F., S. De Salvo, et al. (2014). "Detection of Olfactory Dysfunction Using Olfactory Event Related Potentials in Young Patients with Multiple Sclerosis." PLoS ONE **9**(7).

Cang, J. and J. S. Isaacson (2003). "In vivo whole-cell recording of odor-evoked synaptic transmission in the rat olfactory bulb." J Neurosci **23**(10): 4108-4116.

Carroll, J. L. (2003). "Developmental plasticity in respiratory control." Journal of applied physiology **94**(1): 375-389.

Casjens, S., A. Eckert, et al. (2013). "Diagnostic Value of the Impairment of Olfaction in Parkinson's Disease." PLoS ONE **8**(5).

Castillo, P. E., A. Carleton, et al. (1999). "Multiple and opposing roles of cholinergic transmission in the main olfactory bulb." The Journal of neuroscience : the official journal of the Society for Neuroscience **19**(21): 9180-9191.

Cazakoff, B. N., B. Y. B. Lau, et al. (2014). "Broadly tuned and respiration-independent inhibition in the olfactory bulb of awake mice." Nat Neurosci **17**(4): 569-576.

Cenier, T., F. David, et al. (2009). "Respiration-gated formation of gamma and beta neural assemblies in the mammalian olfactory bulb." Eur J Neurosci **29**(5): 921-930.

Chabaud, P., N. Ravel, et al. (1999). "Functional coupling in rat central olfactory pathways: a coherence analysis." Neuroscience Letters **276**(1): 17-20.

Chen, W. R., W. Xiong, et al. (2000). "Analysis of relations between NMDA receptors and GABA release at olfactory bulb reciprocal synapses." Neuron **25**(3): 625-633.

Coates, E. L., A. Li, et al. (1993). "Widespread sites of brain stem ventilatory chemoreceptors." Journal of applied physiology **75**(1): 5-14.

Cohen, M. I. (1971). "Switching of the respiratory phases and evoked phrenic responses produced by rostral pontine electrical stimulation." J Physiol **217**(1): 133-158.

Cohen, M. I. and C. F. Shaw (2004). "Role in the inspiratory off-switch of vagal inputs to rostral pontine inspiratory-modulated neurons." Respiratory physiology & neurobiology **143**(2-3): 127-140.

Colgin, L. L. (2013). "Mechanisms and functions of theta rhythms." Annual Review of Neuroscience **36**: 295-312.

Colgin, L. L. and E. I. Moser (2009). "Hippocampal theta rhythms follow the beat of their own drum." Nature Neuroscience **12**(12): 1483-1484.

Courtiol, E., C. Amat, et al. (2011). "Reshaping of Bulbar Odor Response by Nasal Flow Rate in the Rat." PLoS ONE **6**(1).

David, F., E. Courtiol, et al. (2015). "Competing Mechanisms of Gamma and Beta Oscillations in the Olfactory Bulb Based on Multimodal Inhibition of Mitral Cells Over a Respiratory Cycle." eNeuro **2**(6).

Davis, B. J. and F. Macrides (1981). "The organization of centrifugal projections from the anterior olfactory nucleus, ventral hippocampal rudiment, and piriform cortex to the main olfactory bulb in the hamster: an autoradiographic study." J Comp Neurol **203**(3): 475-493.

Davison, I. G. and L. C. Katz (2007). "Sparse and selective odor coding by mitral/tufted neurons in the main olfactory bulb." Journal of Neuroscience **27**(8): 2091-2101.

de Almeida, L., M. Idiart, et al. (2013). "A model of cholinergic modulation in olfactory bulb and piriform cortex." Journal of Neurophysiology **109**(5): 1360-1377.

De Saint Jan, D., D. Hirnet, et al. (2009). "External tufted cells drive the output of olfactory bulb glomeruli." J Neurosci **29**(7): 2043-2052.

Delaney, K. R. and B. J. Hall (1996). "An in vitro preparation of frog nose and brain for the study of odour-evoked oscillatory activity." J Neurosci Methods **68**(2): 193-202.

Delmaire, C., E. M. Dumas, et al. (2013). "The structural correlates of functional deficits in early huntington's disease." Human Brain Mapping **34**(9): 2141-2153.

Devore, S. and C. Linster (2012). "Noradrenergic and cholinergic modulation of olfactory bulb sensory processing." Frontiers in behavioral neuroscience **6**: 52.

Di Prisco, G. V. and W. J. Freeman (1985). "Odor-related bulbar EEG spatial pattern analysis during appetitive conditioning in rabbits." Behavioral neuroscience **99**(5): 964-978.

Dietz, S. B. and V. N. Murthy (2005). "Contrasting short-term plasticity at two sides of the mitral-granule reciprocal synapse in the mammalian olfactory bulb." Journal of Physiology-London **569**(2): 475-488.

Dinh, Q. T., D. A. Groneberg, et al. (2003). "Expression of substance P and vanilloid receptor (VR1) in trigeminal sensory neurons projecting to the mouse nasal mucosa." Neuropeptides **37**(4): 245-250.

Dorries, K. M. and J. S. Kauer (2000). "Relationships between odor-elicited oscillations in the salamander olfactory epithelium and olfactory bulb." Journal of Neurophysiology **83**(2): 754-765.

Doty, R. L. (1986). "Odor-guided behavior in mammals." Experientia **42**(3): 257-271.

Doty, R. L. (2007). "Olfaction in Parkinson's disease." Parkinsonism & related disorders **13**: S225-S228.

Doty, R. L. (2012). "Olfaction in Parkinson's disease and related disorders." Neurobiology of Disease **46**(3): 527-552.

Doty, R. L. and V. Kamath (2014). "The influences of age on olfaction: a review." Frontiers in psychology **5**: 20.

Doty, R. L. and V. Kamath (2014). "The influences of age on olfaction: a review." Frontiers in psychology **5**.

Doucette, W., J. Milder, et al. (2007). "Adrenergic modulation of olfactory bulb circuitry affects odor discrimination." Learning & memory **14**(8): 539-547.

Dutschmann, M. and T. E. Dick (2012). "Pontine mechanisms of respiratory control." <u>Comprehensive Physiology</u> **2**(4): 2443-2469.

Dutschmann, M. and H. Herbert (1996). "The Kolliker-Fuse nucleus mediates the trigeminally induced apnoea in the rat." <u>Neuroreport</u> **7**(8): 1432-1436.

Dutschmann, M. and H. Herbert (1997). "Fos expression in the rat parabrachial and Kolliker-Fuse nuclei after electrical stimulation of the trigeminal ethmoidal nerve and water stimulation of the nasal mucosa." <u>Experimental brain research</u> **117**(1): 97-110.

Dutschmann, M. and H. Herbert (2006). "The Kolliker-Fuse nucleus gates the postinspiratory phase of the respiratory cycle to control inspiratory off-switch and upper airway resistance in rat." <u>Eur J Neurosci</u> **24**(4): 1071-1084.

Dutschmann, M. and J. F. Paton (2003). "Whole cell recordings from respiratory neurones in an arterially perfused in situ neonatal rat preparation." <u>Experimental physiology</u> **88**(6): 725-732.

Eckmeier, D. and S. D. Shea (2014). "Noradrenergic plasticity of olfactory sensory neuron inputs to the main olfactory bulb." <u>The Journal of neuroscience : the official journal of the Society for Neuroscience</u> **34**(46): 15234-15243.

Eeckman, F. H. and W. J. Freeman (1990). "Correlations between Unit Firing and Eeg in the Rat Olfactory System." <u>Brain Research</u> **528**(2): 238-244.

Egger, V. and O. Stroh (2009). "Calcium buffering in rodent olfactory bulb granule cells and mitral cells." <u>J Physiol</u> **587**(Pt 18): 4467-4479.

Egger, V., K. Svoboda, et al. (2003). "Mechanisms of lateral inhibition in the olfactory bulb: Efficiency and modulation of spike-evoked calcium influx into granule cells." <u>J Neurosci</u> **23**: 7551-7558.

Egger, V., K. Svoboda, et al. (2005). "Dendrodendritic synaptic signals in olfactory bulb granule cells: Local spine boost and global low-threshold spike." <u>J Neurosci</u> **25**: 3521-3530.

Egger, V. and N. N. Urban (2006). "Dynamic connectivity in the mitral cell-granule cell microcircuit." <u>Seminars in Cell & Developmental Biology</u> **17**(4): 424-432.

Egger, V. and N. N. Urban (2006). "Dynamic connectivity in the mitral cell-granule cell microcircuit." <u>Semin Cell Dev Biol</u> **17**(4): 424-432.

Escanilla, O., S. Alperin, et al. (2012). "Noradrenergic but not cholinergic modulation of olfactory bulb during processing of near threshold concentration stimuli." <u>Behavioral neuroscience</u> **126**(5): 720-728.

Esclassan, F., E. Courtiol, et al. (2012). "Faster, Deeper, Better: The Impact of Sniffing Modulation on Bulbar Olfactory Processing." <u>PLoS ONE</u> **7**(7).

Esclassan, F., E. Courtiol, et al. (2012). "Faster, deeper, better: the impact of sniffing modulation on bulbar olfactory processing." <u>PLoS ONE</u> **7**(7): e40927.

Eyre, M. D., M. Antal, et al. (2008). "Distinct deep short-axon cell subtypes of the main olfactory bulb provide novel intrabulbar and extrabulbar GABAergic connections." <u>J Neurosci</u> **28**(33): 8217-8229.

Eyre, M. D., K. Kerti, et al. (2009). "Molecular diversity of deep short-axon cells of the rat main olfactory bulb." <u>Eur J Neurosci</u> **29**(7): 1397-1407.

Feldman, J. L. and M. D.R., Eds. (2003). <u>Neural control of breathing.</u> Fundamental Neuroscience.

Feldman, J. L. and C. A. Del Negro (2006). "Looking for inspiration: new perspectives on respiratory rhythm." <u>Nature reviews. Neuroscience</u> **7**(3): 232-242.

Feldman, J. L., G. S. Mitchell, et al. (2003). "Breathing: Rhythmicity, plasticity, chemosensitivity." <u>Annual Review of Neuroscience</u> **26**: 239-266.

Fletcher, M. L. and W. R. Chen (2010). "Neural correlates of olfactory learning: Critical role of centrifugal neuromodulation." <u>Learning & memory</u> **17**(11): 561-570.

Fontanini, A., P. Spano, et al. (2003). "Ketamine-xylazine-induced slow (< 1.5 Hz) oscillations in the rat piriform (olfactory) cortex are functionally correlated with respiration." <u>The Journal of neuroscience : the official journal of the Society for Neuroscience</u> **23**(22): 7993-8001.

Forster, H. V. (2003). "Plasticity in the control of breathing following sensory denervation." <u>Journal of applied physiology</u> **94**(2): 784-794.

Fourcaud-Trocme, N., E. Courtiol, et al. (2014). "Two distinct olfactory bulb sublaminar networks involved in gamma and beta oscillation generation: a CSD study in the anesthetized rat." Frontiers in Neural Circuits **8**: 88.

Freeman, W. J. (1978). "Spatial properties of an EEG event in the olfactory bulb and cortex." Electroencephalography and clinical neurophysiology **44**(5): 586-605.

Freeman, W. J. and W. Schneider (1982). "Changes in spatial patterns of rabbit olfactory EEG with conditioning to odors." Psychophysiology **19**(1): 44-56.

Friedrich, R. W. and G. Laurent (2001). "Dynamic optimization of odor representations by slow temporal patterning of mitral cell activity." Science **291**(5505): 889-894.

Fukunaga, I., M. Berning, et al. (2012). "Two distinct channels of olfactory bulb output." Neuron **75**(2): 320-329.

Gaillard, I., S. Rouquier, et al. (2004). "Olfactory receptors." Cellular and molecular life sciences : CMLS **61**(4): 456-469.

Galan, R. F., N. Fourcaud-Trocme, et al. (2006). "Correlation-induced synchronization of oscillations in olfactory bulb neurons." The Journal of neuroscience : the official journal of the Society for Neuroscience **26**(14): 3646-3655.

Galizia, C. G. and P. M. Lledo (2013). "Neurosciences - From Molecule to Behavior: A university textbook." Neuroforum **19**(1): 27-27.

Gallego, J., E. Nsegbe, et al. (2001). "Learning in respiratory control." Behavior modification **25**(4): 495-512.

Gao, Y. and B. W. Strowbridge (2009). "Long-term plasticity of excitatory inputs to granule cells in the rat olfactory bulb." Nature Neuroscience **12**(6): 731-733.

Garaschuk, O., R. I. Milos, et al. (2006). "Targeted bulk-loading of fluorescent indicators for two-photon brain imaging in vivo." Nature protocols **1**(1): 380-386.

Gaykema, R. P., P. G. Luiten, et al. (1990). "Cortical projection patterns of the medial septum-diagonal band complex." J Comp Neurol **293**(1): 103-124.

Gelperin, A. and D. W. Tank (1990). "Odour-modulated collective network oscillations of olfactory interneurons in a terrestrial mollusc." Nature **345**(6274): 437-440.

Gire, D. H., K. M. Franks, et al. (2012). "Mitral cells in the olfactory bulb are mainly excited through a multistep signaling path." J Neurosci **32**(9): 2964-2975.

Gire, D. H. and N. E. Schoppa (2008). "Long-term enhancement of synchronized oscillations by adrenergic receptor activation in the olfactory bulb." Journal of Neurophysiology **99**(4): 2021-2025.

Godoy, M. D., R. L. Voegels, et al. (2015). "Olfaction in neurologic and neurodegenerative diseases: a literature review." International archives of otorhinolaryngology **19**(2): 176-179.

Goutagny, R., J. Jackson, et al. (2009). "Self-generated theta oscillations in the hippocampus." Nature Neuroscience **12**(12): 1491-1493.

Gracia-Llanes, F. J., C. Crespo, et al. (2010). "GABAergic basal forebrain afferents innervate selectively GABAergic targets in the main olfactory bulb." Neuroscience **170**(3): 913-922.

Gray, P. A., W. A. Janczewski, et al. (2001). "Normal breathing requires preBotzinger complex neurokinin-1 receptor-expressing neurons." Nature Neuroscience **4**(9): 927-930.

Gray, P. A., J. C. Rekling, et al. (1999). "Modulation of respiratory frequency by peptidergic input to rhythmogenic neurons in the preBotzinger complex." Science **286**(5444): 1566-1568.

Grosmaitre, X., L. C. Santarelli, et al. (2007). "Dual functions of mammalian olfactory sensory neurons as odor detectors and mechanical sensors." Dual functions of mammalian olfactory sensory neurons as odor detectors and mechanical sensors **10**(3): 348-354.

Gutierrez-Castellanos, N., C. Pardo-Bellver, et al. (2014). "The vomeronasal cortex - afferent and efferent projections of the posteromedial cortical nucleus of the amygdala in mice." European Journal of Neuroscience **39**(1): 141-158.

Guyenet, P. G. and H. Wang (2001). "Pre-Botzinger neurons with preinspiratory discharges "in vivo" express NK1 receptors in the rat." Journal of Neurophysiology **86**(1): 438-446.

Guzman-Aranguez, A., X. Gasull, et al. (2014). "Purinergic Receptors in Ocular Inflammation." Mediators of Inflammation.

Haehner, A., T. Hummel, et al. (2009). "Olfactory dysfunction as a diagnostic marker for Parkinson's disease." Expert Review of Neurotherapeutics **9**(12): 1773-1779.

Haehner, A., T. Hummel, et al. (2011). "Olfactory Loss in Parkinson's Disease." Parkinsons Disease.

Hall, B. and K. Delaney (2001). "Cholinergic modulation of odor-evoked oscillations in the frog olfactory bulb." The Biological bulletin **201**(2): 276-277.

Halpern, M. and A. Martinez-Marcos (2003). "Structure and function of the vomeronasal system: an update." Progress in neurobiology **70**(3): 245-318.

Hamilton, J. M., C. Murphy, et al. (1999). "Odor detection, learning, and memory in Huntington's disease." Journal of the International Neuropsychological Society **5**(7): 609-615.

Heimer, L., D. S. Zahm, et al. (1990). "The basal forebrain projection to the region of the nuclei gemini in the rat; a combined light and electron microscopic study employing horseradish peroxidase, fluorescent tracers and Phaseolus vulgaris-leucoagglutinin." Neuroscience **34**(3): 707-731.

Hummel, T., B. N. Landis, et al. (2011). "Smell and taste disorders." GMS current topics in otorhinolaryngology, head and neck surgery **10**: Doc04.

Hummel, T., P. Mohammadian, et al. (2003). "Pain in the trigeminal system: irritation of the nasal mucosa using short- and long-lasting stimuli." International Journal of Psychophysiology **47**(2): 147-158.

Ichikawa, H. and T. Sugimoto (2002). "The co-expression of ASIC3 with calcitonin gene-related peptide and parvalbumin in the rat trigeminal ganglion." Brain Research **943**(2): 287-291.

Igarashi, K. M., N. Ieki, et al. (2012). "Parallel Mitral and Tufted Cell Pathways Route Distinct Odor Information to Different Targets in the Olfactory Cortex." The Journal of Neuroscience **32**(23): 7970-7985.

Imai, T. (2014). "Construction of functional neuronal circuitry in the olfactory bulb." Seminars in Cell & Developmental Biology **35**: 180-188.

Imai, T. and H. Sakano (2008). "Odorant receptor-mediated signaling in the mouse." Current Opinion in Neurobiology **18**(3): 251-260.

Isaacson, J. S. (1999). "Glutamate spillover mediates excitatory transmission in the rat olfactory bulb." Neuron **23**(2): 377-384.

Isaacson, J. S. and G. J. Murphy (2001). "Glutamate-mediated extrasynaptic inhibition: direct coupling of NMDA receptors to Ca(2+)-activated K+ channels." Neuron **31**(6): 1027-1034.

Isaacson, J. S. and B. W. Strowbridge (1998). "Olfactory reciprocal synapses: dendritic signaling in the CNS." Neuron **20**(4): 749-761.

Ishikawa, T., T. Sato, et al. (2007). "Odor-driven activity in the olfactory cortex of an in vitro isolated guinea pig whole brain with olfactory epithelium." Journal of Neurophysiology **97**(1): 670-679.

Jacquot, L., J. Monnin, et al. (2004). "Influence of nasal trigeminal stimuli on olfactory sensitivity." Comptes rendus biologies **327**(4): 305-311.

Jahr, C. E. and R. A. Nicoll (1980). "Dendrodendritic inhibition: demonstration with intracellular recording." Science **207**(4438): 1473-1475.

Jahr, C. E. and R. A. Nicoll (1982). "Noradrenergic modulation of dendrodendritic inhibition in the olfactory bulb." Nature **297**(5863): 227-229.

Jakus, J., E. Halasova, et al. (2004). "Brainstem areas involved in the aspiration reflex: c-Fos study in anesthetized cats." Physiological research / Academia Scientiarum Bohemoslovaca **53**(6): 703-717.

Jessberger, J., W. Zhong, et al. (2016). "Olfactory Bulb Field Potentials and Respiration in Sleep-Wake States of Mice." Neural plasticity **2016**: 4570831.

Johnson, M. A., L. Tsai, et al. (2012). "Neurons expressing trace amine-associated receptors project to discrete glomeruli and constitute an olfactory subsystem." Proceedings of the National Academy of Sciences of the United States of America **109**(33): 13410-13415.

Kaas, J. H. (2005). "From mice to men: the evolution of the large, complex human brain." Journal of biosciences **30**(2): 155-165.

Kapoor, V., A. C. Provost, et al. (2016). "Activation of raphe nuclei triggers rapid and distinct effects on parallel olfactory bulb output channels." Nature Neuroscience **19**(2): 271-282.

Kass, M. D., M. C. Rosenthal, et al. (2013). "Fear learning enhances neural responses to threat-predictive sensory stimuli." Science **342**(6164): 1389-1392.

Kato, Hiroyuki K., Monica W. Chu, et al. (2012). "Dynamic Sensory Representations in the Olfactory Bulb: Modulation by Wakefulness and Experience." Neuron **76**(5): 962-975.

Kay, L. M. (2003). "Two species of gamma oscillations in the olfactory bulb: dependence on behavioral state and synaptic interactions." Journal of integrative neuroscience **2**(1): 31-44.

Kay, L. M. (2005). "Theta oscillations and sensorimotor performance." Proceedings of the National Academy of Sciences of the United States of America **102**(10): 3863-3868.

Kay, L. M. (2014). "Circuit oscillations in odor perception and memory." Progress in brain research **208**: 223-251.

Kay, L. M. and J. Beshel (2010). "A beta oscillation network in the rat olfactory system during a 2-alternative choice odor discrimination task." Journal of Neurophysiology **104**(2): 829-839.

Kay, L. M., J. Beshel, et al. (2009). "Olfactory oscillations: the what, how and what for." Trends in Neurosciences **32**(4): 207-214.

Kepecs, A., N. Uchida, et al. (2006). "The sniff as a unit of olfactory processing." Chem Senses **31**(2): 167-179.

Keverne, E. B. (2004). "Importance of olfactory and vomeronasal systems for male sexual function." Physiology & behavior **83**(2): 177-187.

Kleinfeld, D., K. R. Delaney, et al. (1994). "Dynamics of propagating waves in the olfactory network of a terrestrial mollusk: an electrical and optical study." Journal of Neurophysiology **72**(3): 1402-1419.

Kollo, M., A. Schmaltz, et al. (2014). "'Silent' mitral cells dominate odor responses in the olfactory bulb of awake mice." Nature Neuroscience **17**(10): 1313-1315.

Kosaka, K., C. W. Heizmann, et al. (1994). "Calcium-binding protein parvalbumin-immunoreactive neurons in the rat olfactory bulb. 1. Distribution and structural features in adult rat." Experimental brain research **99**(2): 191-204.

Kosaka, T. and K. Kosaka (2011). ""Interneurons" in the olfactory bulb revisited." Neuroscience Research **69**(2): 93-99.

Koshiya, N. and J. C. Smith (1999). "Neuronal pacemaker for breathing visualized in vitro." Nature **400**(6742): 360-363.

Lam, Y. W., L. B. Cohen, et al. (2000). "Odors elicit three different oscillations in the turtle olfactory bulb." The Journal of neuroscience : the official journal of the Society for Neuroscience **20**(2): 749-762.

Landis, B. N., C. G. Konnerth, et al. (2004). "A study on the frequency of olfactory dysfunction." Laryngoscope **114**(10): 1764-1769.

Laurent, G. (1999). "A systems perspective on early olfactory coding." Science **286**(5440): 723-728.

Laurent, G. and H. Davidowitz (1994). "Encoding of olfactory information with oscillating neural assemblies." Science **265**(5180): 1872-1875.

Lazic, S. E., A. O. G. Goodman, et al. (2007). "Olfactory abnormalities in Huntington's disease: Decreased plasticity in the primary olfactory cortex of R6/1 transgenic mice and reduced olfactory discrimination in patients." Brain Research **1151**: 219-226.

Lepousez, G., Z. Csaba, et al. (2010). "Somatostatin interneurons delineate the inner part of the external plexiform layer in the mouse main olfactory bulb." J Comp Neurol **518**(11): 1976-1994.

Lepousez, G., A. Nissant, et al. (2014). "Olfactory learning promotes input-specific synaptic plasticity in adult-born neurons." Proceedings of the National Academy of Sciences of the United States of America **111**(38): 13984-13989.

Li, A., L. Zhang, et al. (2012). "Effects of different anesthetics on oscillations in the rat olfactory bulb." Journal of the American Association for Laboratory Animal Science : JAALAS **51**(4): 458-463.

Li, L. M., L. N. Yang, et al. (2016). "Olfactory dysfunction in patients with multiple sclerosis." Journal of the neurological sciences **365**: 34-39.

Li, M. H., S. Q. Liu, et al. (2014). "Acid-sensing ion channels in mouse olfactory bulb M/T neurons." J Gen Physiol **143**(6): 719-731.

Li, Z. (1990). "A model of olfactory adaptation and sensitivity enhancement in the olfactory bulb." Biological cybernetics **62**(4): 349-361.

Liberles, S. D. and L. B. Buck (2006). "A second class of chemosensory receptors in the olfactory epithelium." Nature **442**(7103): 645-650.

Litaudon, P., S. Garcia, et al. (2008). "Strong Coupling between Pyramidal Cell Activity and Network Oscillations in the Olfactory Cortex." Neuroscience **156**(3): 781-787.

Liu, S., J. L. Aungst, et al. (2012). "Serotonin modulates the population activity profile of olfactory bulb external tufted cells." Journal of Neurophysiology **107**(1): 473-483.

Lledo, P. M., M. Alonso, et al. (2006). "Adult neurogenesis and functional plasticity in neuronal circuits." Nature reviews. Neuroscience **7**(3): 179-193.

Llinas, R. and M. Muhlethaler (1988). "An electrophysiological study of the in vitro, perfused brain stem-cerebellum of adult guinea-pig." J Physiol **404**: 215-240.

Llinas, R., Y. Yarom, et al. (1981). "Isolated mammalian brain in vitro: new technique for analysis of electrical activity of neuronal circuit function." Federation proceedings **40**(8): 2240-2245.

Lucassen, E. B., A. Turel, et al. (2016). "Olfactory dysfunction in Multiple Sclerosis: A scoping review of the literature." Multiple sclerosis and related disorders **6**: 1-9.

Ma, L., Q. Qiu, et al. (2012). "Distributed representation of chemical features and tunotopic organization of glomeruli in the mouse olfactory bulb." Proceedings of the National Academy of Sciences of the United States of America **109**(14): 5481-5486.

Ma, M. and M. Luo (2012). "Optogenetic activation of basal forebrain cholinergic neurons modulates neuronal excitability and sensory responses in the main olfactory bulb." The Journal of neuroscience : the official journal of the Society for Neuroscience **32**(30): 10105-10116.

Macrides, F. and S. L. Chorover (1972). "Olfactory bulb units: activity correlated with inhalation cycles and odor quality. ." Science **175**: 84-87.

Malnic, B., J. Hirono, et al. (1999). "Combinatorial receptor codes for odors." Cell **96**(5): 713-723.

Manabe, H., I. Kusumoto-Yoshida, et al. (2011). "Olfactory cortex generates synchronized top-down inputs to the olfactory bulb during slow-wave sleep." The Journal of neuroscience : the official journal of the Society for Neuroscience **31**(22): 8123-8133.

Manabe, H. and K. Mori (2013). "Sniff rhythm-paced fast and slow gamma-oscillations in the olfactory bulb: relation to tufted and mitral cells and behavioral states." Journal of neurophysiology **110**(7): 1593-1599.

Margrie, T. W. and A. T. Schaefer (2003). "Theta oscillation coupled spike latencies yield computational vigour in a mammalian sensory system." J Physiol **546**(Pt 2): 363-374.

Maritan, M., G. Monaco, et al. (2009). "Odorant receptors at the growth cone are coupled to localized cAMP and Ca2+ increases." Proceedings of the National Academy of Sciences of the United States of America **106**(9): 3537-3542.

Markopoulos, F., D. Rokni, et al. (2012). "Functional properties of cortical feedback projections to the olfactory bulb." Neuron **76**(6): 1175-1188.

Martin, C., R. Gervais, et al. (2004). "Learning-induced modulation of oscillatory activities in the mammalian olfactory system: the role of the centrifugal fibres." Journal of physiology, Paris **98**(4-6): 467-478.

Martin, C., R. Gervais, et al. (2006). "Learning-induced oscillatory activities correlated to odour recognition: a network activity." Eur J Neurosci **23**(7): 1801-1810.

Martin, C. and N. Ravel (2014). "Beta and gamma oscillatory activities associated with olfactory memory tasks: different rhythms for different functional networks?" Frontiers in behavioral neuroscience **8**: 218.

McCulloch, P. F., E. A. Warren, et al. (2016). "Repetitive Diving in Trained Rats Still Increases Fos Production in Brainstem Neurons after Bilateral Sectioning of the Anterior Ethmoidal Nerve." Frontiers in physiology **7**: 148.

McLean, J. H. and M. T. Shipley (1987). "Serotonergic afferents to the rat olfactory bulb: I. Origins and laminar specificity of serotonergic inputs in the adult rat." The Journal of neuroscience : the official journal of the Society for Neuroscience **7**(10): 3016-3028.

McLean, J. H., M. T. Shipley, et al. (1989). "Chemoanatomical organization of the noradrenergic input from locus coeruleus to the olfactory bulb of the adult rat." J Comp Neurol **285**(3): 339-349.

Meister, M. (2015). "On the dimensionality of odor space." eLife **4**: e07865.

Meredith, M. (1991). "Sensory processing in the main and accessory olfactory systems: comparisons and contrasts." The Journal of steroid biochemistry and molecular biology **39**(4B): 601-614.

Merkle, F. T., L. C. Fuentealba, et al. (2014). "Adult neural stem cells in distinct microdomains generate previously unknown interneuron types." Nature Neuroscience **17**(2): 207-214.

Millhorn, D. E. and F. L. Eldridge (1986). "Role of ventrolateral medulla in regulation of respiratory and cardiovascular systems." Journal of applied physiology **61**(4): 1249-1263.

Mitchell, G. S. and S. M. Johnson (2003). "Neuroplasticity in respiratory motor control." Journal of applied physiology **94**(1): 358-374.

Mizrahi, A. (2007). "Dendritic development and plasticity of adult-born neurons in the mouse olfactory bulb." Nature Neuroscience **10**(4): 444-452.

Mombaerts, P. (2001). "The human repertoire of odorant receptor genes and pseudogenes." Annual review of genomics and human genetics **2**: 493-510.

Mombaerts, P., F. Wang, et al. (1996). "Visualizing an olfactory sensory map." Cell **87**(4): 675-686.

Monahan, K. and S. Lomvardas (2015). "Monoallelic expression of olfactory receptors." Annual review of cell and developmental biology **31**: 721-740.

Mori, K., K. Kishi, et al. (1983). "Distribution of dendrites of mitral, displaced mitral, tufted, and granule cells in the rabbit olfactory bulb." J Comp Neurol **219**(3): 339-355.

Mori, K., H. Manabe, et al. (2013). "Olfactory consciousness and gamma oscillation couplings across the olfactory bulb, olfactory cortex, and orbitofrontal cortex." Frontiers in psychology **4**: 743.

Munger, S. D., T. Leinders-Zufall, et al. (2010). "An olfactory subsystem that detects carbon disulfide and mediates food-related social learning." Current biology : CB **20**(16): 1438-1444.

Nagayama, S., R. Homma, et al. (2014). "Neuronal organization of olfactory bulb circuits." Frontiers in Neural Circuits **8**: 98.

Najac, M., D. De Saint Jan, et al. (2011). "Monosynaptic and polysynaptic feed-forward inputs to mitral cells from olfactory sensory neurons." J Neurosci **31**(24): 8722-8729.

Nakashima, M., K. Mori, et al. (1978). "Centrifugal influence on olfactory bulb activity in the rabbit." Brain Res **154**(2): 301-306.

Nattie, E. (1999). "CO2, brainstem chemoreceptors and breathing." Progress in neurobiology **59**(4): 299-331.

Nattie, E. (2000). "Multiple sites for central chemoreception: their roles in response sensitivity and in sleep and wakefulness." Respiration physiology **122**(2-3): 223-235.

Neville, K. R. and L. B. Haberly (2003). "Beta and gamma oscillations in the olfactory system of the urethane-anesthetized rat." Journal of Neurophysiology **90**(6): 3921-3930.

Nguyen Chi, V., C. Muller, et al. (2016). "Hippocampal Respiration-Driven Rhythm Distinct from Theta Oscillations in Awake Mice." The Journal of neuroscience : the official journal of the Society for Neuroscience **36**(1): 162-177.

Nunes, D. and T. Kuner (2015). "Disinhibition of olfactory bulb granule cells accelerates odour discrimination in mice." Nature Communications **6**: 8950.

Nunez-Parra, A., R. K. Maurer, et al. (2013). "Disruption of centrifugal inhibition to olfactory bulb granule cells impairs olfactory discrimination." Proceedings of the National Academy of Sciences of the United States of America **110**(36): 14777-14782.

Nusser, Z., L. M. Kay, et al. (2001). "Disruption of GABA(A) receptors on GABAergic interneurons leads to increased oscillatory power in the olfactory bulb network." Journal of Neurophysiology **86**(6): 2823-2833.

Nusser, Z., L. M. Kay, et al. (2001). "Disruption of GABA(A) receptors on GABAergic interneurons leads to increased oscillatory power in the olfactory bulb network." J Neurophysiol **86**(6): 2823-2833.

Olufsen, M. S., M. A. Whittington, et al. (2003). "New roles for the gamma rhythm: population tuning and preprocessing for the Beta rhythm." J Comput Neurosci **14**(1): 33-54.

Onoda, N. and K. Mori (1980). "Depth distribution of temporal firing patterns in olfactory bulb related to air-intake cycles." Journal of Neurophysiology **44**(1): 29-39.

Orona, E., E. C. Rainer, et al. (1984). "Dendritic and axonal organization of mitral and tufted cells in the rat olfactory bulb." J Comp Neurol **226**(3): 346-356.

Otazu, Gonzalo H., H. Chae, et al. (2015). "Cortical Feedback Decorrelates Olfactory Bulb Output in Awake Mice." Neuron **86**(6): 1461-1477.

Pandipati, S., D. H. Gire, et al. (2010). "Adrenergic receptor-mediated disinhibition of mitral cells triggers long-term enhancement of synchronized oscillations in the olfactory bulb." Journal of Neurophysiology **104**(2): 665-674.

Panneton, W. M. (1991). "Primary afferent projections from the upper respiratory tract in the muskrat." J Comp Neurol **308**(1): 51-65.

Parrish-Aungst, S., M. T. Shipley, et al. (2007). "Quantitative analysis of neuronal diversity in the mouse olfactory bulb." J Comp Neurol **501**(6): 825-836.

Paton, J. F. R. (1996). "A working heart-brainstem preparation of the mouse." J Neurosci Methods **65**(1): 63-68.

Perez de Los Cobos Pallares, F., T. G. Bautista, et al. (2016). "Brainstem-mediated sniffing and respiratory modulation during odor stimulation." Respiratory physiology & neurobiology **233**: 17-24.

Perl, O., A. Arzi, et al. (2016). "Odors enhance slow-wave activity in non-rapid eye movement sleep." Journal of Neurophysiology **115**(5): 2294-2302.

Pimentel, D. O. and T. W. Margrie (2008). "Glutamatergic transmission and plasticity between olfactory bulb mitral cells." J Physiol **586**(8): 2107-2119.

Pinching, A. J. and T. P. Powell (1971). "The neuron types of the glomerular layer of the olfactory bulb." J Cell Sci **9**(2): 305-345.

Pressler, R. T., T. Inoue, et al. (2007). "Muscarinic receptor activation modulates granule cell excitability and potentiates inhibition onto mitral cells in the rat olfactory bulb." The Journal of neuroscience : the official journal of the Society for Neuroscience **27**(41): 10969-10981.

Price, J. L. and T. P. Powell (1970). "The morphology of the granule cells of the olfactory bulb." J Cell Sci **7**(1): 91-123.

Ramirez, J. M. and D. W. Richter (1996). "The neuronal mechanisms of respiratory rhythm generation." Current Opinion in Neurobiology **6**(6): 817-825.

Ravel, N., D. Caille, et al. (1987). "A centrifugal respiratory modulation of olfactory bulb unit activity: a study on acute rat preparation." Experimental brain research **65**(3): 623-628.

Restrepo, D., J. Arellano, et al. (2004). "Emerging views on the distinct but related roles of the main and accessory olfactory systems in responsiveness to chemosensory signals in mice." Hormones and behavior **46**(3): 247-256.

Reyher, C. K., W. K. Schwerdtfeger, et al. (1988). "Interbulbar axonal collateralization and morphology of anterior olfactory nucleus neurons in the rat." Brain research bulletin **20**(5): 549-566.

Richter, D. W. and K. M. Spyer (2001). "Studying rhythmogenesis of breathing: comparison of in vivo and in vitro models." Trends in Neurosciences **24**(8): 464-472.

Rinberg, D., A. Koulakov, et al. (2006). "Sparse odor coding in awake behaving mice." J Neurosci **26**(34): 8857-8865.

Riviere, S., L. Challet, et al. (2009). "Formyl peptide receptor-like proteins are a novel family of vomeronasal chemosensors." Nature **459**(7246): 574-577.

Rojas-Libano, D., D. E. Frederick, et al. (2014). "The olfactory bulb theta rhythm follows all frequencies of diaphragmatic respiration in the freely behaving rat." Frontiers in behavioral neuroscience **8**.

Rojas-Libano, D. and L. M. Kay (2012). "Interplay between Sniffing and Odorant Sorptive Properties in the Rat." Journal of Neuroscience **32**(44): 15577-15589.

Rothermel, M. and M. Wachowiak (2014). "Functional imaging of cortical feedback projections to the olfactory bulb." Frontiers in Neural Circuits **8**: 73.

Sailor, K. A., M. T. Valley, et al. (2016). "Persistent Structural Plasticity Optimizes Sensory Information Processing in the Olfactory Bulb." Neuron **91**(2): 384-396.

Sassoe-Pognetto, M. and O. P. Ottersen (2000). "Organization of ionotropic glutamate receptors at dendrodendritic synapses in the rat olfactory bulb." The Journal of neuroscience : the official journal of the Society for Neuroscience **20**(6): 2192-2201.

Schmidt, L. J. and B. W. Strowbridge (2014). "Modulation of olfactory bulb network activity by serotonin: synchronous inhibition of mitral cells mediated by spatially localized GABAergic microcircuits." Learning & memory **21**(8): 406-416.

Schneider, S. P. and F. Macrides (1978). "Laminar distributions of internuerons in the main olfactory bulb of the adult hamster." Brain Res Bull **3**(1): 73-82.

Schoenfeld, T. A. and F. Macrides (1984). "Topographic organization of connections between the main olfactory bulb and pars externa of the anterior olfactory nucleus in the hamster." J Comp Neurol **227**(1): 121-135.

Schoppa, N. E., J. M. Kinzie, et al. (1998). "Dendrodendritic inhibition in the olfactory bulb is driven by NMDA receptors." J Neurosci **18**(17): 6790-6802.

Schwarzacher, S. W., J. C. Smith, et al. (1995). "Pre-Botzinger complex in the cat." Journal of Neurophysiology **73**(4): 1452-1461.

Shipley, M. T. and G. D. Adamek (1984). "The connections of the mouse olfactory bulb: a study using orthograde and retrograde transport of wheat germ agglutinin conjugated to horseradish peroxidase." Brain Res Bull **12**(6): 669-688.

Shusterman, R., M. C. Smear, et al. (2011). "Precise olfactory responses tile the sniff cycle." Nature Neuroscience **14**(8): 1039-1044.

Siegel, M., T. H. Donner, et al. (2012). "Spectral fingerprints of large-scale neuronal interactions." Nature reviews. Neuroscience **13**(2): 121-134.

Silver, W. L., T. R. Clapp, et al. (2006). "TRPV1 receptors and nasal trigeminal chemesthesis." Chem Senses **31**(9): 807-812.

Silver, W. L. and J. A. Maruniak (1981). "Trigeminal Chemoreception in the Nasal and Oral Cavities." Chem Senses **6**(4): 295-305.

Smith, J. C., A. P. Abdala, et al. (2007). "Spatial and functional architecture of the mammalian brain stem respiratory network: a hierarchy of three oscillatory mechanisms." Journal of Neurophysiology **98**(6): 3370-3387.

Smith, J. C., H. H. Ellenberger, et al. (1991). "Pre-Botzinger complex: a brainstem region that may generate respiratory rhythm in mammals." Science **254**(5032): 726-729.

Spors, H. and A. Grinvald (2002). "Spatio-temporal dynamics of odor representations in the mammalian olfactory bulb." Neuron **34**(2): 301-315.

Stamps, J. J., L. M. Bartoshuk, et al. (2013). "A brief olfactory test for Alzheimer's disease." Journal of the neurological sciences **333**(1-2): 19-24.

Steinfeld, R., J. T. Herb, et al. (2015). "Divergent innervation of the olfactory bulb by distinct raphe nuclei." J Comp Neurol **523**(5): 805-813.

Stosiek, C., O. Garaschuk, et al. (2003). "In vivo two-photon calcium imaging of neuronal networks." Proceedings of the National Academy of Sciences of the United States of America **100**(12): 7319-7324.

Sun, Q. J., A. K. Goodchild, et al. (1998). "The pre-Botzinger complex and phase-spanning neurons in the adult rat." Brain Research **809**(2): 204-213.

Suzuki, N. and J. M. Bekkers (2006). "Neural coding by two classes of principal cells in the mouse piriform cortex." The Journal of neuroscience : the official journal of the Society for Neuroscience **26**(46): 11938-11947.

Traub, R. D., A. Bibbig, et al. (2004). "Cellular mechanisms of neuronal population oscillations in the hippocampus in vitro." Annual Review of Neuroscience **27**: 247-278.

Tsuno, Y., H. Kashiwadani, et al. (2008). "Behavioral state regulation of dendrodendritic synaptic inhibition in the olfactory bulb." The Journal of neuroscience : the official journal of the Society for Neuroscience **28**(37): 9227-9238.

Uchida, N., C. Poo, et al. (2014). "Coding and transformations in the olfactory system." Annual Review of Neuroscience **37**: 363-385.

Uhlhaas, P. J. and W. Singer (2006). "Neural synchrony in brain disorders: Relevance for cognitive dysfunctions and pathophysiology." Neuron **52**(1): 155-168.

Urban, N. N. and A. C. Arevian (2009). "Computing with dendrodendritic synapses in the olfactory bulb." Ann N Y Acad Sci **1170**: 264-269.

Vanderwolf, C. H. (1992). "Hippocampal activity, olfaction, and sniffing: an olfactory input to the dentate gyrus." Brain Research **593**(2): 197-208.

Varela, F., J. P. Lachaux, et al. (2001). "The brainweb: phase synchronization and large-scale integration." Nature reviews. Neuroscience **2**(4): 229-239.

Vassar, R., S. K. Chao, et al. (1994). "Topographic organization of sensory projections to the olfactory bulb." Cell **79**(6): 981-991.

Viriyopase, A., R. M. Memmesheimer, et al. (2016). "Cooperation and competition of gamma oscillation mechanisms." Journal of Neurophysiology **116**(2): 232-251.

Wachowiak, M. (2011). "All in a Sniff: Olfaction as a Model for Active Sensing." Neuron **71**(6): 962-973.

Wachowiak, M. and L. B. Cohen (2001). "Representation of odorants by receptor neuron input to the mouse olfactory bulb." Neuron **32**(4): 723-735.

Wallois, F., F. Gros, et al. (1995). "C-Fos-like immunoreactivity in the cat brainstem evoked by sneeze-inducing air puff stimulation of the nasal mucosa." Brain Research **687**(1-2): 143-154.

Wang, H., T. P. Germanson, et al. (2002). "Depressor and tachypneic responses to chemical stimulation of the ventral respiratory group are reduced by ablation of neurokinin-1 receptor-expressing neurons." The Journal of neuroscience : the official journal of the Society for Neuroscience **22**(9): 3755-3764.

Wellis, D. P. and J. S. Kauer (1993). "GABAA and glutamate receptor involvement in dendrodendritic synaptic interactions from salamander olfactory bulb." J Physiol **469**: 315-339.

Wellis, D. P., J. W. Scott, et al. (1989). "Discrimination among odorants by single neurons of the rat olfactory bulb." J Neurophysiol **61**(6): 1161-1177.

Wesson, D. W., E. Levy, et al. (2010). "Olfactory dysfunction correlates with amyloid-beta burden in an Alzheimer's disease mouse model." The Journal of neuroscience : the official journal of the Society for Neuroscience **30**(2): 505-514.

Wesson, D. W., J. V. Verhagen, et al. (2009). "Why Sniff Fast? The Relationship Between Sniff Frequency, Odor Discrimination, and Receptor Neuron Activation in the Rat." Journal of Neurophysiology **101**(2): 1089-1102.

Wesson, D. W., D. A. Wilson, et al. (2010). "Should olfactory dysfunction be used as a biomarker of Alzheimer's disease?" Expert Review of Neurotherapeutics **10**(5): 633-635.

Westecker, M. E. (1970). "Responses of single cells in the olfactory bulb of rabbits to air flow." Pflugers Archiv : European journal of physiology **315**(2): 93-104.

Wilson, D. A., A. R. Best, et al. (2004). "Plasticity in the olfactory system: lessons for the neurobiology of memory." The Neuroscientist : a review journal bringing neurobiology, neurology and psychiatry **10**(6): 513-524.

Wilson, D. A. and R. M. Sullivan (1994). "Neurobiology of associative learning in the neonate: early olfactory learning." Behavioral and neural biology **61**(1): 1-18.

Wilson, R. S., S. E. Arnold, et al. (2009). "Olfactory Impairment in Presymptomatic Alzheimer's Disease." International Symposium on Olfaction and Taste **1170**: 730-735.

Woolf, T. B., G. M. Shepherd, et al. (1991). "Serial reconstructions of granule cell spines in the mammalian olfactory bulb." Synapse **7**(3): 181-192.

Wyatt, T. D. (2003). Pheromones and animal behavior : chemical signals and signatures.

Xiong, W. and W. R. Chen (2002). "Dynamic gating of spike propagation in the mitral cell lateral dendrites." Neuron **34**(1): 115-126.

Yaldizli, O., I. K. Penner, et al. (2016). "The association between olfactory bulb volume, cognitive dysfunction, physical disability and depression in multiple sclerosis." European journal of neurology **23**(3): 510-519.

Yan, Z., J. Tan, et al. (2008). "Precise Circuitry Links Bilaterally Symmetric Olfactory Maps." Neuron **58**(4): 613-624.

Yokoi, M., K. Mori, et al. (1995). "Refinement of odor molecule tuning by dendrodendritic synaptic inhibition in the olfactory bulb." Proc Natl Acad Sci U S A **92**(8): 3371-3375.

Youngentob, S. L., M. M. Mozell, et al. (1987). "A quantitative analysis of sniffing strategies in rats performing odor detection tasks." Physiology & behavior **41**(1): 59-69.

6. Appendix

6.1. Nomenclature

ACIII: adenylil cyclase III

AD: Alzheimer´s disease

AMPAR: α-amino-3-hydroxy-5-methyl-4-isoxazolepropionic acid receptor

AOB: accessory olfactory bulb

AON: anterior olfactory nucleus

ASIC: acid-sensing ion channel

BötzC: Bötzinger complex

BNAOT: bed nucleus of the accessory olfactory tract

BNST: bed nucleus of the stria terminalis

BS: brainstem

cAMP: cyclic adenosin monophosphate

cVRG: caudal VRG

CaCC: calcium activated chloride channels

CN: cranial nerve

CNGC: cyclic nucleotide gated channels

CNQX: 6-cyano-7-nitroquinoxaline-2,3-dione

dSAC: deep short axon cell

DRG: dorsal respiratory group

eTC: external tufted cell

ECx: entorhinal cortex

EEG: electroencephalogram

ESP: exocrine-gland secretion peptide

GABA: gamma - aminobutyric acid

GC: granule cell

GG: Grueneberg Ganglion

GL: glomeruli layer

HD: Huntington´s disease

HPC: hippocampus

KF: Kölliker-Fuse

LFP: local field potential

MeA: medial amygdala

MC: mitral cell

MHC: major histocompability complex

MOB: main olfactory bulb

MOE: main olfactory epithelium

MS: multiple sclerosis

MUP: mouse urine protein

nAChR: nicotinic acetylcholine receptor

NA: nucleus ambigous

NE: noradrenaline

NK1R: neurokinin-1 receptor

NMDAR: N-methyl-D-aspartate receptor

NTS: nucleus of the solitary tract

OB: olfactory bulb

ORN: olfactory receptor neuron (see OSN)

OSN: olfactory sensory neuron

preBötzC: preBötzinger complex

PCx: piriform cortex

PD: Parkinson´s disease

PGC: periglomerular cell

PMCoA: posteromedial amygdala

PRG: pontine respiratory group

P2X: purinergic receptor

rVRG: rostral VRG

sSAC: superficial short axon cell

Sp5C: Spinal trigeminal tract

SO: septal organ

TAAR: trace amine-associated receptor

TC: tufted cell

TR: trigeminal receptor

TRPV1: transient receptor potential cation channel subfamily V member 1

VNO: vomeronasal organ

VRG: ventral respiratory group

VSN: Vomeronasal sensory neuron

6.2. Declaration of contribution to the mentioned papers

Paper 1:

An arterially perfused nose-olfactory bulb preparation of the rat.

Fernando Pérez de los Cobos Pallarés, Davor Stanić, David Farmer, Mathias Dutschmann, Veronica Egger

F.P.d.l.C.P., D.S., D.F., M.D., and V.E. conception and design of research; F.P.d.l.C.P. and M.D. performed experiments; F.P.d.l.C.P., M.D., and V.E. analyzed data; F.P.d.l.C.P., M.D., and V.E. interpreted results of experiments; F.P.d.l.C.P., M.D., and V.E. prepared figures; F.P.d.l.C.P., M.D., and V.E. drafted manuscript; F.P.d.l.C.P., D.F., M.D., and V.E. edited and revised manuscript; F.P.d.l.C.P., M.D., and V.E. approved final version of manuscript.

Paper 2:

Brainstem-mediated sniffing and respiratory modulation during odor stimulation.

Fernando Pérez de los Cobos Pallarés, Tara G. Bautista, Davor Stanić, Veronica Egger, Mathias Dutschmann

F.P.d.l.C.P., M.D., V.E. conception and design of research. F.P.d.l.C.P., M.D. performed experiments. F.P.d.l.C.P., M.D. analyzed data. M.D. edited the manuscript. F.P.d.l.C.P., T.B., D.S., V.E., M.D. reviewed the manuscript

Sniff-Like Patterned Input Results in Long-Term Plasticity at the Rat Olfactory Bulb Mitral and Tufted Cell to Granule Cell Synapse

Mahua Chatterjee, Fernando Pérez de los Cobos Pallarés, Alex Loebel, Michael Lukas, and Veronica Egger

Veronica Egger designed experiments; Mahua Chatterjee, Fernando Perez de los Cobos Pallares, Michael Lukas, and Veronica Egger performed experiments; Mahua Chatterjee, Fernando Perez de los Cobos Pallares, and Veronica Egger analyzed data; Alex Loebel contributed the quantal modeling and the respective parts of the paper; Veronica Egger wrote the paper.

Signature Fernando Perez de los Cobos Pallares

Signature Prof. Dr. Veronica Egger (thesis supervisor)

6.3. <u>Acknowledgements</u>

The performance of this thesis could have not been possible without the advice, support and friendship of many people along these years. For this I would love to thank…

Prof. Dr. Veronica Egger for being my doctoral supervisor. For giving me the chance to develop this thesis in your workgroup. I really appreciate all your help, scientific advice, discussions and support you gave me in the last years. I also enjoyed all the non scientific related chats.

Prof. Dr. Mathias Dutchmann and his workgroup in Australia for sharing with me all your knowledge related to semi intact preparations. Thank you for all your support. You have been such a great collaborator!

My thesis advisory committee (Prof. Dr. Veronica Egger, Prof. Dr. Hans Straka & PD Lars Kunz) for all the scientific advice and support for this thesis.

Prof. Drs. Benedikt Grothe and Inga Neumann for providing lab and office space and for your patience during moving periods from one city to another.

My current and former workgroup (Veronica, Wolfgang, Vanessa, Michael L., Max, Tiffany, Mahua, Michael M., Anne and Hortenzia) for all the laughs and for creating such a nice atmosphere which made my day by day pleasant and enjoyable.

Everyone who shared the office with me (Wolfgang, Mahua, Michael, Vanessa, Max, Tiffany, Daniel, Nicole and Chrisi) for all the good moments and continuous support during stressful moments.

All the TAs (Hortenzia and Anne) for your valuable work which made possible this thesis.

Collegues and friends in both Grothe and Neumann departments for creating a nice atmosphere and for sharing really good moments.

All the secretary and administrative staff in the LMU and UR (Simone Fisher, Kathrin Koros, Eva-Maria Hoffman, Cornelia Bestand, Tanja Janoschek) for all your help with time consuming burocracy papers related to my project.

All my friends for listening me uncountable times talking about my work as well as for all your support.

All my family for all your constant support in all good and bad moments during the last years. I knew you were always there and although you are far away I always felt you really closed.

All who were and are still a part of my life during this journey.

To all of you, thank you very much!

6.4. Short scientific curriculum vitae

Name: Fernando Pérez de los Cobos Pallarés

Date and place of birth: March 20th, 1987 in Madrid, Spain.

Nationality: Spanish

Academic Studies:

2013 to date:	PhD thesis - LMU München / Universität Regesnburg
2012 - 2013:	Research assistant at Department of Biology II, Ludwig - Maximilians Universität München (Prof. Dr. Veronica Egger)
2009 - 2010:	Exchange student at Aarhus University, Denmark
2005 - 2011:	Biotechnology studies (Licenciado) at the University of Vic, Spain

Publication list:

Pérez de los Cobos Pallarés F, Stanić D, Farmer D, Dutschmann M, Egger V.
An arterially perfused nose-olfactory bulb preparation of the rat.
J.Neurophysiol. 2015 Sep;114(3):2033-42.
doi:10.1152/jn.01048.2014

Chatterjee M, **Pérez de los Cobos Pallarés F**, Loebel A, Lukas M, Egger V.
Sniff-like patterned input results in long-term plasticity at the rat olfactory bulb mitral and tufted cell to granule cell synapse. Neural plasticity. 2016 (in press).

Pérez de los Cobos Pallarés F, Bautista TG, Stanić D, Egger V, Dutschmann M.
Brainstem-mediated sniffing and respiratory modulation during odor stimulation. Respir Physiol Neurobiol. 2016;233:17-24.
doi:10.1016/j.resp.2016.07.008

Conferences and Workshops:

August 2013:   Poster presentation ECRO Leuven, Belgium

September 2013:   Poster presentation DZG München, Germany

December 2013:   Oral presentation SPP PhD Meeting München, Germany

September 2014:   Poster presentation ECRO Dijon, France

Febraury 2015:   Oral presentation Neuroseminar Klinikum Regensburg, Germany

July 2015:   Oral presentation NeuroDoWO Symposia Cologne, Germany

November 2016:   Poster presentation SFN Conference San Diego, USA

6.5. Statutory declaration and statement

Ich versichere hiermit an Eides statt, dass die vorgelegte Dissertation von mir selbständig und ohne unerlaubte Hilfe angefertig ist. Der Autor hat zuvor nicht versucht, anderweitig eine Dissertation einzureichen oder sich einer Doktorprüfung zu unterziehen. Die Dissertation wurde keiner weiteren Prüfungskomission weder in Teilen noch als Ganzes vorgelegt.

……………………………   ………………………………………..
  Date and place   Signature Fernando Pérez de los Cobos P.